SPECIAL PAPERS IN PALAEONTOLOGY · 25

Stereom Microstructure of the Echinoid Test

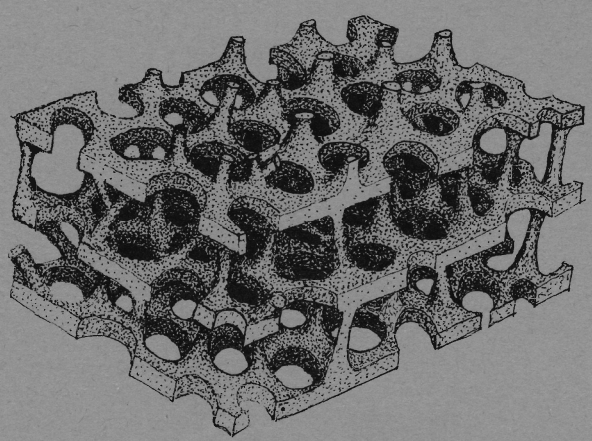

THE PALAEONTOLOGICAL ASSOCIATION

PRICE £15

SPECIAL PAPERS IN PALAEONTOLOGY NO. 25

STEREOM MICROSTRUCTURE OF THE ECHINOID TEST

BY

ANDREW B. SMITH

Department of Geology, University of Liverpool

THE PALAEONTOLOGICAL ASSOCIATION
LONDON

AUGUST 1980

Printed in Great Britain

CONTENTS

ABSTRACT. The stereom of coronal plates from a large number of Recent echinoids has been analysed to provide data for interpreting fossil echinoderm stereom. Both the external surfaces and cross-sections of individual plates have been examined by scanning electron microscopy and six basic three-dimensional lattices are identified and described, plus a further three types of stereom layer. Although all coronal plates examined have the same basic plate construction, details of the stereom composition and relative development of the different layers vary. From the distribution of the different stereom lattices within the plates, the stereom microstructure of the echinoid test is related to phylogeny, growth rate, and soft tissue type. Some stereom arrays are restricted to particular orders reflecting phylogenetic differences. Stereom growth banding in all layers is shown to correspond with 'pigment' banding. The stereoms which alternate to produce the banding are not the same in different plate layers. In most cases, rapid growth is associated with more open stereom and a reduced growth rate produces a denser stereom. In the middle plate layer, periods of minimal plate growth are distinguished by the disruption of the galleried stereom. It is probable that major stereom banding is the product of annual growth cessation which occurs during gonadal development. Certain stereoms are always found in association with a particular tissue, and there is a correlation between the way in which fibres attach to the test and the construction of the stereom of the attachment area. Environmental factors, such as the temperature and the availability of $CaCO_3$, may also influence the stereom construction. Some stereoms are mechanically designed for stress bearing. The growth strategy adopted by a species is reflected in the plate construction and it is therefore possible to identify the difference in emphasis placed on growth, reproduction, and maintenance.

Surface stereom is quantitatively analysed in thirty-two species according to the nature of the overlying tissue. Stereom variation is pronounced both within different areas of one plate and within the same area in different species. The stereom array at the plate surface is dependent largely on the plate design which is, in turn, influenced by the growth rate, the associated soft tissue, and by resorption. There is rarely a simple correlation of one stereom to one tissue and a particular fabric may be associated with a number of different tissues. By using a combination of surface quantitative and qualitative data and cross-sectional construction, it is possible to differentiate areas of sutural collagen fibres, catch apparatus fibres, muscle fibres, and epithelial tissue in nearly all species examined. Stereom interpretation can be successful only with a sound knowledge of the plate construction and growth.

The ecological significance of the superficial stereom construction is considered and rejected. Resorptional features of the plate are described. Areas where tubercles have been resorbed have a distinctive stereom and the filler stereom laid down behind ambulacral pores, as they move marginally by resorption, is different from normal plate stereom. Lateral movement of tubercles is clearly evident from growth banding in cross-section. The similarities and differences between echinoid stereom and crinoid and ophiuroid stereom are discussed, emphasizing the care which must be taken in interpreting stereom fabrics in fossil echinoderms. There is a wealth of biological information encoded in the stereom microstructure.

INTRODUCTION

THE SKELETAL PLATES which form the test of echinoids are composed of a high-magnesium calcite (Weber, 1969) and are mesodermal in origin. Each plate is composed of a three-dimensional mesh of trabeculae, termed stereom, which behaves as a single crystal. The interconnecting pore space of the plate is filled with connective tissue, termed stroma. Echinoderm stereom is varied, both in porosity and in constructional design (Nissen, 1969; Weber, 1969; Weber *et al.*, 1969), which has never previously been explained. A correlation between stereom fabric and the associated soft tissue has been described in crinoids by Roux (1970, 1971, 1974, 1975, 1977) and Macurda and Meyer (1975) and in ophiuroids by Macurda (1976). Although a number of morphological studies have recently described the microstructure of echinoid spines, pedicellariae, and lantern apparatus, only Jensen (1972) has examined echinoid plate microstructure in any detail. Prior to this, the only other work on plate microstructure was carried out by S. Becher (1914) and E. Becher (1924) using light microscopy. Recently, Oldfield (1976) described the stereom of the outer surface of the plates of a number of regular echinoids and Regis (1977) has discussed the surface fabric of *Paracentrotus*.

This paper sets out to describe and analyse the variation found both in plate construction and in stereom microstructural organization. Observations are largely confined to Recent species with the aim of providing a broadly based study for the interpretation of the stereom microstructure of fossil echinoderms.

MATERIALS AND METHODS

From a total of fifty-four species of echinoid, which were examined using a scanning electron microscope (S.E.M.), thirty-two species were selected for stereom analysis, and plate construction was studied in twenty-seven species (Table 1). These were selected to cover the widest range of stereom variation. Interambulacral and ambulacral plates of each were removed and cleansed of organic material in a 10% solution of sodium hypochlorite. To examine the plate construction, individual plates were sectioned transversely, using a dentist's drill, ensuring that at least one major tubercle was bisected. These were then ground smooth using fine carborundum powder, washed and air dried. All specimens were gold coated and placed in an S.E.M. Stereopair photomicrographs were taken by rotating the stage through $7\frac{1}{2}^{\circ}$ and recentring. Plates of *Psammechinus miliaris* and *Echinus esculentus* were treated to display their growth lines, following the methods given by Jensen (1969*a*) and Moore (1935). These were then sectioned transversely and photographed using a light microscope before being cleaned and gold coated for the S.E.M.

The histology of the associated soft tissue was also examined. Pieces of test were removed from preserved specimens using a dentist's drill and were decalcified in a solution of E.D.T.A. neutralized to a pH of 7. This took between one and ten days depending upon the thickness of the test. After being washed, specimens were dehydrated and embedded in paraffin wax. Serial sections were cut at a thickness of between 6 μm and 10 μm and stained using the Modified Massons Technique outlined by Humason (1972) though substituting 2 minutes in Aniline Blue for the recommended 15 seconds or so in Light Green.

STEREOM MICROSTRUCTURAL ORGANIZATION

Although variation in stereom microstructure has been known for some time (Valentin, 1841), very few workers have attempted to describe this variation in any but the broadest terms. Becher (1914) was the first to provide a detailed description of the echinoid plate, and recognized five different areas of stereom: a central unorganized *Fullmasse*, marginally developed *Suturstruktur* showing alignment parallel to the plate surface, vertically aligned *Muskelstruktur* in the tubercle, and two dense layers, a lower *Wabenstruktur* and an upper *glassartige gefarbte Schicht*. Jensen (1972), in an S.E.M. study of *Strongylocentrotus*, differentiated between an inner *reticular* or *spongy* stereom and an outer *meshwork of skeletal trabeculae*. She also identified two thin *compact layers*. Roux (1970, 1971, 1974*a*, 1975, 1977), in S.E.M. studies of Recent and fossil crinoid columnals, recognized two basic patterns

of stereom organization, which he termed α and β. α stereom is a regular meshwork of stereom trabeculae producing long parallel canals in at least one direction. β stereom is composed of an irregular meshwork of trabeculae showing no pore alignment whatsoever. This terminology was applied to echinoid stereom by Regis (1977). Macurda and Meyer (1975) described the stereom of a large number of Recent crinoids, and brought attention to the variety of stereom fabrics, which they made little attempt to classify. They identified *galleried* stereom, in which stereom pores show

TABLE 1. Species in which plate construction was studied.

ORDER CIDAROIDA
Cidaris cidaris (Linnaeus)—N. Atlantic
Poriocidaris purpurata Wyville Thomson—off Morocco

ORDER ECHINOTHURIOIDA
Calveriosoma hystrix (Wyville Thomson)—N. Atlantic
Phormosoma placenta Wyville Thomson—N. Atlantic

ORDER DIADEMATOIDA
Centrostephanus longispinus (Philippi)—Mediterranean
Centrostephanus nitidus Koehler

ORDER PHYMOSOMATOIDA
Stomopneustes variolaris (Lamarck)—Aldabra

ORDER ARBACIOIDA
Arbacia lixula (Troschal)—Gulf of Naples

ORDER TEMNOPLEUROIDA
Temnopleurus hardwickii (Gray)
Sphaerechinus granularis (Lamarck)—Gulf of Naples
Tripneustes gratilla (Linnaeus)—Pacific

ORDER ECHINOIDA
Echinus esculentus (Linnaeus)—S.W. England
Paracentrotus lividus (Lamarck)—S.W. Ireland
Psammechinus miliaris (Gmelin)—S.W. England
Colobocentrotus atratus (Linnaeus)
Echinometra mathaei (de Blainville)—Aldabra
Echinostrephus molaris (de Blainville)—Aldabra

ORDER HOLECTYPOIDA
Echinoneus cyclostomus (Gray)—Aldabra

ORDER CLYPEASTEROIDA
Clypeaster rarispina de Meijere—Bahamas
Clypeaster rosaceus (Linnaeus)—Florida
Mellita quinquiesperforata (Leske)—Alabama
Encope michelini Agassiz—Florida

ORDER CASSIDULOIDA
Apatopygus recens (Milne-Edwards)—New Zealand
Echinolampas crassa (Bell)—South Africa

ORDER SPATANGOIDA
Brissopsis lyrifera (Forbes)—S.W. England
Spatangus raschi Loven—Scilly Isles
Echinocardium cordatum (Pennant)—S.W. England
Eupatagus hastingiae Forbes—Eocene, Hampshire
Paramaretia peloria (Clark)—Australia

EXPLANATION OF PLATE 1

Fig. 1. Stereo view of the outer plate surface of an aboral interambulacral plate of *Eucidaris metularia*. Rectilinear stereom overlain by integument.
Fig. 2. Stereo view of stereom forming the areole of the primary tubercle of an ambital interambulacral plate of *Poriocidaris purpurata*. Rectilinear stereom associated with muscle attachment.
Fig. 3. Stereo view of stereom forming the outer plate layer of *Cidaris cidaris* seen in a broken ambital interambulacral plate section.

Scale bar = 40 μm.

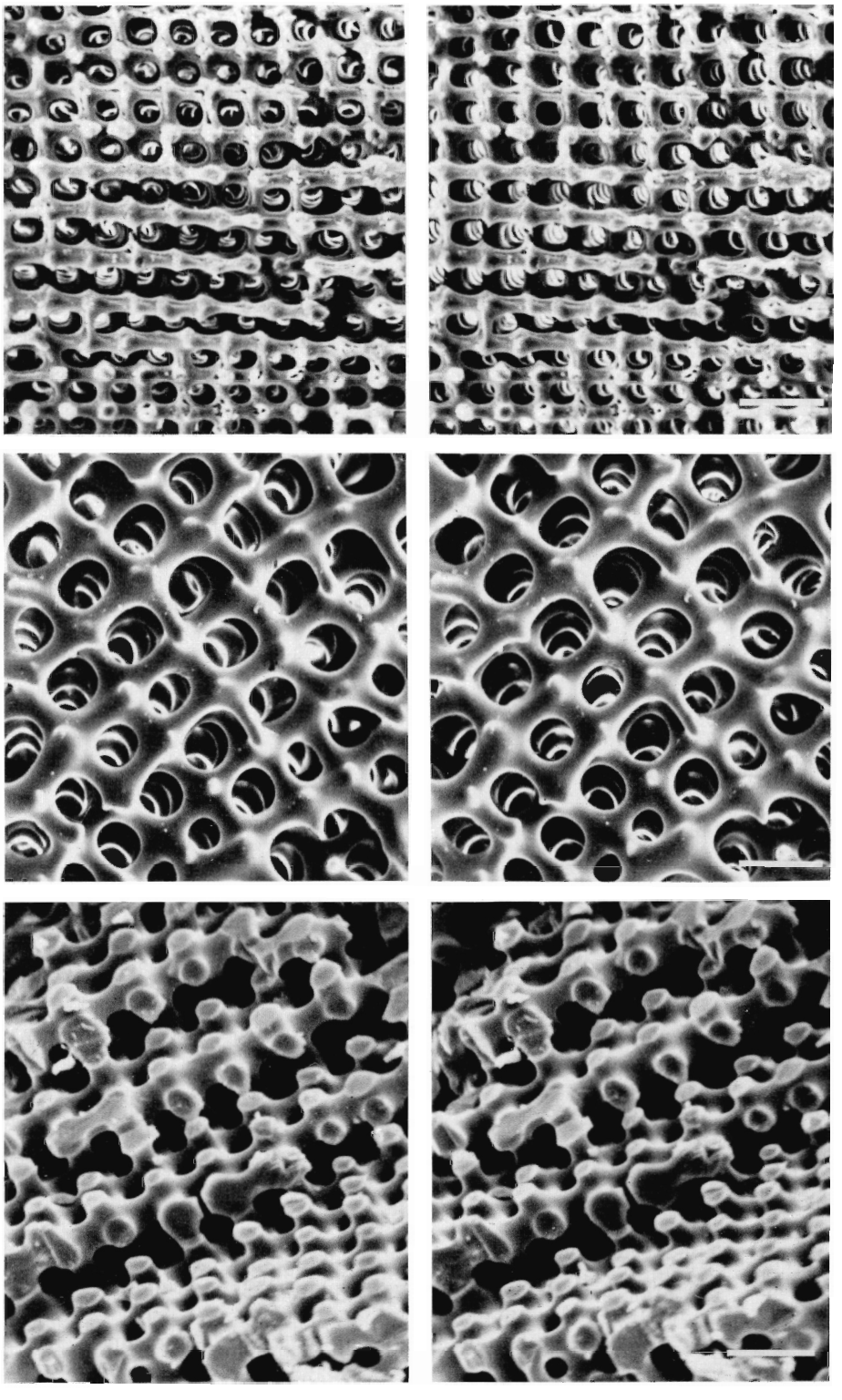

1

2

3

SMITH, rectilinear stereom

good alignment producing long parallel galleries, and distinguished *rectilinear* galleried stereom from other galleried stereoms. In addition they described a number of *irregular* stereom arrangements and *massive* stereom arrangements. They also described a *labyrinthic* stereom, characteristic of the muscle fossae of most commatulid crinoids, typified by having ovoid interconnecting pores showing no internal alignment.

A major contribution to our knowledge of stereom microstructure was provided by the S.E.M. study of stereom growth in regenerating spines carried out by Heatfield (1971). He found two patterns of stereom growth. In one the microspines remain distinct, narrow, and pointed, and horizontal bridges are formed at intervals between adjacent spines, resulting in a delicate meshwork which may show some alignment. In the other type of growth, microspine tips bifurcate shortly after they are formed and fuse with those of adjacent spines forming a series of arches and eventually producing a dense stereom array. In the present study of echinoid stereom a number of distinct structural patterns were identified and it became clear that the present stereom nomenclature was inadequate. As it is important to be able to identify the microstructural organization of a plate before attempting to interpret surface stereom patterns, the following classification of stereom fabrics is proposed. The relationship between this and previous nomenclature is given in Table 2.

TABLE 2. Comparison of stereom nomenclature in this paper with previous usage.

This paper	Macurda and Meyer (1975)	Roux (1970)	Becher (1914)	Jensen (1972)
Rectilinear	Rectilinear galleried	α	—	—
Microperforate	—	—	—	—
Laminar	—	—	—	—
Galleried	Galleried	α	Muskelstruktur Suturstruktur	Skeletal trabeculae
Fascicular	—	—	—	—
Labyrinthic	Labyrinthic	β	Fullmasse	spongy
Retiform	—	—	—	—
Simple perforate	—	—	Waben strukture	compact
Irregular perforate	—	—	Glasige Pigmentschicht	compact
Imperforate	Massive	—	—	—

Rectilinear Stereom. Trabeculae are arranged in a cubic or orthorhombic lattice structure with well-developed pore alignment in three directions, perpendicular or near perpendicular to one another (text-fig. 1). Pores are equally well developed in all three directions and have a diameter equal to or greater than the thickness of the trabeculae. Trabecular intersections may be slightly swollen. Where this stereom is found on the external surface of the plate it forms a planar or stepped surface (Pl. 1, fig. 2). All interior pores show extremely good alignment producing long galleries which penetrate deep into the test. Broken sections show preferential separation along planes producing a distinctive sheet arrangement with regularly arrayed trabecular struts (Pl. 1, fig. 3). In ground sections, long parallel canals are seen running in one direction, or sometimes in two directions approximately perpendicular to each other, depending upon the orientation of the section (Pl. 2, fig. 1).

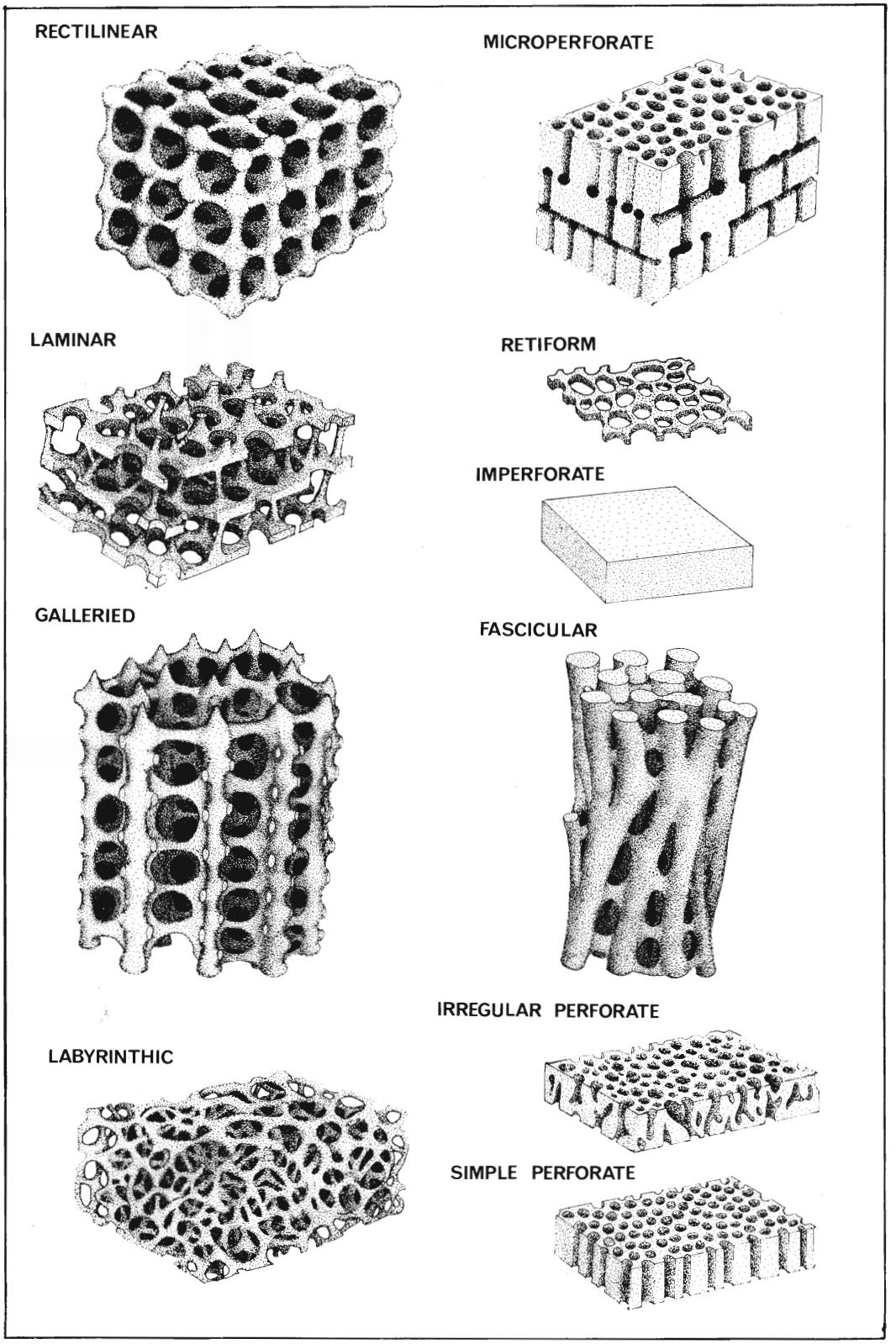

TEXT-FIG. 1. Composite block diagrams of stereom fabrics.

Microperforate Stereom. This is a multilaminar, low-porosity stereom perforated by channels which run in three directions perpendicular to one another. These perforations are extensive in two directions and criss-cross each other to impart a distinct layered texture to the stereom (text-fig. 1). Perforations perpendicular to the layering are randomly arranged with little continuity of channels across the layers. The whole structure has a brickwork appearance when viewed parallel to the layering (Pl. 3, fig. 1). These perforations are cylindrical in cross-section with a diameter of between 12 μm and 18 μm and each layer is approximately 50 μm thick. When viewed perpendicular to the layering the stereom forms a dense, planar surface perforated by an irregular arrangement of circular pores (Pl. 3, fig. 2).

Galleried Stereom. This stereom possesses long parallel galleries running in one direction only and shows no pore alignment perpendicular to this direction. It is composed of parallel trabecular rods which are interconnected by struts in such a way as to produce cylindrical passages paralleling the rods (text-fig. 1). Viewed parallel to the galleries the pores are seen to be in an irregular polygonal arrangement with rods at the intersections of trabeculae (Pl. 2, figs. 3 and 4). Internal pore alignment is moderately well-developed so that each gallery penetrates deep into the test. This pore alignment is not normally as marked as it is in rectilinear stereom. When viewed perpendicular to the galleries the long straight rods and passageways can be seen (Pl. 2, fig. 2; Pl. 4, fig. 5). There is no alignment of lateral pores and these are usually smaller in diameter than the galleried pores. This gives a more irregular appearance to galleried stereom compared with rectilinear stereom.

Laminar Stereom. This is a multilamellar construction built up of thin sheets of stereom separated by trabecular struts (text-fig. 1). Each sheet is retiform in structure and the separation distance between sheets is much greater than the thickness of individual sheets. Trabecular struts are usually thin and are orientated more or less perpendicular to the lamellae (Pl. 2, fig. 5). Some slight alignment of the struts may give a vague galleried effect parallel to the lamella. When viewed perpendicular to the lamination this stereom has a planar surface perforated by numerous closely spaced pores of large diameter (Pl. 2, fig. 6; Pl. 4, fig. 6).

Fascicular Stereom. This is a fairly dense irregular stereom composed of branching trabecular rods which run more or less in parallel. These rods are circular to ovoid in cross-section and are fairly closely spaced so that the inter-trabecular space is small and irregular (text-fig. 1). These rods interconnect with each other not only by major trabecular branching but also by small trabecular struts usually running perpendicular to the rods (Pl. 4, fig 2). Sections cut across the rods show an irregular

---

EXPLANATION OF PLATE 2

Fig. 1. Rectilinear stereom of the outer plate layer of an ambital interambulacral plate of *Cidaris cidaris*, seen in cross-section.

Fig. 2. Galleried stereom of the middle plate layer of an ambital interambulacral plate of *Sphaerechinus granularis*, seen in cross-section.

Fig. 3. Stereo view of galleried stereom of the boss of a primary ambital interambulacral tubercle of *Tripneustes gratilla* viewed perpendicular to the plate surface.

Fig. 4. Galleried stereom of the boss of a primary interambulacral tubercle of *Eucidaris metularia* viewed perpendicular to the plate surface.

Fig. 5. Laminar stereom seen in a cross-section of an aboral interambulacral plate of *Paramaretia peloria* (inner plate layer). Lamellae parallel inner plate surface.

Fig. 6. Stereo view of laminar stereom forming the inner plate layer of an ambital interambulacral plate of *Eupatagus hastingiae*, seen in cross-section. Galleried stereom of the middle plate layer can be seen in the bottom left.

Scale bar in Figs. 3, 4 = 20 μm; Figs. 1, 2, 5 = 40 μm; Fig. 6 = 100 μm.

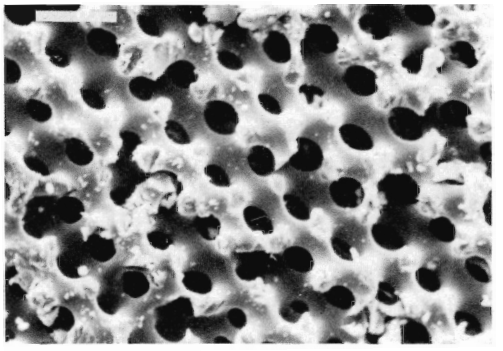

1

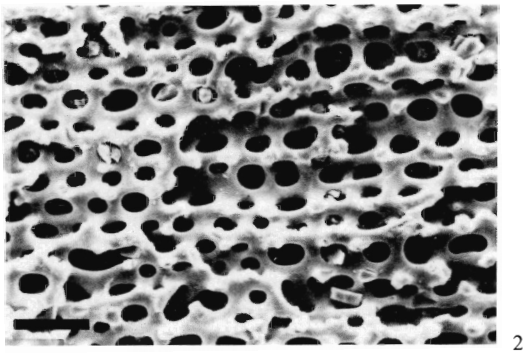

2

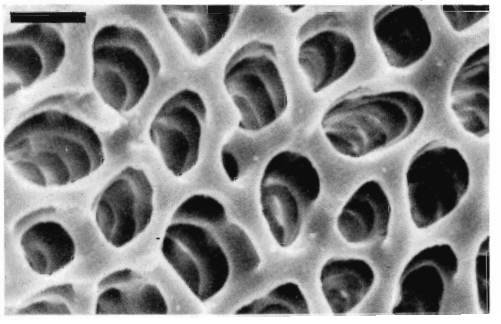

3

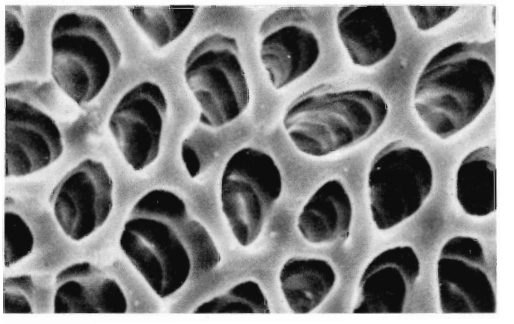

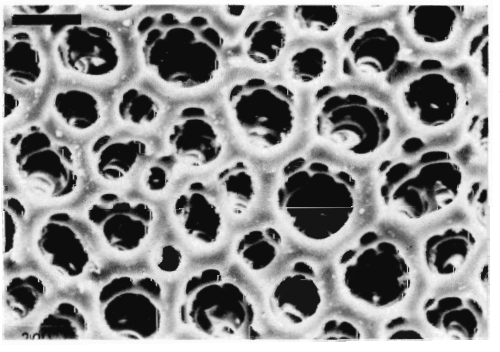

4

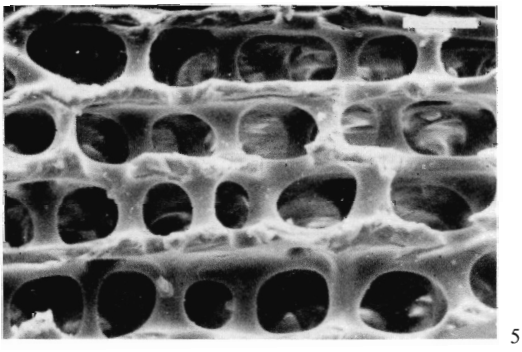

5

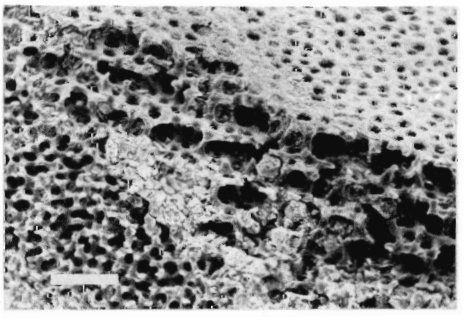

6

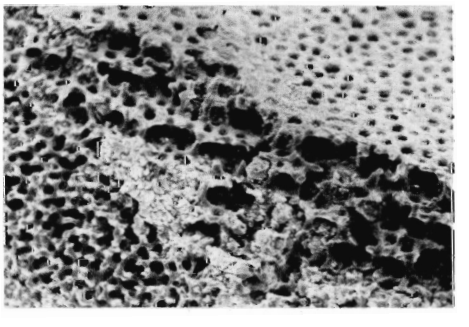

SMITH, stereom organisation

and dense array of subcircular calcite trabeculae with some interconnecting struts (Pl. 4, fig. 1). When viewed perpendicular to the rods the stereom is seen to be composed of thick parallel rods with the interconnecting struts defining irregular and usually elongate pores (Pl. 4, fig. 4).

Labyrinthic Stereom. This takes the form of a completely unorganized mesh of trabeculae (text-fig. 1). Any section (Pl. 3, figs. 3–6) reveals a three-dimensional tangle of interconnecting trabeculae. It may form a very coarse, open structure (Pl. 3, fig. 6) or a finer, more compact structure (Pl. 3, fig. 5). Pores are usually ovoid but are difficult to define as this stereom never forms a planar surface.

In addition to the stereom arrays described above, which form extensive three-dimensional constructions, single layers of stereom may also be found (text-fig. 1).

Retiform Stereom Layer. This forms a thin layer of interconnecting trabeculae in one plane only. The thickness of this layer is less than the average maximum diameter of its pores (Pl. 5, figs. 2, 3). The pores are usually small and closely spaced and may or may not be linearly arranged (Pl. 5, figs. 1, 4).

Perforate Stereom Layer. This is a fairly thick layer, usually thicker than the average maximum diameter of the pores which perforate it. These pores are small, circular and irregularly arranged over the surface of the sheet (Pl. 8, fig. 4). These pores may be cylindrical, unbranched, and more or less perpendicular to the surface (Pl. 8, fig. 7), in which case it is termed *simple* perforate stereom, or they may be sinuous and branched (Pl. 8, fig. 1), in which case it is termed *irregular* perforate stereom.

Imperforate Stereom Layer. This is a solid calcite layer, which, as the name implies, lacks any stromal canals (Pl. 8, fig. 5).

To define a particular stereom fabric fully, not only does the constructional design have to be identified and its orientation given, but also some measure of the coarseness of the array and the density of trabeculae. If, for a given stereom surface, we define $\bar{A}$ as the average maximum diameter of the pores and $\bar{t}$ as the average minimum trabecular thickness between adjacent pores then $\bar{A}$ can be used as an indicator of stereom coarseness and $\bar{A}/\bar{t}$ as a measure of trabecular density (see later). The following terminology is adopted in this paper. *Stereom coarseness*: $\bar{A} > 25$ μm—coarse; 10 μm $< \bar{A} < 25$ μm—medium; $\bar{A} < 10$ μm—fine; *trabecular density*: $\bar{A}/\bar{t} < 1$—compact; $2 > \bar{A}/\bar{t} > 1$—dense; $4 > \bar{A}/\bar{t} > 2$—open; $\bar{A}/\bar{t} > 4$—sparse.

EXPLANATION OF PLATE 3

Fig. 1. Microperforate stereom of the inner plate layer of an ambital interambulacral plate of *Echinolampas crassa*, seen in cross-section. Inner surface of plate to the bottom.

Fig. 2. Microperforate stereom of an ambital interambulacral plate of *Apatopygus recens*. Perpendicular view of inner plate surface.

Fig. 3. Open labyrinthic stereom forming the inner surface of an ambital interambulacral plate of *Echinus esculentus*.

Figs. 4, 6, 7. *Calveriosoma hystrix*. 4, labyrinthic stereom forming the inner surface of an aboral interambulacral plate. 6, another view of labyrinthine stereom on inner plate layer seen in cross-section. 7, stereo view of the irregular laminar stereom of the outer plate layer of an aboral interambulacral plate seen in cross-section. This overlies labyrinthic stereom of the inner plate layer.

Fig. 5. Labyrinthic stereom from the middle plate layer of an aboral interambulacral plate of *Tripneustes gratilla*, seen in cross-section.

Scale bar in Figs. 2, 5–7 = 40 μm; Figs. 1, 3, 4 = 100 μm.

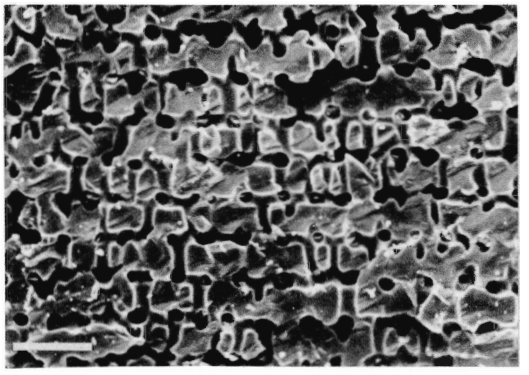

1

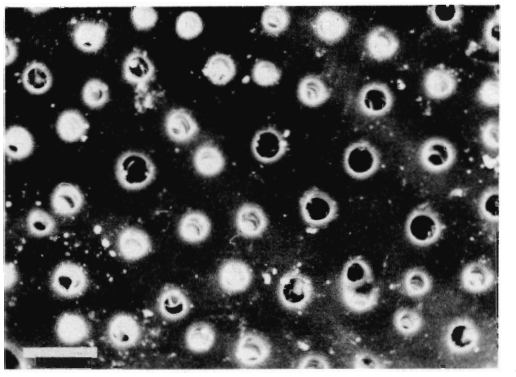

2

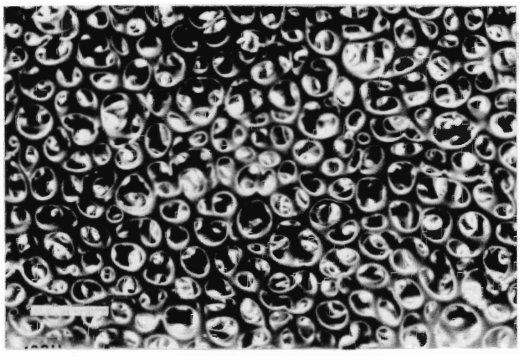

3

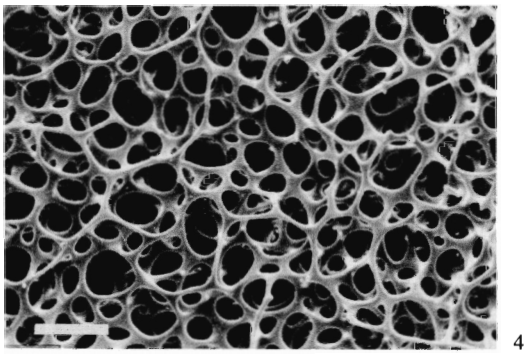

4

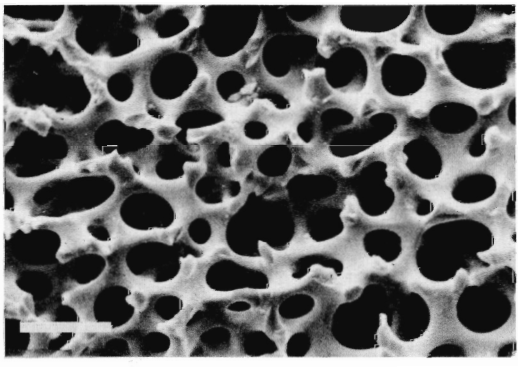

5

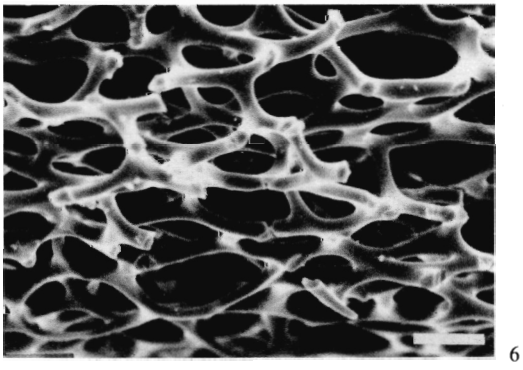

6

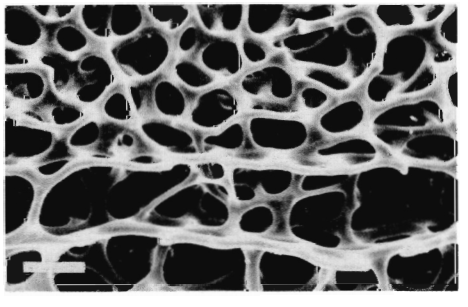

7

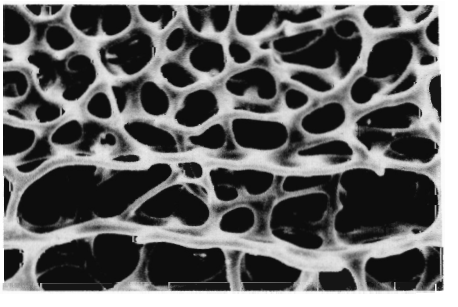

SMITH, stereom organisation

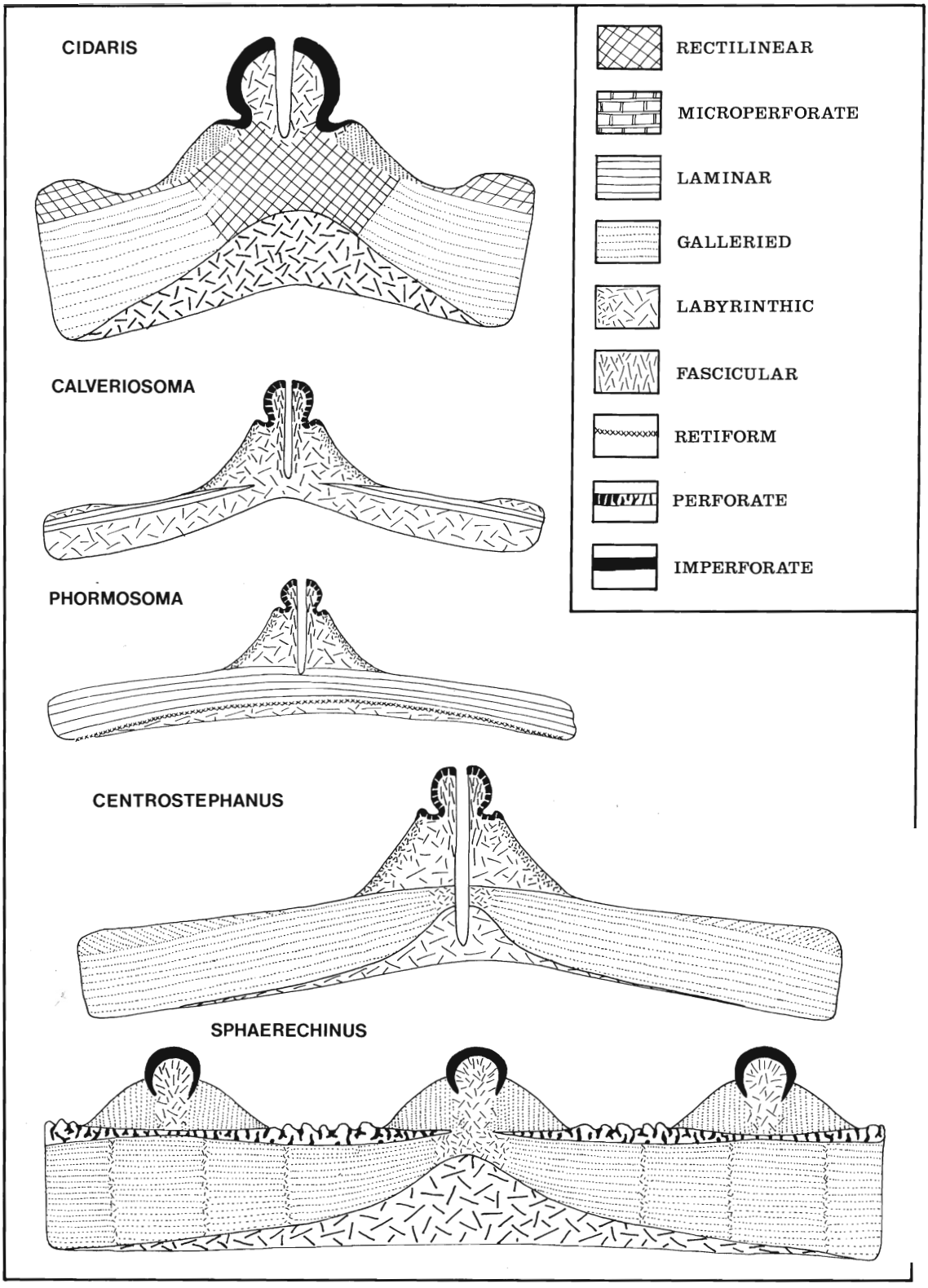

TEXT-FIG. 2. Schematic cross-sectional plans of interambulacral plates showing the distribution of stereom fabrics.

PLATE CONSTRUCTION

The first detailed description of echinoid plate construction was provided by Becher (1914). He found that the plates of *Echinus esculentus* possess a small central region of labyrinthic stereom. Extending laterally from this central region comes galleried stereom which thickens peripherally. As the plate increases in thickness a 'filler' of labyrinthic stereom is laid down on the inner surface. The internal and external surfaces are both bounded by a perforate stereom layer. The outer surface of the test has overlying tubercles which have a central core of compact calcite with radial striae surrounded by vertically aligned galleried stereom. Jensen (1972) found more or less the same plate construction in *Strongylocentrotus droebachiensis* although she notes that the inner, compact, perforate stereom layer lies between the galleried stereom and the labyrinthic stereom and does not form the inner plate surface. Pearse and Pearse (1975) also illustrate a cross-section of an echinoid plate and identify an *outer dense layer*, *middle layer*, and coarse inner *callus*. This study shows that, although the basic plate design is much the same in all species examined, the stereom fabric is varied. Descriptions of the more important variations are given below.

Cidaroids

The external surface of interambulacral plates of all four cidaroid species examined is composed of rectilinear stereom (Pl. 1, figs. 1–3) with the exception of the boss and mamelon of primary tubercles (Pl. 6, fig. 1). The small ambulacral plates, which were not sectioned, have open labyrinthic stereom on their outer surface. The internal surface of interambulacral plates is composed of a coarse, open to sparse labyrinthic stereom. In cross-section (text-fig. 2) there are two layers: an inner labyrinthic stereom layer and an outer rectilinear stereom region (Pl. 6, fig. 2). In *Cidaris cidaris* the outer layer of rectilinear stereom shows a change in orientation which coincides approximately with the base of the boss (Pl. 6, fig. 3). The stereom peripheral to this change shows a preferred development of galleries running perpendicular to the suture face. Towards the margin of the plate, the central and inner stereom of this layer changes into galleried stereom (Pl. 6, fig. 2), although the outer stereom remains rectilinear (Pl. 6, fig. 6). A large part of the suture face is, therefore, composed of galleried stereom with rectilinear stereom retained only in the outermost part of the plate. A similar discontinuity in stereom orientation was observed in *Poriocidaris*. The rectilinear stereom of the plate continues upwards into the tubercle without discontinuity (Pl. 6, figs. 2, 4). A wedge-shaped ring of medium, open, galleried stereom lies immediately beneath the surface of the boss. Galleries of this stereom are orientated perpendicular to the plate surface. The mamelon has a core of labyrinthic stereom which consolidates outwards and changes into a compact fascicular stereom (Pl. 6, fig. 4) or an imperforate stereom (Pl. 6, fig. 2). Apart from the marked zone of stereom realignment, growth lines are evident only in the galleried stereom of the boss. The sharp change in stereom orientation may result from the onset of rigid plate suturing during growth.

Echinothuriids

The plates of *Calveriosoma hystrix* are composed of two layers of stereom; a thick inner layer of coarse, sparse labyrinthic stereom, which does not thin peripherally, and a thin outer layer of rather irregular, coarse, sparse, laminar stereom which thins towards the centre of the plate (text-fig. 2). The upper, laminar stereom parallels the plate surface and is only a few layers thick (Pl. 3, fig. 7). Away from the primary tubercle this laminar layer is overlain by a thin layer of coarse, sparse, labyrinthic stereom. The tubercles themselves overlie the laminar stereom of the plate and each has an extensive central core of labyrinthic stereom. This becomes very much finer just below the surface of the boss where it changes to a medium, sparse, labyrinthic stereom. Towards the mamelon the central core of labyrinthic stereom merges into a fascicular stereom (Pl. 4, fig. 1) which consolidates to form a compact perforate layer on the outer surface of the mamelon. The central perforation penetrates to the base of the tubercle. A central region of open labyrinthic stereom appears to represent the first formed part of the plate. Growth lines were not observed in *Calveriosoma* or in *Phormosoma*. The plate construction of *Phormosoma placenta* differs slightly from that of

Calveriosoma. Plates of *Phormosoma* possess a single retiform layer which is underlain by open labyrinthic stereom and overlain by stereom which, although very irregular shows some lamination (text-fig. 2). The exterior of the plate is always an open, planar surface (Pl. 15, fig. 6). Aboral tubercles are similar in construction to tubercles of *Calveriosoma*, and they overlie the planar surface of the plate. Oral interambulacral tubercles, which support large, hoofed spines are, however, sunken below the level of the retiform layer (Pl. 5, fig. 5). The areole forms a raised rim around the boss.

Diadematoids

The plates of *Centrostephanus nitidus* and *C. longispinus* show the same basic construction with two stereom layers (text-fig. 2). Each plate has an outer region of medium, open to dense, galleried stereom, which thickens marginally, and an inner layer of coarse, open, labyrinthic stereom, which is only developed towards the centre of the plate. In *C. nitidus* the galleried stereom is overlain by a thin surface layer of labyrinthic stereom but this is absent over most of the plate surface of *C. longispinus*. Throughout most of the outer region of the plate, galleried stereom is aligned with galleries running parallel to the plate surface. Marginally, in plates of *C. longispinus*, the outermost stereom has galleries which are angled to the plate surface (Pl. 8, fig. 6). Towards the lateral margins of the plates of both species the galleried stereom becomes organized into sheets and may become laminar centrally (Pl. 6, fig. 7). The primary tubercle, which overlies the galleried layer of each plate, has a large central core of coarse, sparse, labyrinthic stereom. This changes, just beneath the surface of the boss, to a superficial fine to medium, open, labyrinthic stereom. The mamelon is composed of fascicular stereom which consolidates outwards to produce a compact perforate stereom layer at the outer surface. The central perforation of the tubercle penetrates down to the inner labyrinthic stereom layer. Growth banding was not seen in either species.

Echinacea

Sphaerechinus. As in all other Echinacea, plates of *Sphaerechinus granularis* possess a middle layer of galleried stereom, aligned perpendicular to suture faces, and an inner layer of coarse labyrinthic stereom (text-fig. 2; Pl. 7, figs. 1, 5). Labyrinthic stereom is thickest at the plate centre and thins towards the periphery. Galleried stereom thickens away from the centre and is overlain by an outer layer of perforate stereom which forms the external surface of the plate between tubercles (Pl. 7, figs. 5–7). This layer is absent beneath the centre of the primary tubercle but only thins under other major tubercles. Tubercles have a central core of coarse, labyrinthic stereom which becomes denser towards the mamelon, eventually consolidating to produce a compact perforate or imperforate surface layer (Pl. 8, fig. 2). This core is surrounded by vertically aligned, galleried stereom which forms the boss. At the centre of the plate there is a small region of medium-sized labyrinthic stereom which changes abruptly into galleried stereom (Pl. 7, fig. 5). Stereom growth banding can be seen in both plate and tubercles (Pl. 7, figs. 5, 6).

EXPLANATION OF PLATE 4

Fig. 1. Stereo view of fascicular stereom forming the mamelon of an aboral interambulacral tubercle of *Phormosoma placenta*. Top of the mamelon broken off during sectioning.

Fig. 2. Superficial layer of fascicular stereom forming the upper part of the base of a primary interambulacral spine of *Centrostephanus longispinus*. This is the area of attachment for spine muscle.

Fig. 3. Labyrinthic stereom of the internal surface (central) of an ambital interambulacral plate of *Echinus esculentus*.

Fig. 4. Stereo view of fascicular stereom forming the platform and mamelon neck of a primary interambulacral tubercle of *Poriocidaris purpurata*.

Fig. 5. Galleried stereom at the periphery of an ambital interambulacral plate of *Cidaris cidaris* (inner plate surface). The rods forming the galleried stereom extend as pegs at the lateral suture face, seen at the top.

Fig. 6. Laminar stereom of the inner surface of an aboral interambulacral plate of *Spatangus raschi*.

Scale bar in Figs. 1, 3, 5 = 40 μm; Fig. 6 = 100 μm; Figs. 2, 4 = 200 μm.

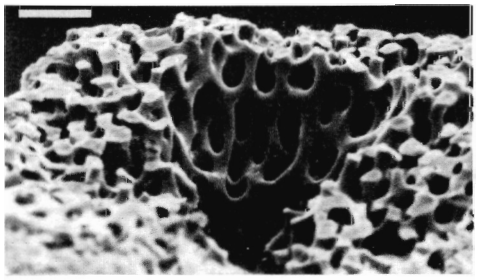

1

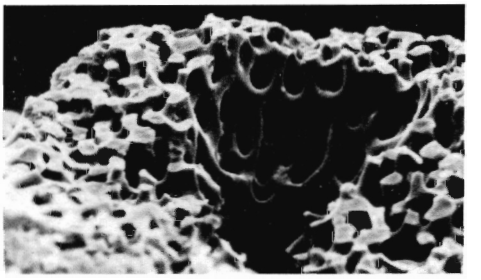

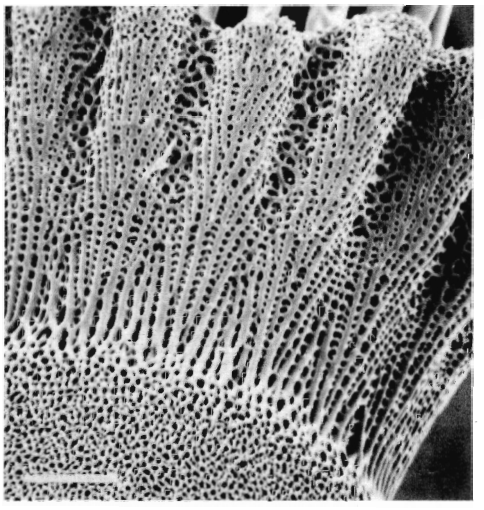

2

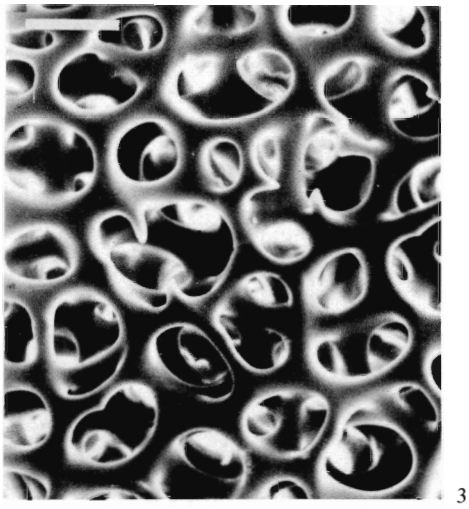

3

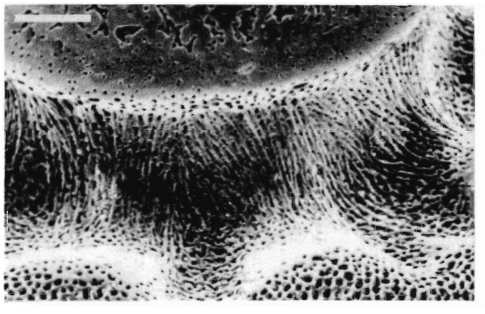

4

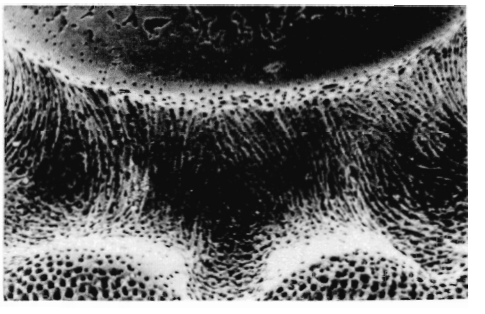

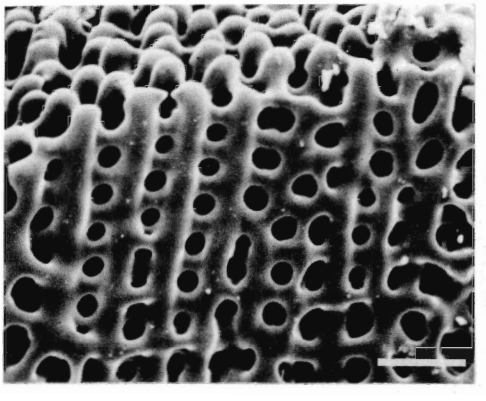

5

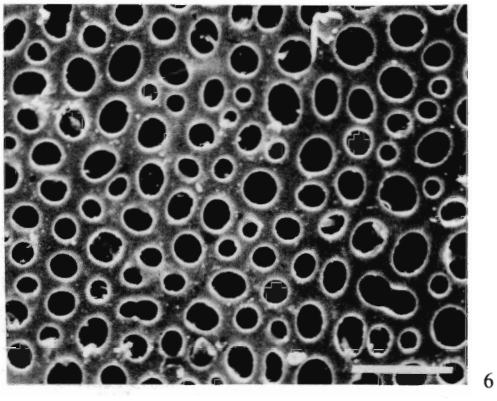

6

SMITH, stereom organisation

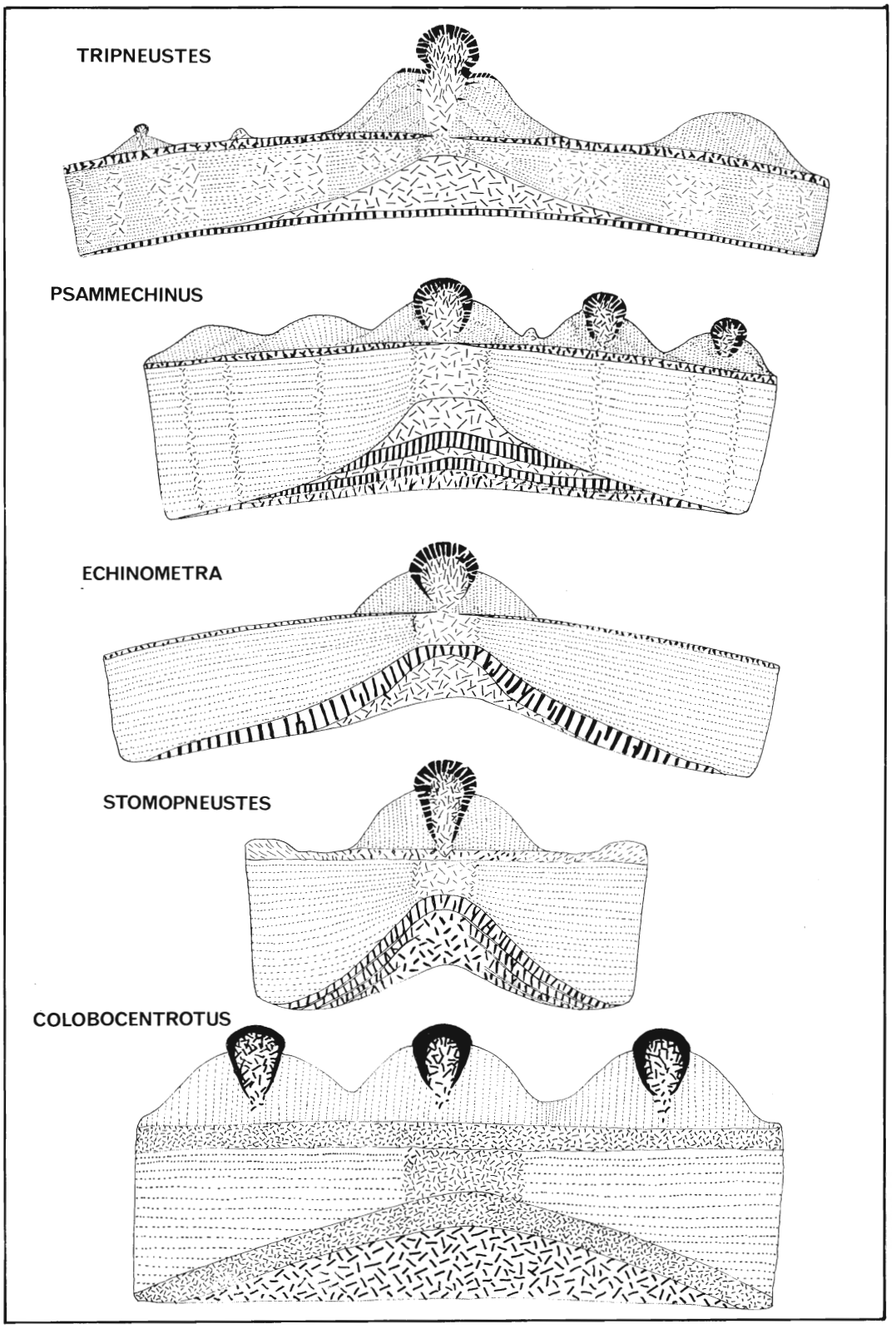

TEXT-FIG. 3. Schematic cross-sectional plans of interambulacral plates showing the distribution of stereom fabrics. Hatching as in text-fig. 2.

Tripneustes. Plates of *Tripneustes gratilla* are similar to those of *Sphaerechinus*, with both an inner labyrinthic stereom layer and a middle galleried stereom layer (text-fig. 3; Pl. 8, fig. 8). The outer surface of interambulacral plates is composed of a compact perforate stereom layer (Pl. 7, fig. 2) which thins and disappears peripherally. This perforate layer is absent from ambulacral plates. However, unlike *Sphaerechinus*, the whole of the inner surface of larger plates is composed of a compact, perforate stereom layer. These two compact layers give the plate a sandwich structure. Tubercles are situated on top of the perforate stereom layer. They have a central core of dense labyrinthic or fascicular stereom which consolidates outwards to produce a compact, perforate stereom capping to the mamelon. Stereom banding is very pronounced in the plates of *Tripneustes*. In the outer plate layer, bands of galleried stereom alternate with bands of slightly more open labyrinthic stereom. Labyrinthic bands are best developed near the centre of this layer whilst galleried stereom is more or less continuous in the inner and outer regions of this layer. The junction between galleried stereom and labyrinthic stereom is sharp and linear whereas the change from labyrinthic to galleried stereom is much less clearly defined. A similar banding is also developed in the stereom of the boss (Pl. 7, fig. 4).

Echinometra and Paracentrotus. Plate construction in *Echinometra mathaei*, and in *Paracentrotus lividus*, differs from that found in *Tripneustes* primarily in the location of the inner perforate stereom layer. In plates of *Echinometra* and *Paracentrotus* this layer lies between the galleried stereom and the labyrinthic stereom (text-fig. 3; Pl. 9, figs. 6–8). The inner surface of each plate has, in consequence, a central area of labyrinthic stereom surrounded by a marginal, dense or compact, perforate stereom (Pl. 7, fig. 8). A thin perforate stereom layer forms the outer surface of the plates and, in *Paracentrotus*, this layer is overlain by a thin veneer of dense labyrinthic stereom (Pl. 15, fig. 2). Tubercles have a central core of dense or compact labyrinthic stereom which tends towards a radially arranged fascicular stereom. This becomes exceedingly compact towards the surface of the mamelon. Around this core, galleried stereom with vertical alignment forms the boss. *Echinometra* shows no stereom growth banding in its plates though vague banding was observed in the stereom of the tubercles. Stereom banding is much more obvious in plates of *Paracentrotus*.

Stomopneustes and Arbacia. Plates of *Stomopneustes variolaris* and *Arbacia lixula* are very similar in structure to those of *Echinometra*. They differ in having a much thicker and more compact inner plate stereom (text-fig. 3). In both species labyrinthic stereom is found only towards the centre of each plate (Pl. 9, figs. 1, 2). Marginally, labyrinthic stereom gives way to thick layers of perforate stereom (Pl. 9, figs. 3, 4), which thin rapidly towards the plate edge. In *Arbacia*, the galleried stereom of the plate is overlain by a well-developed perforate stereom layer, but in *Stomopneustes* no such compact layer is found. Instead, the galleried stereom of the plate is overlain by a thick layer of dense labyrinthic stereom which becomes more open towards the surface. Tubercle construction is similar to that in *Echinometra* and no stereom growth banding was observed in either species.

Psammechinus. The plates of *Psammechinus miliaris* have a middle galleried stereom region and an inner labyrinthic stereom region, both of which show stereom microstructural banding (text-fig. 3). The inner labyrinthic stereom region, which is best developed towards the centre of the plate, shows alternating layers of open labyrinthic stereom and simple perforate stereom (Pl. 12, figs. 4, 7). The first formed and most central stereom is labyrinthic. Towards the inner plate surface, the bands of labyrinthic stereom become narrower and more or less disappear, so that the inner surface is composed of perforate stereom. A thick layer of irregular perforate stereom overlies the galleried stereom of the plate (Pl. 13, figs. 5–7) and this, in turn, is overlain by the tubercles. Tubercle construction is similar to that described in *Echinometra*. The central, compact, fascicular stereom is radially arranged towards the mamelon surface. Both *Echinus esculentus* (Pl. 10, figs. 4, 5) and *Temnopleurus hardwickii* (Pl. 10, figs. 1–3) have a rather similar plate construction to *Psammechinus*. In these species the inner region of the plates show stereom microstructural banding but, unlike *Psammechinus*, perforate stereom layers are not developed. Stereom banding is produced by variation in

the density of the labyrinthic stereom. The stereom of the outer surface of the plates of *Temnopleurus* is less dense and considerably thinner than the same stereom in *Psammechinus* (Pl. 9, fig. 5; Pl. 10, fig. 3). This layer may even be lacking altogether in ambulacral plates and around the periphery of interambulacral plates.

Colobocentrotus. *Colobocentrotus atratus* possesses very thick plates which are composed of rather dense stereom. The inner plate layer is composed of a medium, dense, labyrinthic stereom which has in parts a zig-zag trabecular arrangement (Pl. 10, fig. 6). This is separated from the middle plate layer of galleried stereom by a broad band of fine, dense, labyrinthic stereom (Pl. 10, fig. 7). A similar broad layer overlies the galleried stereom layer of the plate (text-fig. 3; Pl. 10, fig. 8). The outer layer of the plate is formed of vertically orientated, galleried stereom and this is developed outwards to form the boss. No stereom microstructural banding was observed in the specimen available but Deutler (1925) records the presence of growth lines in this genus.

Holectypoids

Plates of *Echinoneus cyclostomus* have a small central area of open labyrinthic stereom which changes laterally into a region composed predominantly of galleried stereom (text-fig. 4). This region thickens marginally and the stereom galleries parallel the outer surface of the plate. Narrow bands of labyrinthic stereom alternate with broader areas of galleried stereom. The inner plate layer, which is thickest at the centre of the plate, is composed of a dense labyrinthic stereom. A layer of simple perforate stereom forms the inner surface of the plate away from the centre. Above the galleried stereom of the plate, a well-developed irregular perforate stereom layer is found (Pl. 11, figs. 1–3). Marginally, this layer lies near the surface but it becomes deeply sunken towards the centre of the plate. Tubercle stereom originates from this layer, each tubercle having a central core of labyrinthic stereom, which gives rise to the mamelon, and a surrounding area of galleried stereom, producing the boss (Pl. 11, fig. 3). Between tubercles there occur 'glassy granules' and these are produced by the upward growth and consolidation of the underlying perforate layer. These are composed almost entirely of imperforate stereom (Pl. 11, fig. 2). Between the tubercles and 'glassy granules' a more open labyrinthic stereom is found (Pl. 11, fig. 4).

Cassiduloids

A similar plate construction is found in *Echinolampas crassa* and *Apatopygus recens*. The inner region of the thick plates of *Echinolampas* is composed of microperforate stereom orientated with the stereom layering paralleling the inner plate surface (Pl. 3, fig. 1). With the exception of a large region of dense labyrinthic stereom at the centre of the plate, the middle layer of the plate is composed of dense galleried stereom (text-fig. 4). An irregular perforate stereom layer is present above the galleried stereom and this, in turn, is overlain by tubercles and inter-tubercle ridges in much the same way as in *Echinoneus*. Fascicular stereom from the perforate stereom layer forms a core to

---

EXPLANATION OF PLATE 5

Figs. 1–3. *Brissopsis lyrifera*. 1, stereo view of a retiform stereom layer forming the areole of an aboral interambulacral tubercle of *Brissopsis lyrifera*. 2, stereo view of a retiform stereom layer forming the areole of an aboral interambulacral tubercle, seen in cross-section. The outer perforate plate layer is easily seen. 3, stereo view—enlargement of Fig. 2.

Fig. 4. Retiform stereom layer forming the areole of an ambital ambulacral tubercle of *Echinocardium cordatum* showing a linear arrangement of pores.

Fig. 5. Retiform stereom layer seen in a cross-section of an oral interambulacral plate of *Phormosoma placenta*.

Scale bar in Figs. 1, 3, 4 = 40 μm; Figs. 2, 5 = 100 μm.

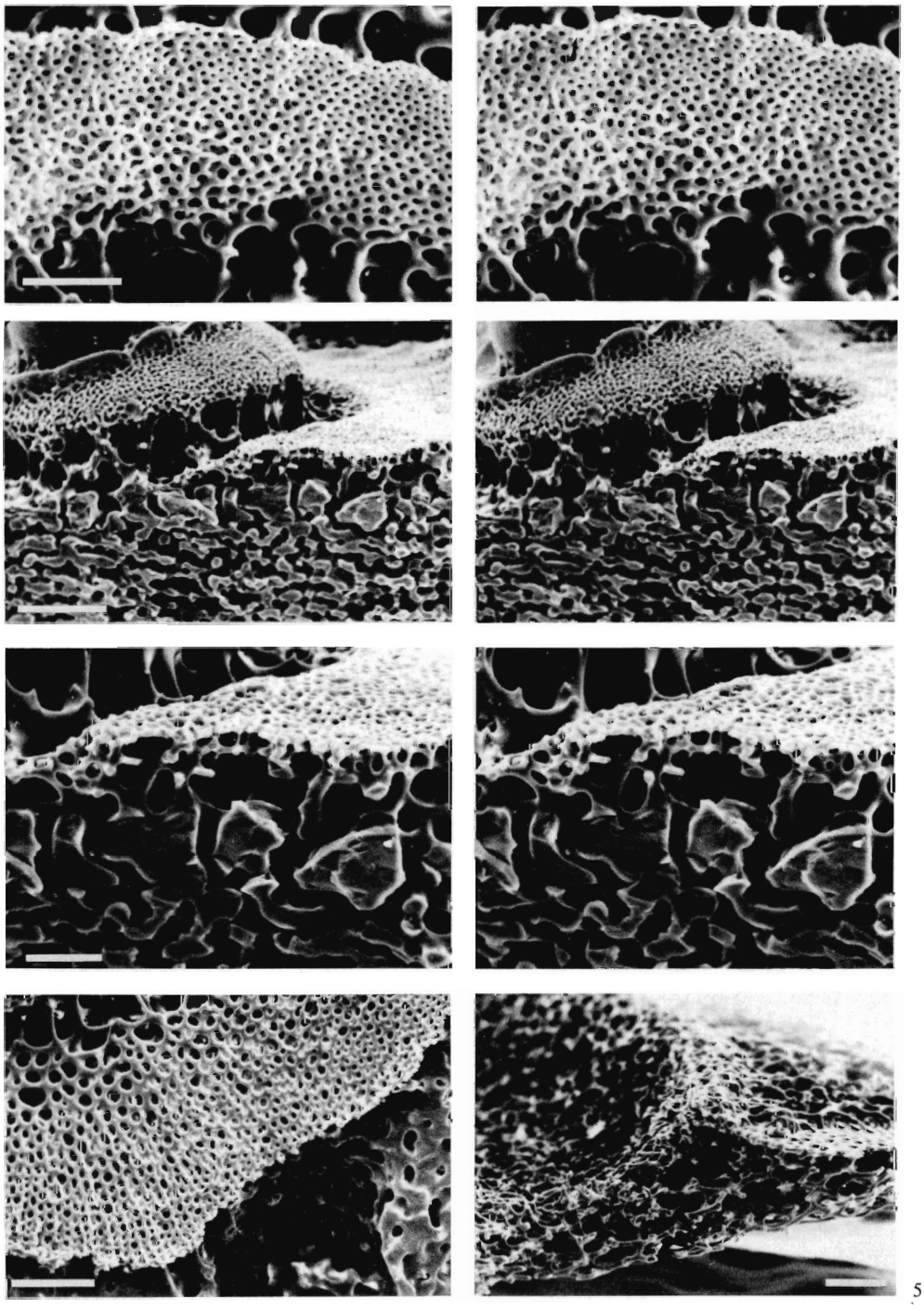

1

2

3

4

5

SMITH, retiform stereom

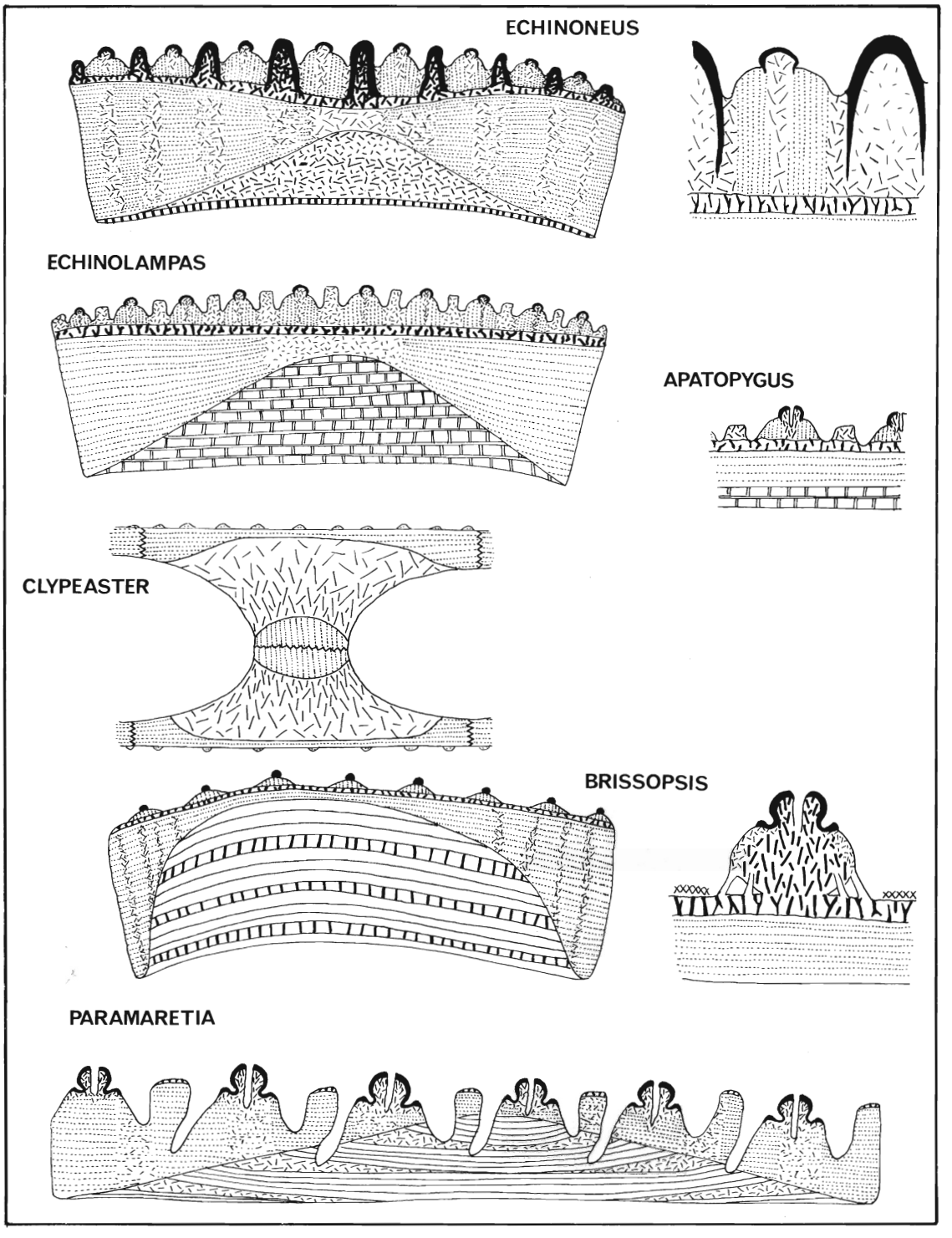

TEXT-FIG. 4. Schematic cross-sectional plans of interambulacral plates showing the distribution of stereom fabrics. Hatching as in text-fig. 2.

each tubercle and consolidates outwards to produce the imperforate cap of the mamelon. Surrounding this, galleried stereom with vertical alignment forms the boss. Ridges between tubercles are formed of a dense labyrinthic stereom which may consolidate to give a superficial compact layer of perforate stereom to granules. *Apatopygus* has very much thinner plates than *Echinolampas* and, in consequence, the inner, microperforate stereom is only a few lamellae thick although it extends over a broad area. In the galleried stereom of the plates of *Apatopygus* there is a tendency towards a rectilinear arrangement in places. No stereom microstructural banding was observed in either species.

Clypeasteroids

All three species of clypeasteroids examined have the same basic plate construction and the simplest arrangement is found in *Clypeaster rarispina*. The plates of *Clypeaster* have a thin outer layer of galleried stereom which thickens peripherally (Pl. 11, figs. 5, 7). The galleries of this stereom parallel the plate surface. This stereom is overlain by a thin veneer of open labyrinthic stereom. Underlying the galleried stereom is an expansive region of labyrinthic stereom which forms the bulk of the plate (text-fig. 4; Pl. 11, fig. 5). Where pillars are developed this labyrinthic stereom gives rise to fascicular stereom which runs up the length of the pillars (Pl. 11, figs. 6, 7). This stereom becomes progressively finer, towards the end of the pillar, and is replaced by galleried stereom with vertical alignment. This is well displayed in sections through fused pillars (Pl. 11, fig. 8). No compact stereom layers are developed in *Clypeaster*. In *Mellita quinquiesperforata* and *Encope michelini* the plate construction, although basically the same as in *Clypeaster*, is complicated by the extensive development of pillars and canals (Pl. 11, fig. 9). These species do, however, possess a thin, outer, compact layer from which large thorns are derived (Pl. 11, fig. 10). This layer is best developed on aboral surfaces and open labyrinthic stereom forms much of the outer surface of oral plates. The tubercles of these clypeasteroids are similar in construction to spatangoid tubercles.

Spatangoids

Brissopsis and Echinocardium. A large part of the plates of *Brissopsis lyrifera* and *Echinocardium cordatum* is composed of laminar stereom, which makes up the inner region of the plate (text-fig. 4). The plates of *Brissopsis* are considerably thicker than plates of *Echinocardium* and the laminar stereom more dense. In *Brissopsis*, slightly thicker layers of perforate stereom are developed periodically in some specimens giving a stereom microstructural banding to this region. The laminar stereom is overlain by a thin development of galleried stereom which thickens dramatically near the plate margin (Pl. 14, fig. 2). Above the galleried stereom, a thin, dense, perforate stereom layer forms the external surface of the plate. From this layer large struts extend outwards to form the core of the tubercles (Pl. 5, figs. 3, 4). Consolidation of this fascicular stereom produces the mamelon and a fine labyrinthic stereom forms a superficial layer to the boss (Pl. 14, fig. 1). The areole, surrounding each tubercle, is composed of a layer of retiform stereom supported above the perforate stereom layer by trabecular struts (Pl. 14, figs. 5, 6). Stereom banding is found in both species. *Eupatagus hastingiae* is very similar in plate construction to *Brissopsis*, except that the lower layer is composed entirely of laminar stereom (Pl. 2, fig. 6) and no stereom banding is found.

Paramaretia. *Paramaretia peloria* has deeply sunken primary tubercles over its aboral interambulacral plates, and the plate construction is very different from that of *Brissopsis*. The inner part of these plates gradually thins away from the centre and is composed of a laminar stereom with wedges of labyrinthic stereom (Pl. 13, fig. 8; Pl. 14, fig. 3). The middle layer of each plate is composed largely of open galleried stereom with narrow bands of labyrinthic stereom. Overlying this, and forming the outer surface of the plates, is a thin, planar layer of open stereom. The large primary tubercles appear to be formed by resorption of the plate as the stereom forming the tubercles is continuous with the stereom of the plate (text-fig. 4; Pl. 14, fig. 3). The only modification of the tubercle stereom occurs in the vicinity of the mamelon where an imperforate layer caps the outer surface and an irregular stereom occurs immediately beneath (Pl. 8, fig. 5). Secondary tubercles lie on top of the thin perforate stereom layer and are similar to other spatongoid tubercles.

GROWTH LINES

Although Jackson (1912) stated that 'sectioning a sea urchin plate we find no trace of its earlier shape or character within', growth banding in echinoid plates had been reported over 130 years ago (McClelland, 1841). However, it was not until the meticulous work of Deutler (1926), in which growth lines were shown to be present in a large number of echinoids, that their importance was fully realized. Working on the growth lines of *Echinus esculentus*, he not only demonstrated the changes that occur in plate shape during growth but also identified the presence of plate resorption around the peristome. This has recently been questioned by Markel (1975, 1976). Since then growth-line studies have been carried out on a number of Recent echinoids (Kume, 1929; Moore, 1935; Durham, 1955; Birkland and Chia, 1971; Kawamura, 1966, 1973; Jensen, 1969*a*, *b*; Dix, 1972; Taki, 1972*a*, *b*; Sumich and McCauley, 1973; Pearse and Pearse, 1975; Markel, 1975; Crapp and Willis, 1975; Allain, 1978) while Raup (1968) has taken a more theoretical approach to plate growth using computer models. Growth has been shown to take place both by the addition of new plates at the apex and by peripheral growth of those plates already formed (Deutler, 1926; Swan, 1966; Moss and Meehan, 1968; Markel, 1975, 1976). Both of these processes may continue throughout the animal's life (Swan, 1966; Kier, 1974) or plate growth may come to dominate in later life (Hsia, 1948; Durham, 1955). Growth-line studies (Deutler, 1926) and tetracycline labelling experiments (Kobayashi and Taki, 1969; Markel, 1975, 1976) have shown that plate growth occurs in different directions at different rates and that greatest plate growth proceeds along the lateral plate margins. Inward plate thickening is also important, especially in newly formed plates.

Pearse and Pearse (1975) have recently reviewed the state of knowledge about growth lines. They suggest that growth lines are the product of periodic variation in the stereom construction of the plate and report that the stereom of opaque zones has relatively smaller pores, larger trabeculae and a greater degree of alignment than the stereom of translucent zones. In order to verify their findings, interambulacral plates of *Psammechinus miliaris* and *Echinus esculentus* were treated to display growth lines, sectioned and photographed before being examined under an S.E.M. Perfect correlation was found between the stereom microstructure and the growth banding (Pl. 12, figs. 3–7). Growth lines are present in all layers of the plate as well as in the tubercles. In the middle plate layer, broad opaque zones are composed of galleried stereom and the sharp junction between an inner opaque zone and an outer translucent zone coincides with a discontinuity of the galleried stereom (Pl. 13, figs. 2–4). This stereom disruption is produced by a narrow zone of irregular labyrinthic stereom. The stereom of the translucent zone, which follows outwards from the discontinuity, is a rather irregular galleried stereom that has relatively thinner trabeculae and slightly larger pores than galleried stereom of the opaque zone (Pl. 13, fig. 4). The change from a translucent zone outwards to an opaque zone is usually gradual (Pl. 12, fig. 2). Each sharp translucent line coincides with a thin

---

EXPLANATION OF PLATE 6

Fig. 1. An aboral interambulacral plate of *Eucidaris metularia*. Rectilinear stereom forms all the plate surface outside the boss of the primary tubercle.

Figs. 2, 3, 5, 6. *Cidaris cidaris*. 2, sectioned interambulacral plate showing change in stereom orientation in the outer plate layer. Plate margin to the right. 3, sectioned interambulacral plate of *Cidaris cidaris*. 5, sectioned aboral interambulacral plate. Galleried stereom of the outer plate layer occurs in the top left and labyrinthic stereom of the inner plate layer in the bottom right of the micrograph. 6, rectilinear stereom forming the areole of a primary interambulacral tubercle.

Fig. 4. Sectioned tubercle of an aboral interambulacral plate of *Poriocidaris purpurata* showing the mamelon construction.

Fig. 7. Stereo view of the lateral face of an ambital ambulacral plate of *Centrostephanus longispinus*. A laminar arrangement is developed towards the centre of the outer plate layer. Outer surface to the bottom right.

Scale bar in Fig. 7 = 40 μm; Figs. 5, 6 = 100 μm; Figs. 1–4 = 400 μm.

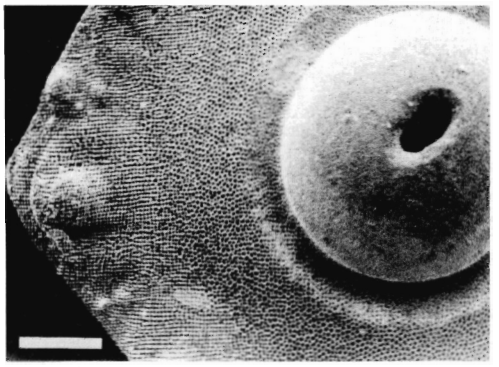

1

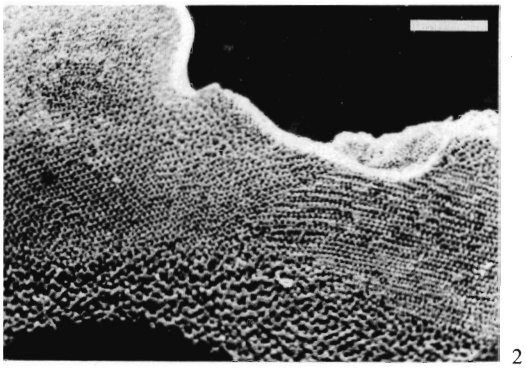

2

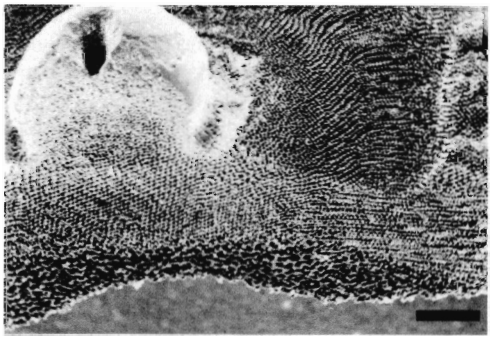

3

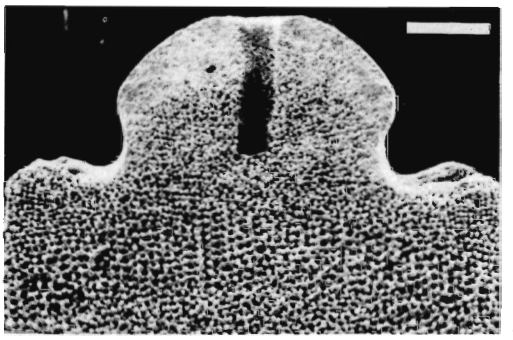

4

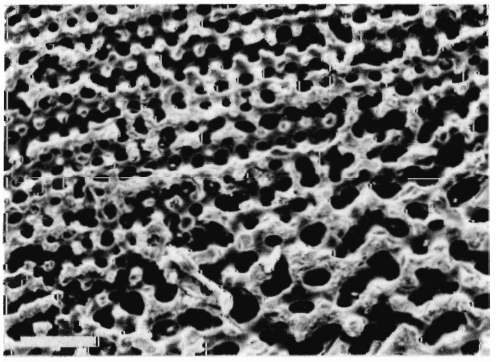

5

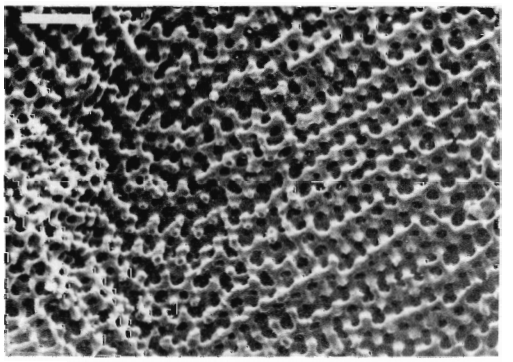

6

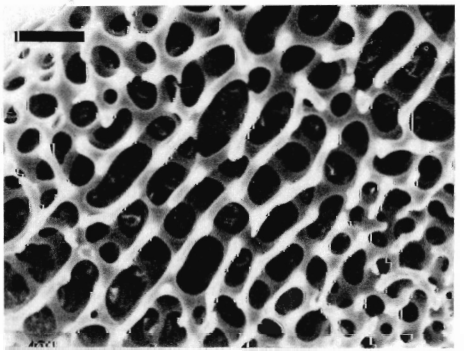

7

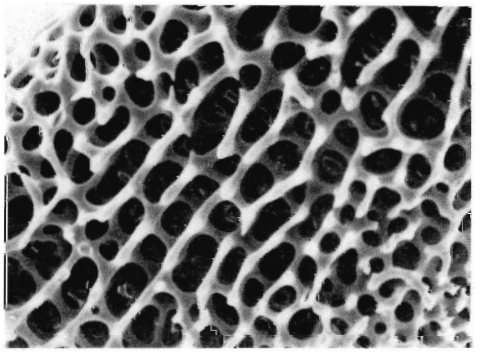

SMITH, plate construction

zone of stereom disruption and there may be a number of sharp lines in one broad translucent band (Pl. 13, fig. 1).

In the inner plate stereom, opaque zones correspond with dense perforate stereom layers whilst translucent zones are formed of a more open labyrinthic stereom (Pl. 12, figs. 3, 4, 7, 8). Towards the inner surface of the plate, individual perforate stereom layers become less distinct and tend to merge to form an irregular perforate stereom (Pl. 12, figs. 3, 4) though they can still be distinguished as opaque and translucent zones. Each growth band in the middle layer of the plate has a corresponding growth band in the inner layer. The opaque zone of galleried stereom is associated with the opaque zone of perforate stereom whilst the translucent zones of labyrinthic stereom coincide. In tubercles of *Psammechinus*, growth banding of opaque and translucent zones is also found. Here galleried stereom of the boss forms the translucent zones and opaque zones are found where there is discontinuity in alignment and dense irregular stereom is deposited. Some of the galleried stereom with relatively thicker trabeculae may also form part of this opaque zone.

Periodic variation in stereom microstructure was observed in a number of other echinoids. In *Tripneustes* broad zones of open labyrinthic stereom are developed towards the centre of the middle plate layer and these alternate with zones of open galleried stereom. Galleried stereom is more or less continuous along the inner and outer parts of this layer (text-fig. 3). The tubercles of *Tripneustes* also have broad bands of labyrinthic stereom which alternate with thin zones of galleried stereom (Pl. 7, fig. 4). It therefore appears that, although growth banding is the result of periodic stereom microstructural variation, opaque and translucent zones cannot be correlated with particular stereom arrays. The major difference between these zones appears to be one of porosity, opaque zones having a denser stereom than translucent zones. Although most workers are agreed that growth lines are laid down annually, opinions on just when or why these bands form are confused and contradictory, largely because of the different methods used for displaying growth lines. This has resulted in a great deal of uncertainty about the usage of the terms *light*, *dark*, *pigmented*, and *non-pigmented* which have been applied to growth lines (Pearse and Pearse, 1975). By applying the methods of Moore (1935), Jensen (1969*a*), and Dix (1972) to specimens of *Echinus* and *Psammechinus* it has been possible to ascertain that the pigment zones of Jensen (1969*b*) are translucent zones, whereas the pigment zones of Moore (1935) and Dix (1972) correspond to the outer part of the opaque zones of the plate. These latter pigment zones are found only in the outer dense stereom which overlies the galleried stereom layer of the plate. They are true pigment zones, formed by the incorporation of spinochromes into the calcite of the trabeculae (Pearse and Pearse, 1975) and are often sharply defined, especially at their outer, marginal edge. When the stereom of this layer is examined in cross-section, marginally overstepping layers of alternating trabecular density can be distinguished (Pl. 13,

---

EXPLANATION OF PLATE 7

Figs. 1, 5–7, *Sphaerechinus granularis*. 1, ambital interambulacral plate section showing junction between the inner labyrinthic stereom layer and the outer galleried stereom layer. 5, ambital interambulacral plate section showing the construction of a major tubercle. 6, same plate seen towards margin showing a well-developed perforate stereom layer at the outer plate surface. 7, ambital interambulacral primary tubercle of *Sphaerechinus granularis* in cross-section.

Figs. 2–4. *Tripneustes gratilla*. 2, ambital interambulacral plate section showing the outer compact layer overlying the middle layer of galleried stereom towards the plate periphery. 3, lateral suture face of ambital interambulacral plate. Galleried stereom is developed near the outer surface (top of photograph) whereas labyrinthic stereom predominates centrally. 4, section of boss of primary interambulacral tubercle of *Tripneustes gratilla* showing alternating bands of galleried and labyrinthic stereom. Outer surface towards the top.

Fig. 8. Ambital interambulacral plate of *Paracentrotus lividus*. Inner plate surface showing the development of a marginal rim of very dense irregular stereom to the left-hand side of the photograph.

Scale bar in Figs. 2 and 4 = 40 μm; Figs. 1 and 3 = 100μm; Figs. 5–7 = 200 μm; Fig. 8 = 400 μm.

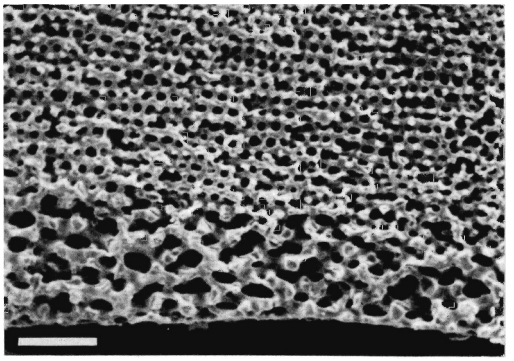

1

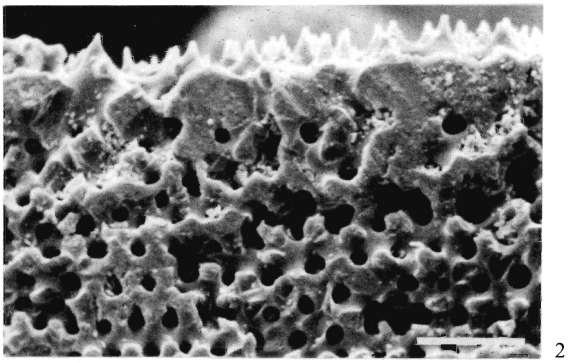

2

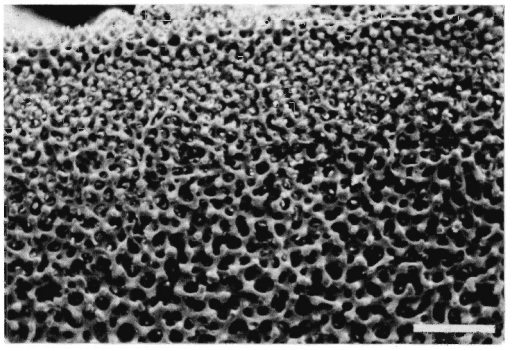

3

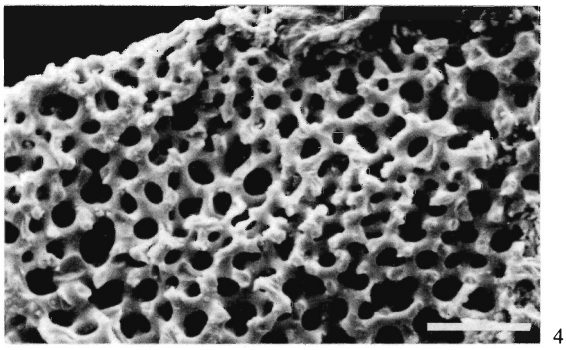

4

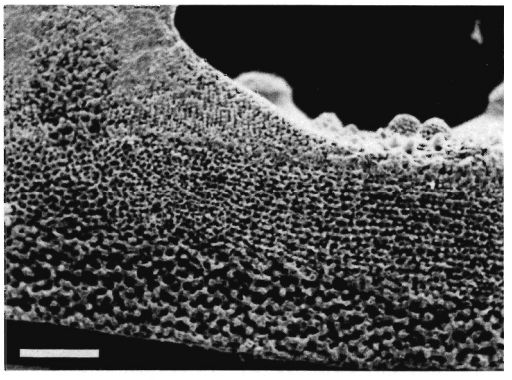

5

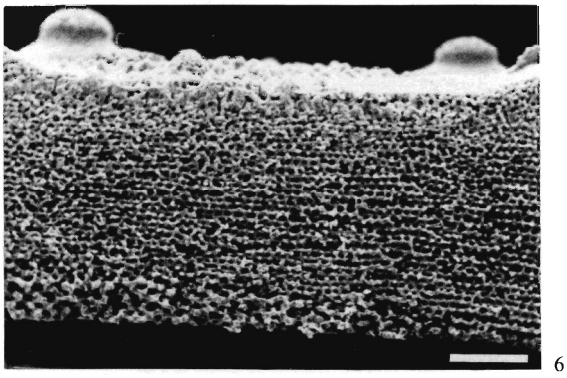

6

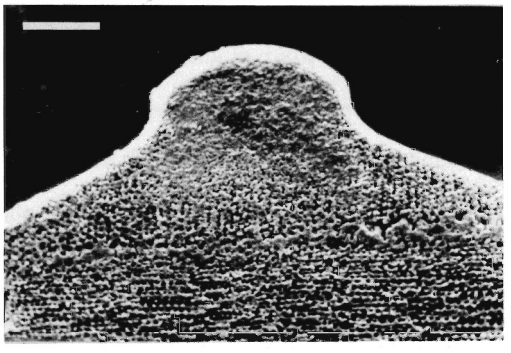

7

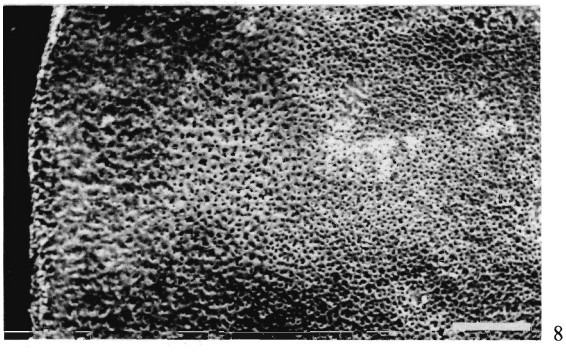

8

SMITH, plate construction

figs. 5–7). Each compact stereom layer commonly accompanies a stereom discontinuity in the underlying galleried stereom (text-fig. 5). Each is overstepped marginally by a dense labyrinthic stereom which gives way outwards to another horizon of compact stereom. Tongues of compact stereom impinge a little deeper into the underlying layer than the intervening dense stereom (Pl. 13, figs. 5–7) giving the pigment zone its characteristic sawtooth base line (see Moore, 1935; Kawamura, 1966).

Seasonal growth. Test growth is known to be seasonal in many echinoids. Some more or less cease growth during part of the year (Moore, 1935, 1937; Moore *et al.*, 1963*b*; McPherson, 1965; Hines and Kenny, 1967; Jensen, 1969*b*; Crapp and Willis, 1975) and may even show negative growth rates (Ebert, 1967, 1968), while others just undergo a seasonal decrease in growth rate (Lewis, 1958; Moore, 1936*a*; Fuji, 1967; Kobayashi and Taki, 1969; Ferber and Lawrence, 1976). This growth hiatus has been attributed to seasonal gonadal development (Lewis, 1959; Fuji, 1967; Jensen, 1969*b*;

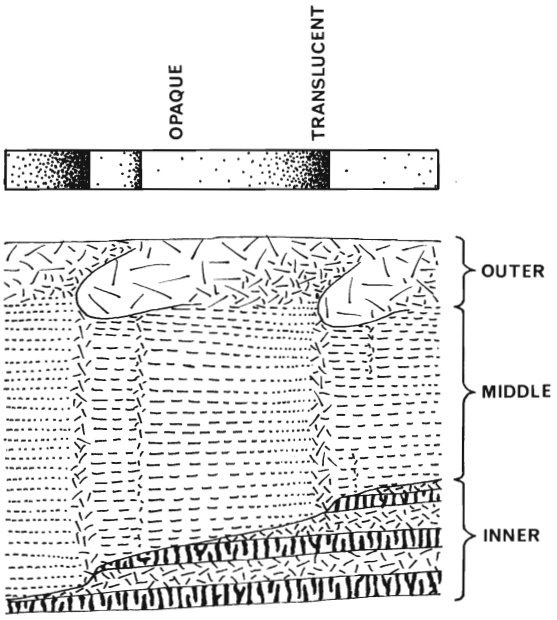

TEXT-FIG. 5. Diagrammatic cross-section of an interambulacral plate of *Psammechinus miliaris* illustrating the stereom banding in the different plate layers and their relationship to translucent and opaque zones. Growth from right to left. Hatching as in text-fig. 2 except that galleried stereom is indicated by dashed, as well as dotted lines. Galleried stereom with large pores and thin trabeculae (dotted lines) changes outwards into a denser stereom with smaller pores (dashed lines).

EXPLANATION OF PLATE 8

Fig. 1. Aboral interambulacral plate section of *Echinus esculentus* showing galleried stereom of the middle plate layer overlain by an outer dense perforate stereom layer.

Figs. 2, 3. *Sphaerechinus granularis*. 2, Ambital interambulacral primary tubercle in cross-section. 3, domed perforate stereom, covered by integument in life, forming the outer plate surface of aboral interambulacral plates.

Fig. 4. Perforate stereom layer. Inner surface of an aboral interambulacral plate of *Tripneustes gratilla* towards the plate margin.

Fig. 5. Cross-section of the parapet of a primary aboral (interambulacral) tubercle of *Paramaretia peloria* showing imperforate stereom.

Fig. 6. Cross-section through an ambital interambulacral plate of *Centrostephanus longispinus* towards the plate margin. Galleried stereom changes in orientation near the outer plate surface.

Figs. 7, 8. *Tripneustes gratilla*. 7, cross-section of an ambital interambulacral plate of *Tripneustes gratilla*. The perforate stereom layer of the internal plate surface lies beneath labyrinthic stereom of the inner plate layer. 8, same plate showing galleried and labyrinthic stereom of the middle plate layer in the top right corner, the coarser labyrinthic stereom forms part of the middle plate layer. Inner surface to the bottom.

Scale bar in Figs. 4, 6, 7 = 40 μm; Figs. 1–3, 5, 8 = 100 μm.

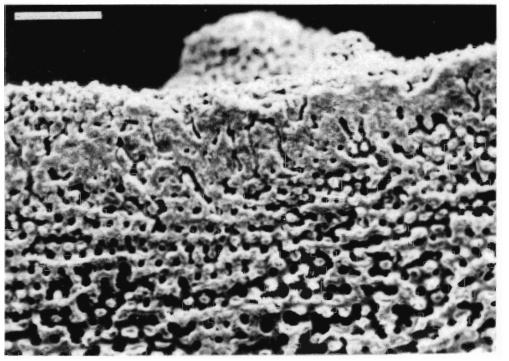

1

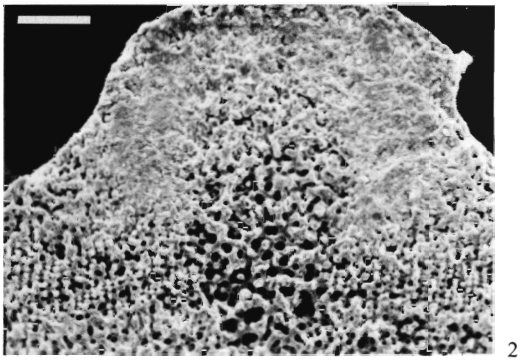

2

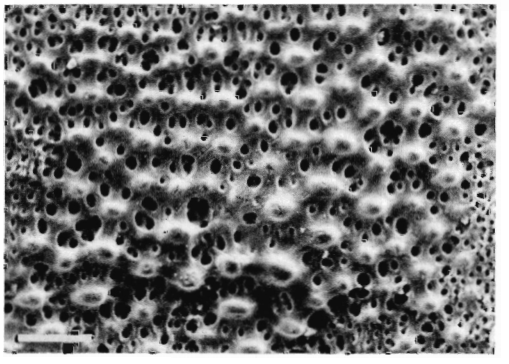

3

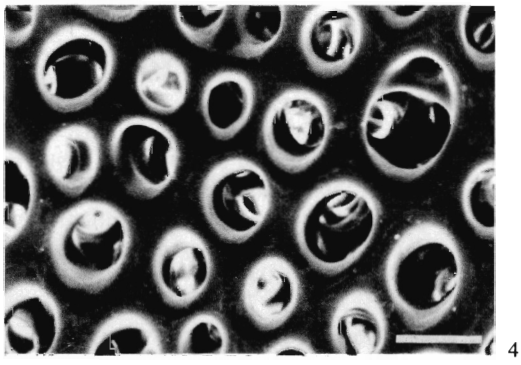

4

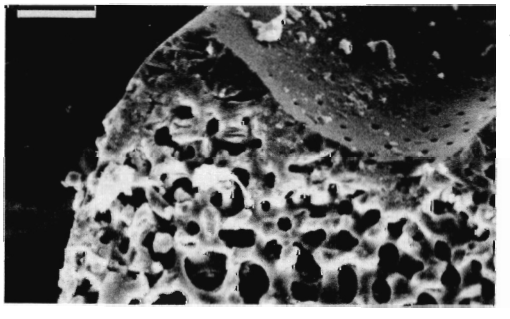

5

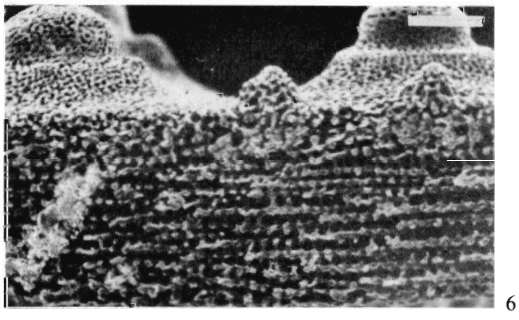

6

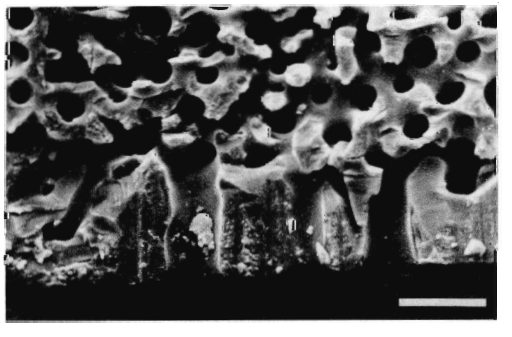

7

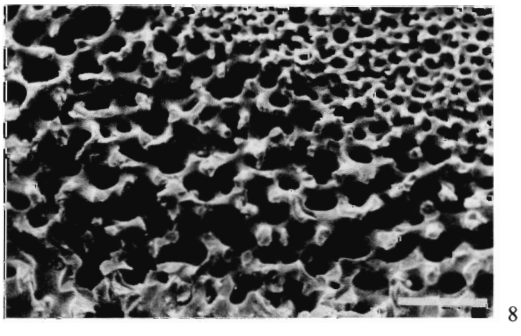

8

SMITH, plate construction

Sumich and McCauley, 1973), to variation in food availability and suitability (Ebert, 1968; Pearse and Pearse, 1975; Vadas, 1977) and to annual variation in temperature (Moore *et al.*, 1963*a*, *b*, 1965; McPherson, 1965). Dix (1972) found no fluctuation in the growth rate of *Evechinus chloroticus* over a six-month period covering the largest seasonal change in temperature.

Although the majority of echinoids examined display growth lines there are a number which do not. *Centrostephanus*, *Calveriosoma*, and *Phormosoma* show no evidence of stereom banding whatsoever while *Cidaris* and *Poriocidaris* have stereom banding only in their tubercles. In addition *Stomopneustes variolaris*, *Salmacis bicolor*, *Echinometra mathaei*, *Toxopneustes pileolus*, *Echinolampas crassa*, and *Apatopygus recens* show no clear evidence of either pigment banding (Deutler, 1926) or stereom banding. Many workers have noted that growth rate decreases, or even ceases, during gonad development and Jensen (1969*b*) and Dix (1972) have correlated growth banding with the stage of gonad development. Information available on *Strongylocentrotus* (Boolootian, 1966; Pearse and Pearse, 1975; Kawamura, 1973; Fuji, 1967; Taki, 1972*b*) and *Echinus* (Moore, 1935, 1936*b*) also shows some correlation. Sumich and McCauley (1973) have reported a half-yearly growth zone banding in *Allocentrotus fragilis* which they correlate with the biannual gonad development and spawning. However, Crapp and Willis (1975) found that pigmented stereom was deposited annually in *Paracentrotus lividus* whereas spawning was biannual. Similar growth data are not available for the echinoids which do not display growth banding but it is interesting to note that *Salmacis bicolor* and *Stomopneustes variolaris* have been reported to display continuous reproduction (Boolootian, 1966; Giese *et al.*, 1964) and that *Echinometra mathaei* has been shown to have continuous reproduction throughout much of its geographical range (Pearse, 1968, 1969; Pearse and Phillips, 1968). *Centrostephanus coronatus* is also reported to show a monthly reproductive rhythm throughout much of the year (Pearse, 1972).

Growth rates. The rate of plate growth and the stereom fabric appear to be linked. Pearse and Pearse (1975) found that urchins which were fed and which showed fast growth rates produced aligned stereom (galleried stereom) in the middle plate layer whereas urchins which were starved and which showed slow growth rates produced irregular (labyrinthic) stereom. Heatfield (1971), on the other hand, reports that fast growth is associated with an open meshwork stereom and that consolidation of the stereom to produce dense or compact stereom layers takes place when stereom growth slows. Raup (1966) also reports that faster growing stereom is more open than slower growing stereom. Jensen (1969*a*, *b*) states that narrow 'pigment' (translucent) zones are deposited in spring and early summer during periods of minimal growth and that broad 'unpigmented' (opaque) zones are formed in fall and winter during rapid test growth. Taki (1972*b*) also found that 'unpigmented' (translucent) bands were deposited during periods of minimal growth. Pigmented stereom was found to be laid down in the outer plate layer of *Echinus* during periods of minimal growth (Moore, 1935, 1936*b*)

EXPLANATION OF PLATE 9

Figs. 1–3, 5. *Stomopneustes variolaris*. 1, ambital interambulacral plate in cross-section. 2, enlargement of Fig. 1 showing the central region of the inner, labyrinthic stereom layer. 3, enlargement of Fig. 1 showing the marginal region of the inner plate layer. 5, enlargement of Fig. 1 showing the labyrinthic outer plate layer overlying galleried stereom of the middle plate layer.

Fig. 4. The inner plate layer of an ambital interambulacral plate of *Arbacia lixula* seen in cross-section showing the very dense construction.

Figs. 6–8. *Echinometra mathaei*. 6, ambital interambulacral plate in cross-section. 7, enlargement of Fig. 6 showing the construction of the centre of the plate. 8, enlargement of Fig. 6 showing the inner plate layer. A dense stereom is developed between the upper galleried stereom of the middle plate layer and the lower labyrinthic stereom of the inner plate layer.

Scale bar in Figs. 3–5 and 8 = 100 μm; Figs. 2 and 7 = 200 μm; Figs. 1 and 6 = 400 μm.

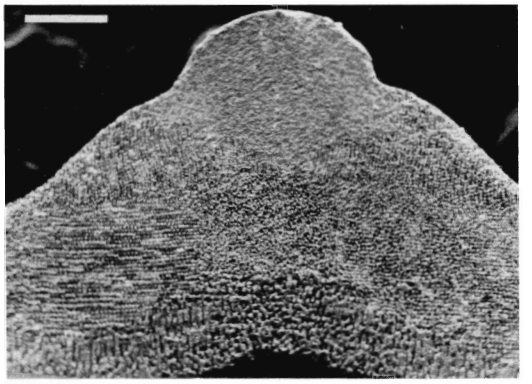

1

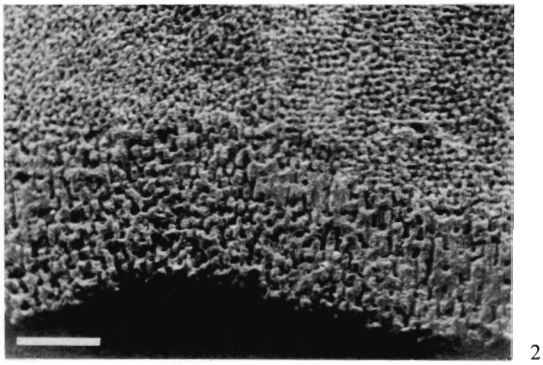

2

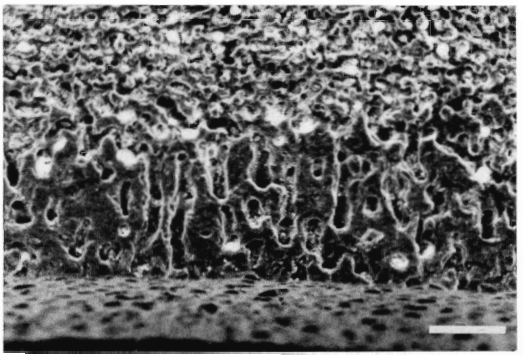

3

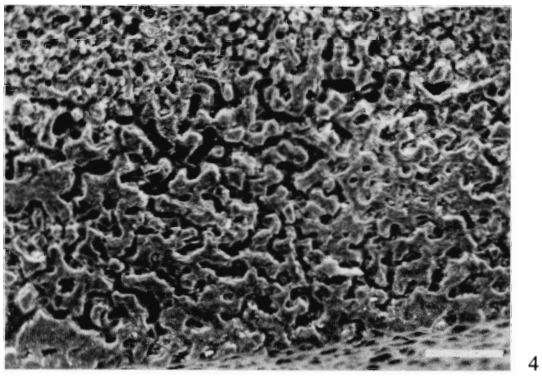

4

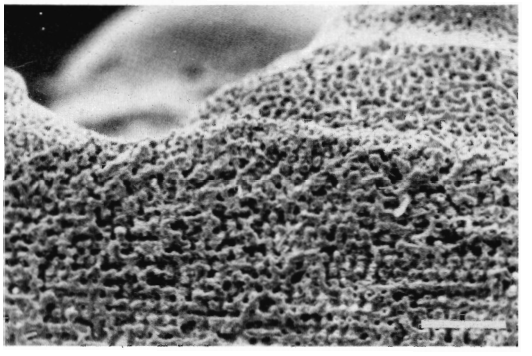

5

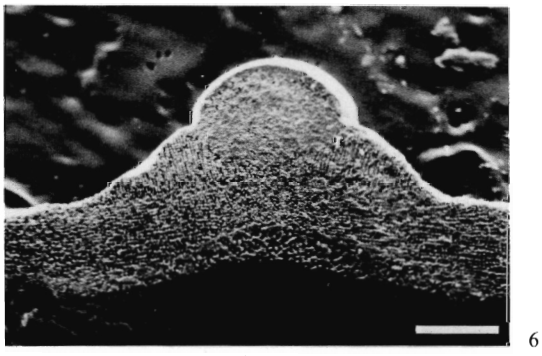

6

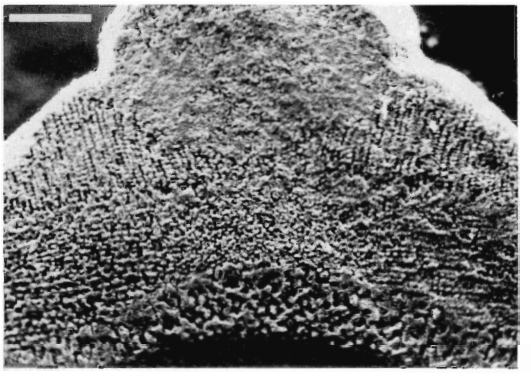

7

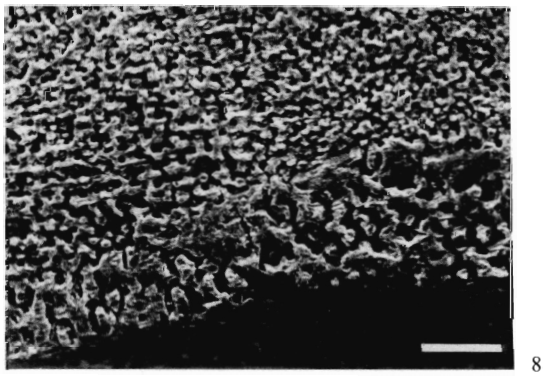

8

SMITH, plate construction

but pigmented stereom was found to be deposited during periods of rapid growth in *Paracentrotus* (Crapp and Willis, 1975). This suggests that the deposition of spinochromes may by controlled by seasonal factors and is independent of growth rate.

Stereom discontinuities in the middle plate layer of *Psammechinus* seem to be produced during periods of growth cessation. The galleried stereom, deposited between one major discontinuity and the next, is formed during a period of continuous growth. Multiple discontinuities, associated with one translucent band, may be produced by fluctuations in the growth rate, either towards the end of the growth period or during growth cessation when conditions have become favourable for short periods. Markel (1975), using tetracycline labelling, found that aquarium urchins, kept under uniform conditions, deposited a number of alternating growth bands within a period of five months. Pearse and Pearse (1975) clearly demonstrated that growth banding could be induced by alternately feeding and starving aquarium urchins. Variation in the porosity of the galleried stereom between two discontinuities may be due to a change in the rate of calcite production and availability or to a change in the growth rate. As growth in *Psammechinus* is initially rapid and slows down later in the season (Jensen, 1969*b*) it appears that a faster growth rate is associated with a more open galleried stereom and that denser galleried stereom is deposited as the growth rate slows.

Gross variation in the stereom fabric can therefore be related to the growth rate of the plate. Galleried stereom is always associated with collagenous fibres which penetrate into the test along the galleries to a depth of between 25 μm and 100 μm. These fibres are never found to extend to any great depth within each plate (Foucart, 1966; personal observation) and must die off internally as growth proceeds. During periods of continuous growth these fibres restrict trabecular growth so as to maintain pore alignment. During periods of little or no growth these fibres may change structurally or become reorganized so that, when the next bout of growth is initiated, sutural fibres have become misaligned with previous growth. Kobayashi and Taki (1969) report a marked seasonal change in the sutural collagen fibres related to a change in the growth rate. In *Tripneustes* open labyrinthic stereom is deposited over much of the middle plate layer following each discontinuity. If this is associated with a bout of rapid growth the change in stereom construction is most likely to be caused by a reduction or loss of all but the inner and outermost collagen fibres at the start of each growth period. This would give a weaker bond between plates easing the rapid expansion of the stereom. With a slowing of plate growth, collagen fibres may be reinstated centrally.

Growth of the inner layer in plates of *Psammechinus* is relatively straightforward. Periods of rapid peripheral plate growth also increase the plate thickness at the margins. In order to maintain a uniform plate thickness, stereom must be deposited on the inner surface towards the centre of the plate. When plate thickness increases rapidly during the early stages of a bout of plate growth, open labyrinthic stereom is deposited on the inner surface, but when plate growth slows or ceases, consolidation of the inner layer of stereom takes place producing a compact, perforate stereom layer.

EXPLANATION OF PLATE 10

Figs. 1–3. *Temnopleurus hardwickii*. 1, aboral interambulacral plate showing stereom banding. 2, enlargement of Fig. 1 showing variation in galleried stereom in middle plate layer. The inner plate layer of labyrinthic stereom can be seen to the bottom left. 3, enlargement of Fig. 1 showing the thin layer of labyrinthic stereom forming the outer plate layer and overlying galleried stereom of the middle plate layer.

Figs. 4, 5. *Echinus esculentus*. 4, aboral interambulacral plate. 5, enlargement of Fig. 4 showing a section of the mamelon of the primary tubercle of *Echinus esculentus*.

Figs. 6–8. *Colobocentrotus atratus*. 6, aboral interambulacral plate section showing the zig-zag arrangement of labyrinthic stereom in the inner plate layer. 7, same plate showing inner plate layer of labyrinthic stereom separated from the middle plate layer of galleried stereom by a broad band of finer labyrinthic stereom. 8, same plate showing the upper galleried stereom of the boss separated from the lower galleried stereom of the middle plate layer by a broad band of finer labyrinthic stereom.

Scale bar in Fig. 6 = 40 μm; Figs. 2, 3, 5, and 8 = 100 μm; Fig. 7 = 200 μm; Fig. 1 = 400 μm; Fig. 4 = 1 mm.

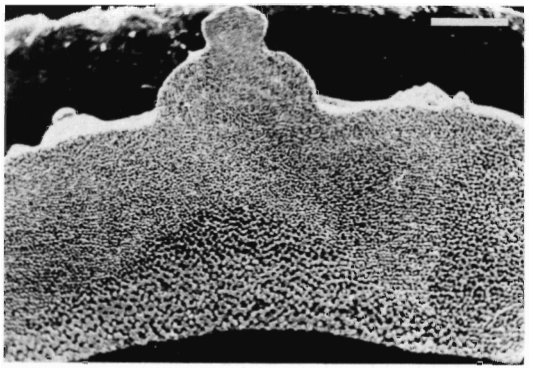

1

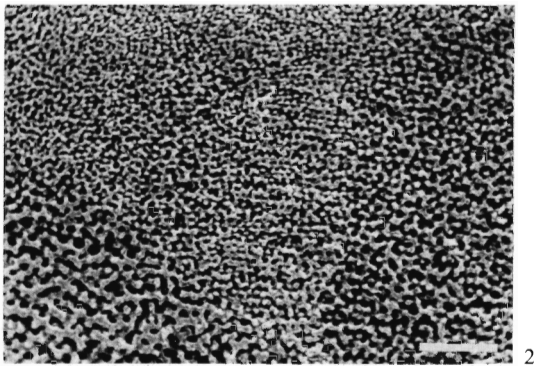

2

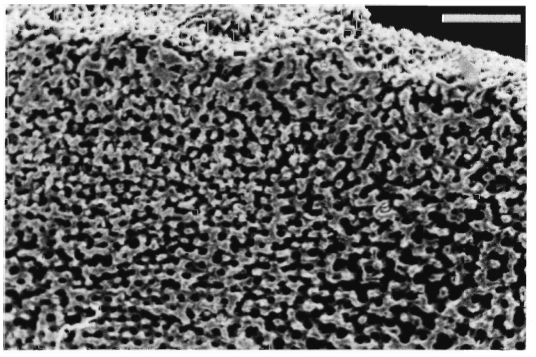

3

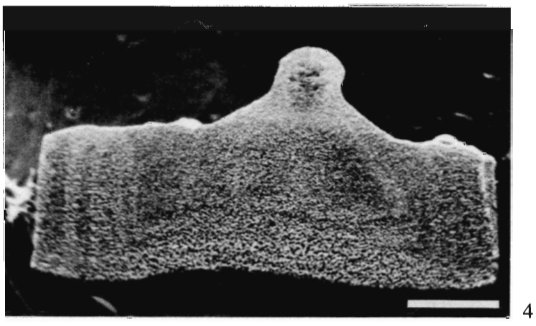

4

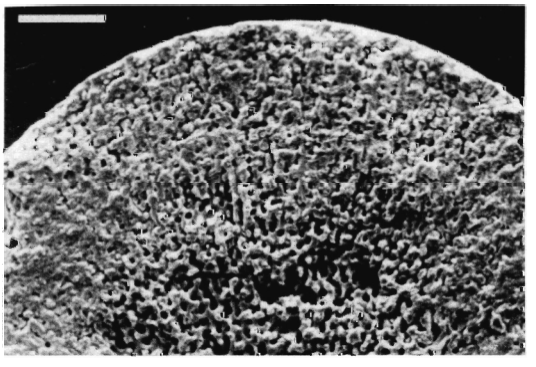

5

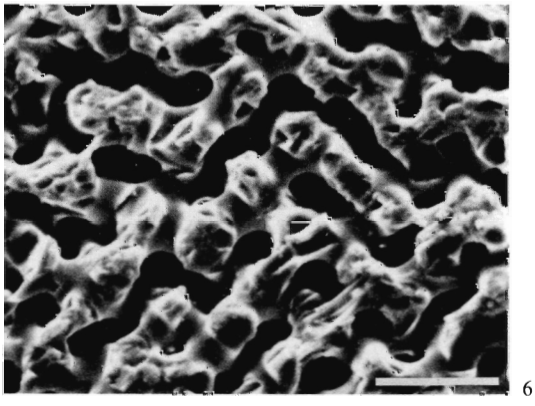

6

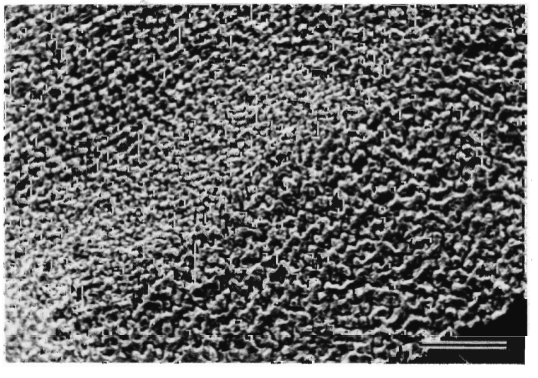

7

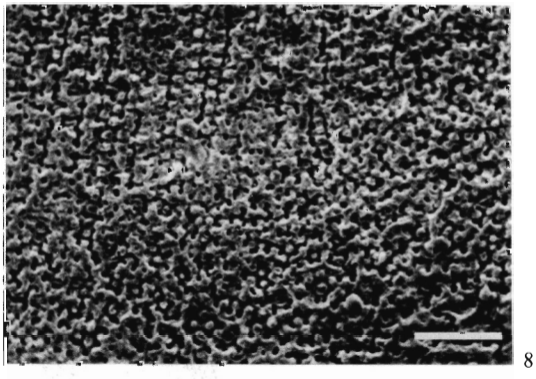

8

SMITH, plate construction

With the next bout of plate growth further labyrinthic stereom is laid down. As the plate nears its final thickness the thickness of stereom which needs to be deposited on the inner surface diminishes and the relatively slower growth rate results in the deposition of irregular perforate stereom. A similar situation is found in the outer plate layer. Towards the end of a period of growth stereom of the outer layer is consolidated, forming a compact stereom, and this is associated with the incorporation of spinochrome pigmentation. During periods of more rapid growth dense labyrinthic stereom is deposited.

Tubercles. In tubercles, collagenous catch apparatus fibres from the spine penetrate into the galleried stereom of the boss. It is not known whether the growth banding evident in tubercles forms seasonally accompanying a variation in growth rate, or forms each time the associated spine is lost. Swan (1952) and Ebert (1968) observed that tubercles of *Strongylocentrotus* from which spines are removed quickly change in appearance from glassy to opaque, and only regain their glassy sheen after a period of four to five months. This change in appearance from glassy to opaque is almost certainly produced by an increase in surface porosity, suggesting that following spine loss a more open stereom takes the place of the more usual compact, perforate stereom layer of the mamelon. Presumably then spine loss will result in the growth of a further layer on to the tubercle. Jensen (1969*b*) observed that *Psammechinus* drops its spines during the period of growth cessation and regenerates new ones. Complete spine regeneration has also been recorded by Chadwick (1929) and Hobson (1930). Galleried stereom is thought to be deposited during growth in the presence of catch apparatus fibres. Tubercle growth following spine loss would be expected to form wide labyrinthic stereom bands, whereas seasonal growth cessation should result in discontinuity of the galleried stereom.

PLATE GROWTH

Studies in plate growth, using natural growth banding (Deutler, 1926; Raup, 1968) or tetracycline labelling (Kobayashi and Taki, 1969; Markel, 1975, 1976) have been largely concerned with changes in shape of the outer surface of the plate. In cross-section the manner of plate growth in rigid- and flexible-tested echinoids is obviously different. The earliest formed part of the plate of non-cidarid echinoids with rigid tests is composed of labyrinthic stereom. Growing outwards from this, and expanding in thickness, is galleried stereom. The central part of the plate is built up on the inner surface, to match the peripheral thickness, by the deposition of an inner layer of labyrinthic, laminar, or microperforate stereom. Additional dense or compact layers may be deposited internally and externally. The change from labyrinthic to galleried stereom in the middle plate layer presumably reflects the onset of rigid plate suturing during early plate growth. In echinoids with flexible tests, individual plates are embedded in a layer of connective tissue fibres and no rigid plate suturing occurs.

EXPLANATION OF PLATE 11

Figs. 1–4. Cross-sections of aboral interambulacral plates of *Echinoneus cyclostomus*. 1, section through a 'glassy tubercle' near the plate margin. 2, section through the outer plate layer near the centre of the plate. A perforate stereom layer can be seen at the base. 3, section through the galleried stereom of a tubercle and the imperforate stereom of a 'glassy tubercle'. 4, enlargement of Fig. 3 showing the different stereoms.

Figs. 5–8. *Clypeaster rarispina*. 5, section through an aboral interambulacral plate. 6, buttress extending from an oral interambulacral plate. Galleried stereom can be seen at the tip: fascicular stereom forms the rest. 7, section through an interambulacrum. Test margin to the left and aboral surface uppermost. 8, section through a buttress. Aboral surface uppermost.

Figs. 9, 10. *Mellita quinquiesperforata*. 9, section through part of an ambulacrum. Oral surface uppermost: aboral surface just off the bottom of the micrograph. 10, oral ambulacral surface and cross-section showing outermost layer of perforate stereom.

Scale bar in Fig. 4 = 40 μm; Figs. 1–3, 10 = 100 μm; Figs. 6, 8 = 200 μm; Figs. 5, 7, 9 = 400 μm.

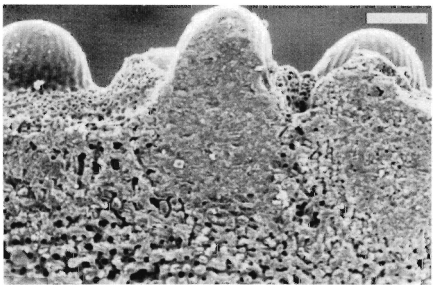
1

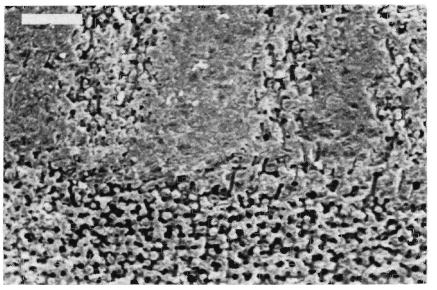
2

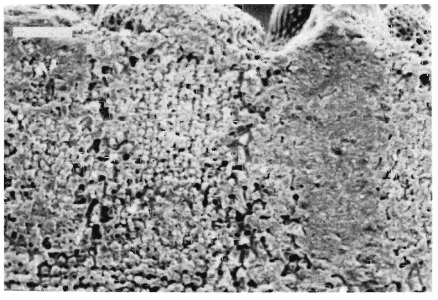
3

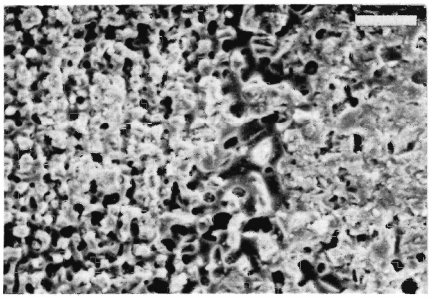
4

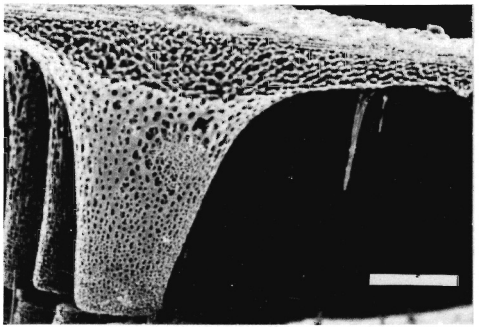
5

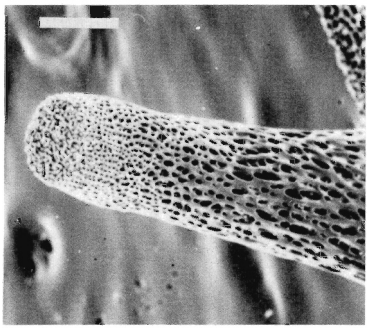
6

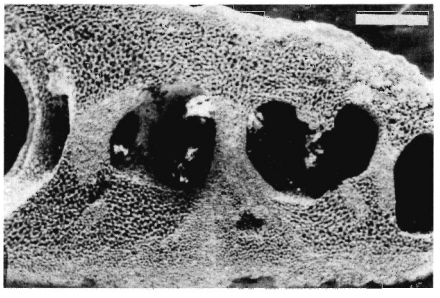
7

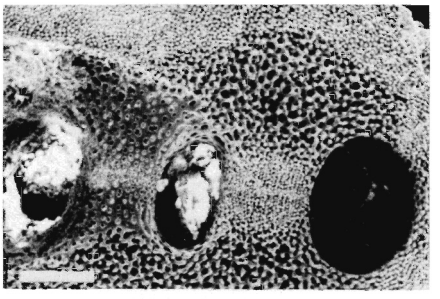
8

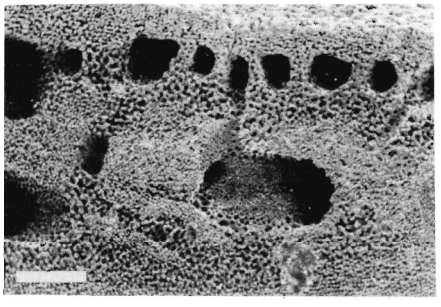
9

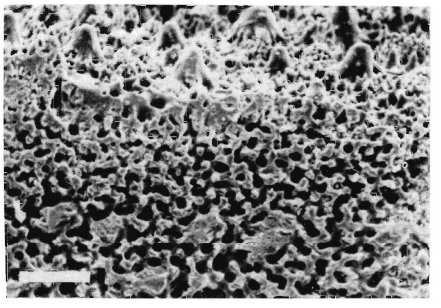
10

SMITH, plate construction

Galleried stereom is therefore absent from these plates and the major part of each plate is composed of labyrinthic stereom which continues to the plate margin with no decrease in thickness.

The thickness of the middle, galleried stereom layer was plotted against distance away from the plate growth centre (text-fig. 6). This shows that different echinoids have adopted different growth strategies. Regular echinoids, such as *Echinus esculentus*, *Temnopleurus hardwickii*, and *Tripneustes gratilla*, build up plate thickness rapidly during early growth and continue this thickening, though to a lesser extent, throughout later growth. *Psammechinus miliaris*, *Stomopneustes variolaris*, *Arbacia lixula*, and *Colobocentrotus atratus* all show a more gradual increase in plate thickness though again a rather more rapid increase in plate thickness occurs during early growth. *Sphaerechinus granularis*,

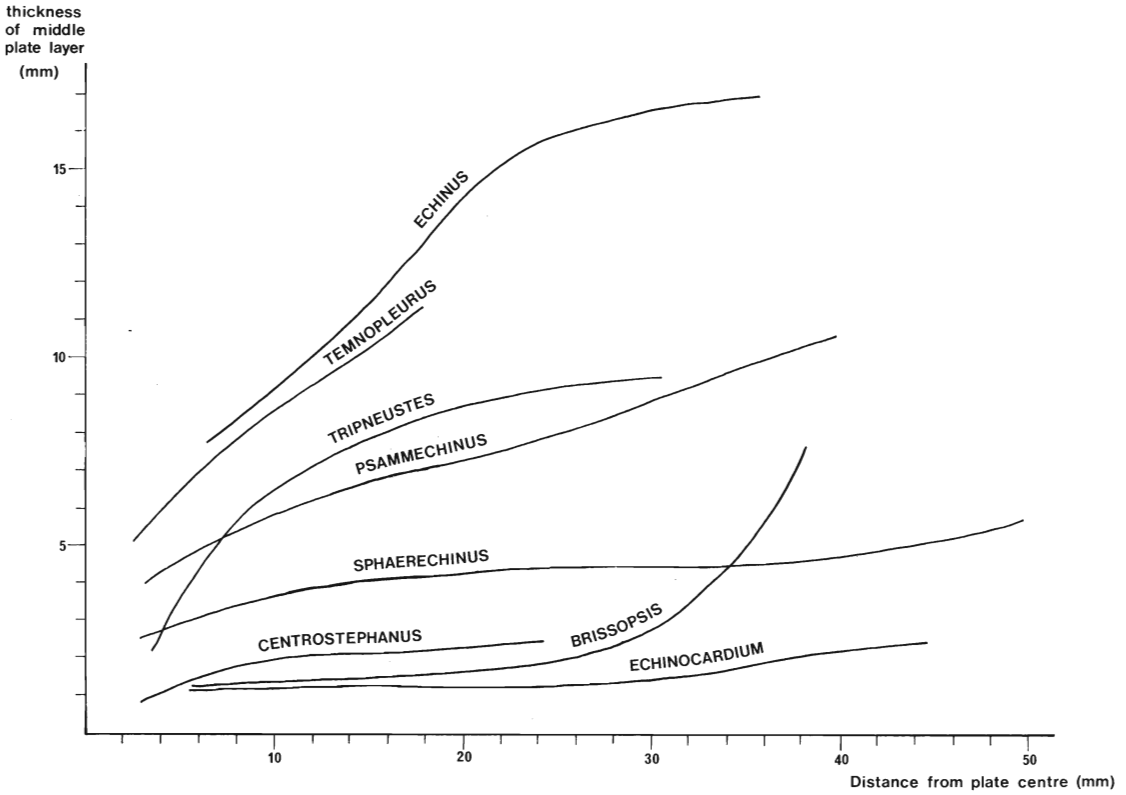

TEXT-FIG. 6. Growth of the middle plate layer. The thickness of the middle plate layer is plotted against the distance from the growth centre. Measurements were taken from S.E.M. micrographs of interambulacral plate sections.

EXPLANATION OF PLATE 12

Figs. 1–8. *Psammechinus miliaris*. Figs. 1–3, photomicrographs of an ambital interambulacral plate section treated to display light (opaque) and dark (translucent) zones, 1, ×8.6, 2, detail of plate margin, ×27, 3, detail of central region of plate, ×28. 4, electron micrograph of the same plate with soft tissue removed. Scale bar = 400 μm. 5, photomicrograph of the same plate showing the first broad opaque zone (growth from right to left), ×41. 6, electron micrograph of the same plate showing the stereom construction of the area in Fig. 5. V indicates zone of galleried stereom disruption. Scale bar = 200 μm. 7, electron micrograph of the same plate showing the stereom banding in the inner plate layer. Scale bar = 100 μm. 8, photomicrograph of a cross-section of an ambital interambulacral plate of another specimen showing growth banding of the inner plate layer, ×18.

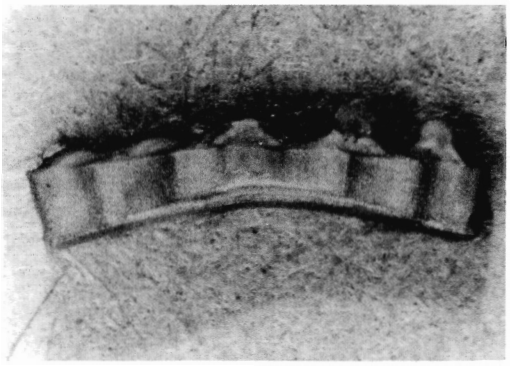

1

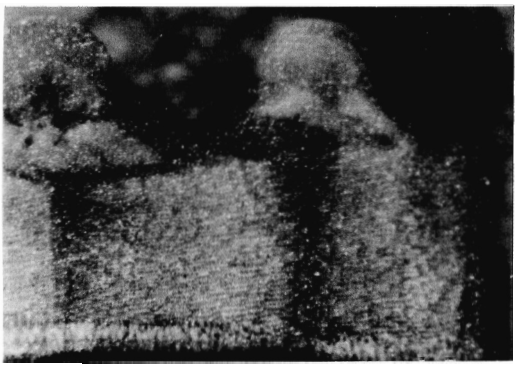

2

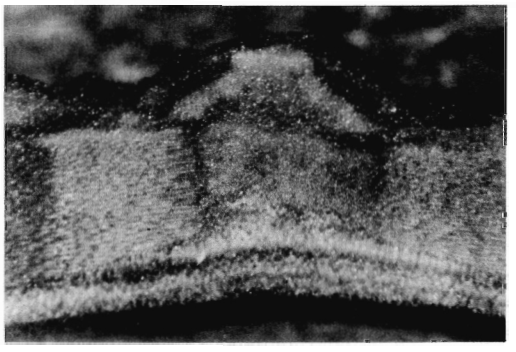

3

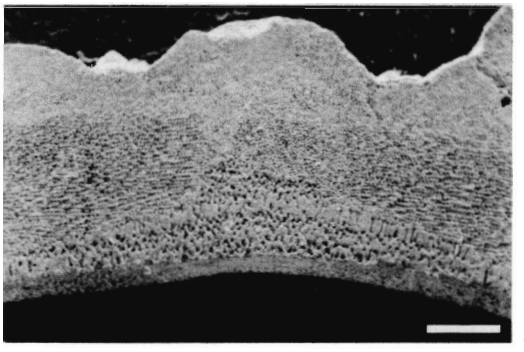

4

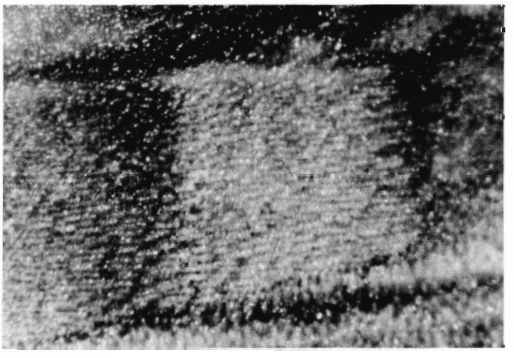

5

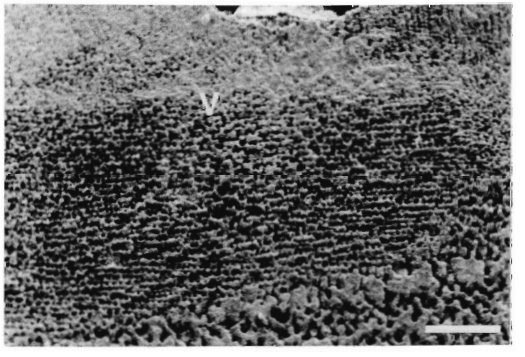

6

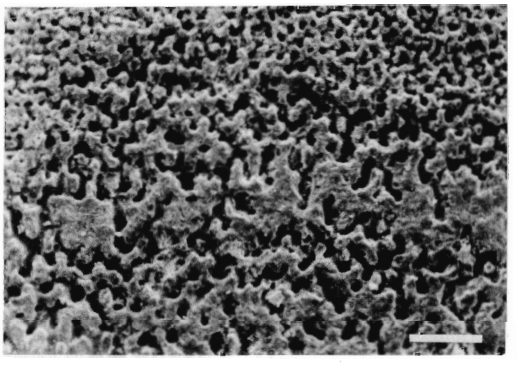

7

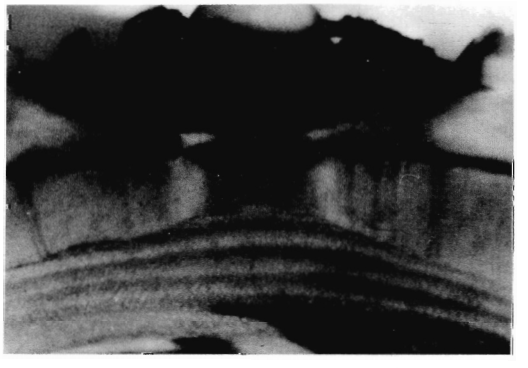

8

SMITH, growth banding

Centrostephanus longispinus, and *Echinometra mathaei* all have thinner tests and achieve their full plate thickness during the early growth of the plate. Further plate enlargement is extensive but this is accompanied by very little plate thickening. The spatangoids *Brissopsis lyrifera*, *Echinocardium cordatum*, and *Eupatagus hastingiae* increase rapidly in plate size with very little accompanying plate thickening. In *Brissopsis* and *Eupatagus* test thickness starts to increase rapidly only when the plate nears its maximum size. Plates of *Echinocardium* show only a small increase in thickness during later growth. The differences in plate construction which result from these differing growth strategies can be seen in text-figs. 2, 3, and 4.

Ebert (1975) found a correlation between the growth and mortality rates of echinoids and suggested that this relationship could be explained by considering the allocation of limited resources amongst growth, reproduction, and maintenance. Since plate thickening increases the strength of the test, the emphasis given to increasing plate thickness during growth can be used as an indication of the stress placed on maintenance. Although no firm conclusions can be drawn from the very limited data available, it appears as though echinoids from more turbulent environments allocate more of their resources to maintenance and build up their test thickness at the expense of rapid growth. Both Moore (1935), working on *Echinus*, and Giese (1967), working on *Strongylocentrotus* noted that shallow-water populations had thicker tests than deeper-water populations. Echinoids which inhabit more protected environments can increase their test size rapidly without expending much energy on plate thickening (and strengthening). In many spatangoids plate thickening occurs only after considerable lateral plate growth. Precedence of growth over maintenance during the early life of such echinoids may be linked to their specialized life style. Spatangoids possess specific morphological modifications for burial and for feeding and it may be that these only become efficient once appropriate numbers of spines and tube feet have been achieved. Early growth would therefore have to proceed rapidly at the expense of maintenance and only later, once a suitable size had been achieved, could resources be switched to plate strengthening. In *Meoma ventricosa* test growth is known to be rapid during the first year or so and tails off in later life (Chester, 1969). The spatangoid *Paramaretia peloria* lacks a specialized anterior ambulacrum and probably does not bury itself. Unlike other spatangoids *Paramaretia* shows a fairly constant increase in plate thickness during growth. Paul (1971) has figured and described plate growth in cystoids which shows remarkable similarity to echinoid plate growth.

FUNCTIONAL DESIGN OF PLATE STEREOM

The factors which produce the observed stereom variation in echinoid plates appear to be partly genetic and partly physiological. The restricted occurrence of individual stereom fabric gives some clues as to why a particular arrangement may be developed in preference to others.

EXPLANATION OF PLATE 13

Figs. 1–7. *Psammechinus miliaris*. 1, photomicrograph of ambital interambulacral plate margin showing multiple dark banding associated with a major dark (translucent) zone, × 50. 2, electron micrograph of another specimen showing a central zone of irregular stereom which interrupts the galleried stereom of the middle plate layer. Ambital interambulacral plate section. 3, same specimen, stereom between two translucent zones (v) in the middle plate layer, with growth from right to left. 4, ambital interambulacral plate taken from third specimen in cross-section showing the stereom of the middle plate layer between two translucent zones (v). Growth from left to right. 5, same specimen, outer plate layer showing variation in the stereom density. Growth from right to left. 6, ambital interambulacral plate of fourth specimen in cross-section. Outer plate layer with two coarse layers (c) separated by a more porous, finer stereom. Growth from left to right. 7, same specimen showing coarser area of stereom (c) in outer plate layer associated with a broad translucent zone, and a pair of bands of irregular stereom (Λ). Growth from right to left.

Fig. 8. Aboral interambulacral plate of *Paramaretia peloria* seen in cross-section. Inner plate layer of laminar stereom with a labyrinthic stereom wedge. Inner surface of the plate towards the top.

Scale bar in Fig. 2 = 40 μm; Figs. 3–8 = 100 μm.

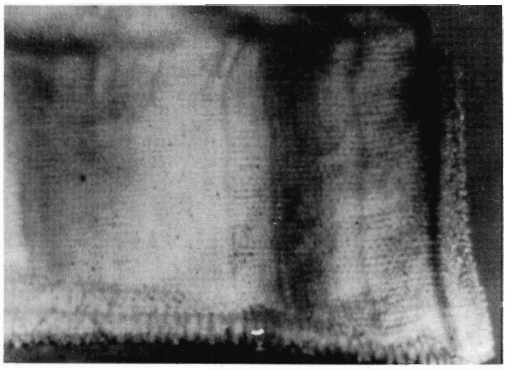

1

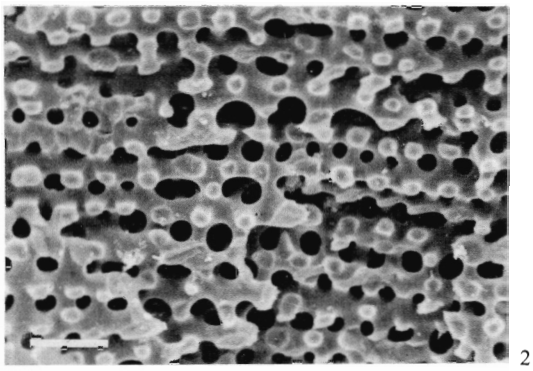

2

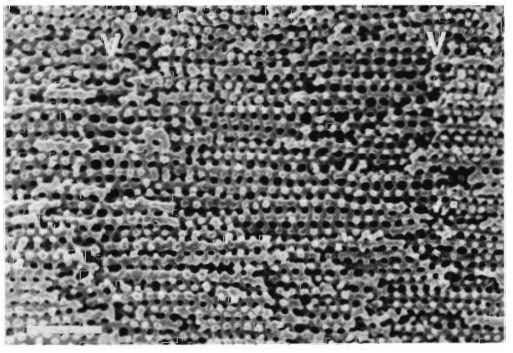

3

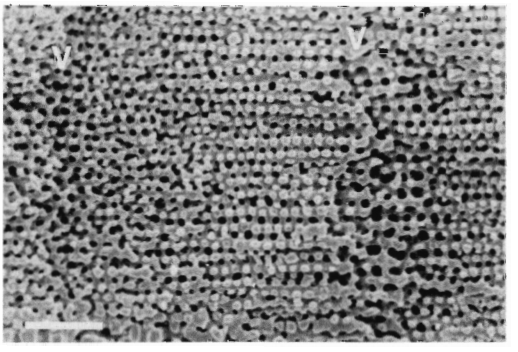

4

5

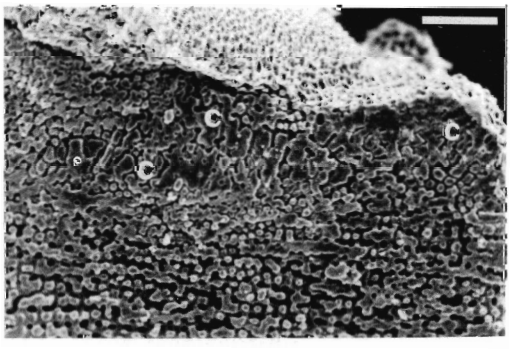

6

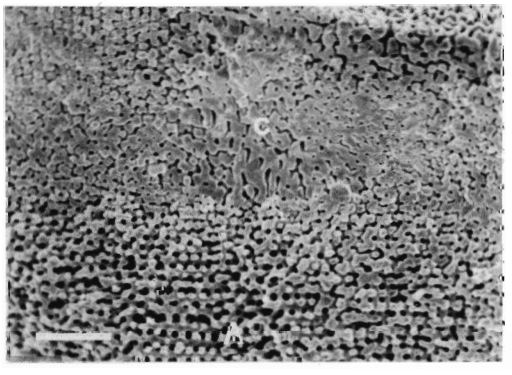

7

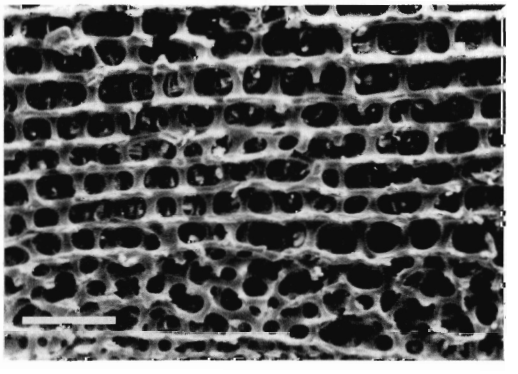

8

SMITH, growth banding

Galleried Stereom. This arrangement is always found associated with long bundles of collagen fibres, 4 μm to 12 μm in diameter, which form the sutural fibres of the plate (Foucart, 1966) and the catch apparatus fibres of the tubercle boss (Kawaguti and Kamishima, 1965). These fibre bundles penetrate into the plate following the long galleries of the stereom. The more detailed relationship between collagen fibres and galleried stereom will be dealt with in a later section. Stereom growth appears to be restricted by the presence of these fibres and that, while growth proceeds at a moderate pace, pore alignment is maintained.

Laminar Stereom. This stereom is found in only two groups of echinoids, the spatangoids and the diadematoids. In spatangoid plates, laminar stereom is deposited in the inner layer of the plate with the lamellae paralleling the inner plate surface. Because of the mode of growth of spatangoid plates, laminar stereom forms the greater part of each plate. This stereom arrangement has two possible advantages. It is economical in calcite, which is important as extensive plate thickening has to occur over a large area, and it also acts to strengthen the plate against stresses acting perpendicular to the plate surface, which are extremely dangerous to broad thin plates. Stereom growth rate must be fairly constant as thicker perforate stereom layers are deposited during periods of minimal growth. The labyrinthic stereom wedges observed in *Paramaretia* may be the result of periods of rapid growth. A more irregular laminar stereom is found in echinothuriids and in *Centrostephanus*. In *Calveriosoma* and *Phormosoma* it forms the outer layer of the plate and supports the tubercles. Here again this construction may help to strengthen the plates while being economical in calcite.

Fascicular Stereom. This appears to be associated with regions of rapid unidirectional growth. It is commonly found in the central core of tubercles and may be derived from a perforate stereom layer or from labyrinthic stereom.

Labyrinthic Stereom. This arrangement is found in a wide variety of sites and associated with all types of tissue. It forms the small central region of the plates in all non-cidaroid echinoids with rigid tests. This is the first part of the plate to be formed prior to the development of sutural collagen fibres. Labyrinthic stereom is also deposited in the inner layer of many plates where it acts as a filler. Here it is associated with moderate or fast stereom growth. Decrease in the stereom growth rate results in the deposition of a denser stereom leading to the production of a perforate stereom layer by consolidation. In echinoids, such as *Stomopneustes*, labyrinthic stereom may be deposited centrally whilst perforate stereom is laid down peripherally, where relatively much slower growth occurs. Labyrinthic stereom in the middle plate layer is formed during periods of minimal plate growth. In *Tripneustes*, broad labyrinthic stereom bands may be deposited during rapid plate growth in the absence of sutural collagen fibres. Labyrinthic stereom is also commonly present in the outer plate layer and in the core of tubercles. It may also form the stereom of the boss and the areole. The associated soft tissue influences the microstructure of the labyrinthic stereom. Labyrinthic stereom is the basic constructional design adopted by echinoids with the exception of the cidaroids and possibly the extinct bothriocidaroids. The isotropic trabecular arrangement ensures that the stereom is equally strong in all directions and that growth can proceed in any direction. A coarse texture is economical in materials but forms a weaker construction than dense stereom, which is more expensive in materials. There is some evidence that echinoids from higher-energy environments have denser labyrinthic stereom, suggesting that environmental factors may influence the stereom microstructure.

Microperforate Stereom. This stereom was found only in the inner plate layer of the two cassiduloid species examined. In a third cassiduloid, *Conolampas sigsbei*, the inner plate layer is composed of laminar stereom. Whether microperforate stereom is the product of physiological or genetic factors is not known since little is known about the growth of cassiduloids. Recently, Gladfelter (1978) has shown that *Cassidulus caribboearum* has more or less continuous growth and reproduction. *Echinolampas crassa* has, however, a biannual spawning (Thum and Allen, 1976). Microperforate stereom, which is basically a multilamellar perforate stereom, may be associated with slow but continous

growth. The extreme thickness and density of the plates of *Echinolampas* may be due largely to predatory pressures from boring gastropods.

Retiform Stereom. With the exception of the single retiform layer in the centre of plates of *Phormosoma* this stereom is always associated with muscle insertion. It is found in the areoles and spine bases of a number of echinoids.

Perforate Stereom. Simple perforate stereom is laid down in the inner plate layer during periods of slow stereom growth. The deposition of dense calcite layers on both the inner and outer surfaces gives the plate a sandwich structure which increases the plate's resistance to bending stresses (Wainwright *et al.*, 1976). The outer dense calcite layer, with its associated spinochromes, may also function to deter the settlement of parasitic algae (Vevers, 1966). The most important function of this outer dense layer is in the increased protection it gives against surface abrasion in turbulent conditions. Echinoids living in protected environments either have no outer layer or have only a thin development of this layer whereas echinoids from highly turbulent intertidal areas have a thick outer plate layer.

Imperforate Stereom. This is found at articular surfaces of larger tubercles and spines. Imperforate stereom provides a strong and smooth surface which is minimally resistant to sliding movements of the spine. This stereom is reported to by polycrystalline (Towe, 1967; Markel *et al.*, 1971). Imperforate stereom is also found to form the glassy tubercles of *Echinoneus* which support no appendages. The function of these glassy tubercles is unknown.

Rectilinear Stereom. The galleried appearance of rectilinear stereom is not formed in association with collagen fibres and it may be found with various tissue types. It has been found only in post-Palaeozoic cidaroids. A latex mould of plates of *Neobothriocidaris* suggests that rectilinear stereom may also have been present in this genus. In cidaroids, rectilinear stereom, rather than labyrinthic stereom, forms the core to each interambulacral plate and this appears to reflect a difference in the basic plate construction of the Perischoechinoidea and the Euechinoidea (Nissen, 1969).

ANALYSIS OF SURFACE STEREOM MICROSTRUCTURE

Although there is only a limited number of three-dimensional stereom fabrics in echinoid plates, the microstructure at the surface of the test is strikingly varied. Similar variation is apparent in well-preserved fossil material, and correct interpretation of the stereom microstructure could yield valuable biological information. Previous quantitative stereom analysis by Roux (1970, 1971, 1974*b*, 1975) and by Macurda and Meyer (1975) on Recent crinoids has shown that there is a relationship between the surface stereom microstructure and the associated soft tissue. Using Recent echinoid material in which the precise relationship between the stereom and the associated soft tissue can be examined from histological preparations, I hoped to detect a scheme for identifying soft tissue from the stereom of fossil echinoderms. This proved to be partly successful, although the correlation between tissue and stereom was found to be much more complicated than previously suggested.

Stereom parameters

Ambulacral and interambulacral plates, from the species listed in Table 3, were placed in an S.E.M. I selected areas where the associated soft tissue was known from histological thin sections and photographed them at high magnification. Stereom from the following regions was analysed in most cases: external surface away from tubercles—(ectoderm); boss—(collagenous catch apparatus); areole—(muscle); gap between boss and areole—(collagen membrane); tube foot attachment area—(collagen/muscle); interporal area—(coelomic epithelium); suture face—(collagen); internal surface: central—(coelomic epithelium); internal surface: marginal (if different)—(coelomic epithelium); pore wall—(densely ciliated epithelium); plus any other special features. Measurements from enlargements of the photomicrographs were taken for each area. The maximum pore diameter (A) and, in some cases, the pore diameter (B) perpendicular to A were measured as was the minimum trabecular thickness separating adjacent pores (t). Wherever possible, a minimum of twenty-five measurements were made for each parameter, working from the centre of the photomicrograph outwards and including all

TABLE 3. Species in which plate stereom was quantitatively analysed.

1. *Cidaris cidaris* (Linnaeus)
2. *Eucidaris metularia* (Lamarck)
3. *Calveriosoma hystrix* (Wyville Thomson)
4. *Phormosoma placenta* Wyville Thomson
5. *Micropyga tuberculata* Agassiz
6. *Centrostephanus nitidus* Koehler
7. *Centrostephanus longispinus* (Philippi)
8. *Stomopneustes variolaris* (Lamarck)
9. *Arbacia lixula* (Troschal)
10. *Temnopleurus hardwickii* (Gray)
11. *Sphaerechinus granularis* (Lamarck)
12. *Tripneustes gratilla* (Linnaeus)
13. *Echinus acutus* Lamarck
14. *Echinus esculentus* (Linnaeus)
15. *Psammechinus miliaris* (Gmelin)
16. *Paracentrotus lividus* (Lamarck)
17. *Colobocentrotus atratus* (Linnaeus)
18. *Echinometra mathaei* (de Blainville)
19. *Echinostrephus molaris* (de Blainville)
20. *Plesiechinus ornatus* (Buckman)
21. *Echinoneus cyclostomus* (Gray)
22. *Clypeaster rarispina* de Meijere
23. *Fellaster zelandiae* (Gray)
24. *Mellita quinquiesperforata* (Leske)
25. *Encope michelini* Agassiz
26. *Cassidulus cariboearum* Lamarck
27. *Echinolampas crassa* (Bell)
28. *Apatopygus recens* (Milne-Edwards)
29. *Brissopsis lyrifera* (Forbes)
30. *Spatangus raschi* Loven
31. *Echinocardium cordatum* (Pennant)
32. *Eupatagus hastingiae* Forbes

possible measurements within the area defined. Where the stereom was variable the number of individual measurements was increased and, in some cases, results from more than one photomicrograph were combined. In addition, the surface pore space (P) of the stereom was calculated using a 1000-point grid placed centrally on the photomicrograph. At least two independent counts were taken from adjacent areas and if the results were not consistent further counts were made and the results averaged and converted to a percentage. The number of pores lying within a known area (between 50 μm^2 and 250 μm^2 depending upon the magnification of the photomicrographs taken) was counted in two randomly selected areas and further counts were taken if the results proved to be unacceptably variable. The average was then recalculated to give pores per mm^2(N). Measurements of A and t are accurate to 0.25 μm, unless otherwise stated and, for each area, the sample size, mean, standard deviation, and coefficient of variation were calculated. P is better than $\pm 5\%$ and N is considered accurate to $\pm 10\%$. All data are tabulated in Smith (1978*b*).

There are a number of possible sources of error in measuring properties of stereom. First, there is the question of whether the stereom analysed is typical of the area it represents. In most cases a visual check shows that this is not a problem. Occasionally the stereom was found to be atypical because of its great variability, when a second region was chosen and the results combined. Variation in stereom construction also occurs during growth. Roux (1971, 1975) has demonstrated that there is a change in stereom pore size during growth and similar fluctuations in pore size have been observed in this study. Where growth banding was observed the number of measurements taken was increased so that the area covered took in the range of pore sizes found.

The measurement of pore diameters on non-planar surfaces also posed problems because of the difficulty in defining the pores (see Pl. 3 fig. 4). By using a narrow focus on the S.E.M. and by always taking the uppermost pore rim, much of the ambiguity was eliminated. The best separation of stereom types was achieved by using a plot of average maximum pore dameter ($\bar{A}$) against average minimum trabecular thickness ($\bar{t}$). The ratio $\bar{A}/\bar{t}$ can be used as an approximate measure of the surface pore space as can be seen from a plot of $\bar{A}/\bar{t}$ against P (text-fig. 7). The correlation is not precise because of the variation in pore shape. Plots of P against N gave similar but less distinct separation of stereom groups.

Description of Surface Stereom Organization

The surface stereom of each area will be dealt with in turn. Terminology for microstructural features is drawn largely from Oldfield (1976). Trabecular intersections may be smooth (Pl. 3, fig. 2), swollen (Pl. 2, fig. 3), or may have sharp-pointed thorns (Pl. 14, figs. 4, 6) or blunt pegs (Pl. 4, fig. 5). In compact stereom, domes may be developed between the small pores (Pl. 8, fig. 3). A distinctive texture, typical of the areole, is characterized by an abundance of free-ended trabeculae in all orientations which define angular and often 'incomplete' pores (Pl. 14, fig. 7).

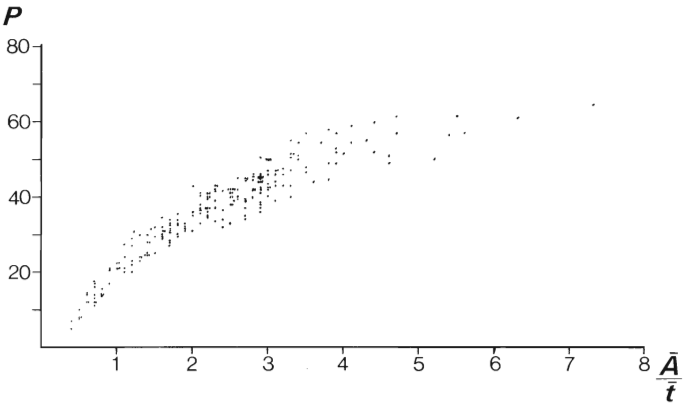

TEXT-FIG. 7. The relationship between the $\bar{A}/\bar{t}$ ratio and the surface pore space (P) based on a plot of all data available. The correlation is not precise because of differences in stereom pore elongation.

Plate Surface

This is covered in life by the integument which is composed of an outer layer of lightly ciliated epithelial cells, around 10 μm to 25 μm in thickness, and an underlying nerve plexus (Pl. 23, fig. 9). A thin basal membrane separates this from the mesodermal connective tissue of the plate. A more detailed description of the integument of an echinoid is given by Kawaguti and Kamishima (1964). In the echinothuriids a layer of collagenous fibres separates the sub-epidermal nerve plexus from the connective tissue of the plates. The stereom underlying the integument is quite varied, as can be seen from text-fig. 8, and can be divided into the following categories:

1. Rectilinear. Typical rectilinear stereom, with squarish, uniformly sized pores showing good alignment, is found beneath the integument of *Cidaris* and *Eucidaris* in interambulacral plates. This stereom is open in texture and small thorns are commonly developed at trabecular intersections (Pl. 1, fig. 1).

2. Open labyrinthic. This stereom has variable-sized, sub-circular to oval pores which are irregularly arranged (Pl. 15, fig. 1). Underlying trabeculae can be seen clearly beneath the surface layer. Trabeculae are fairly uniform in size and small thorns are present at all intersections, except in the stereom of *Calveriosoma*, which has smooth intersections. Open labyrinthic stereom forms the plate surface in *Calveriosoma*, *Centrostephanus*, *Micropyga*, *Temnopleurus*, *Stomopneustes*, *Clypeaster*, *Fellaster*, *Mellita*, and *Encope*. In addition, it also forms the surface of the ambulacral plates of *Cidaris* and small parts of the same plates of *Eucidaris*. In the sand dollars *Fellaster*, *Mellita*, and *Encope* suitably large areas of plate stereom were found only in the oral interambulacra. Aborally there appears to be a rather more compact stereom but the great density of tubercles prevents any quantitative analysis.

3. Dense labyrinthic. In the cassiduloids *Echinolampas*, *Apatopygus*, and *Cassidulus* dense labyrinthic stereom with medium or fine-sized pores underlies the integument. Stereom pores are roundish, variable in size, and show no orderly arrangement (Pl. 15, fig. 3). Trabeculae are thick and all intersections have prominent thorns. A similar stereom is present in *Tripneustes*, *Echinus esculentus*, *Paracentrotus* (Pl. 15, fig. 2), *Echinostrephus*, and *Echinoneus*, all of which have well-developed thorns at trabecular intersections. In *Echinometra* the pores are small and trabeculae are very variable in thickness. Trabecular intersections are broad and developed into small peg-like domes (Pl. 15, fig. 8). The labyrinthic stereom of the plate surface of *Colobocentrotus* shows a more organized arrangement of pores with pegs at all intersections (Pl. 15, fig. 4). The stereom over the plate surface of *Salenocidaris profundi* is difficult to place as it varies from imperforate stereom to galleried stereom orientated parallel to the plate's outer surface (Pl. 22, fig. 6). Over the larger part of the plate there is a single layer of dense irregular trabeculae overlying the galleried stereom of the middle plate layer. All plate surface stereoms have thorns at trabecular intersections.

4. Perforate. The outer surface of spatangoid plates is composed of perforate stereom. This is typically a planar, compact, stereom layer perforated by small circular pores with an average diameter of less than 15 μm (Pl. 15, fig. 5). Large thorns are present at all intersections and the pores are often aligned. In some cases there may be low ridges between pores and in the posterior oral ambulacra of *Brissopsis*, where few tubercles are found, the normally planar stereom develops prominent peg-like domes (Pl. 15, fig. 7). Perforate stereom was found underlying the integument of *Arbacia*, *Psammechinus*, and *Echinus acutus* as well as the spatangoids *Brissopsis*, *Spatangus*, and *Echinocardium*. It also formed the plate surface of *Eupatagus* (Pl. 14, fig. 6).

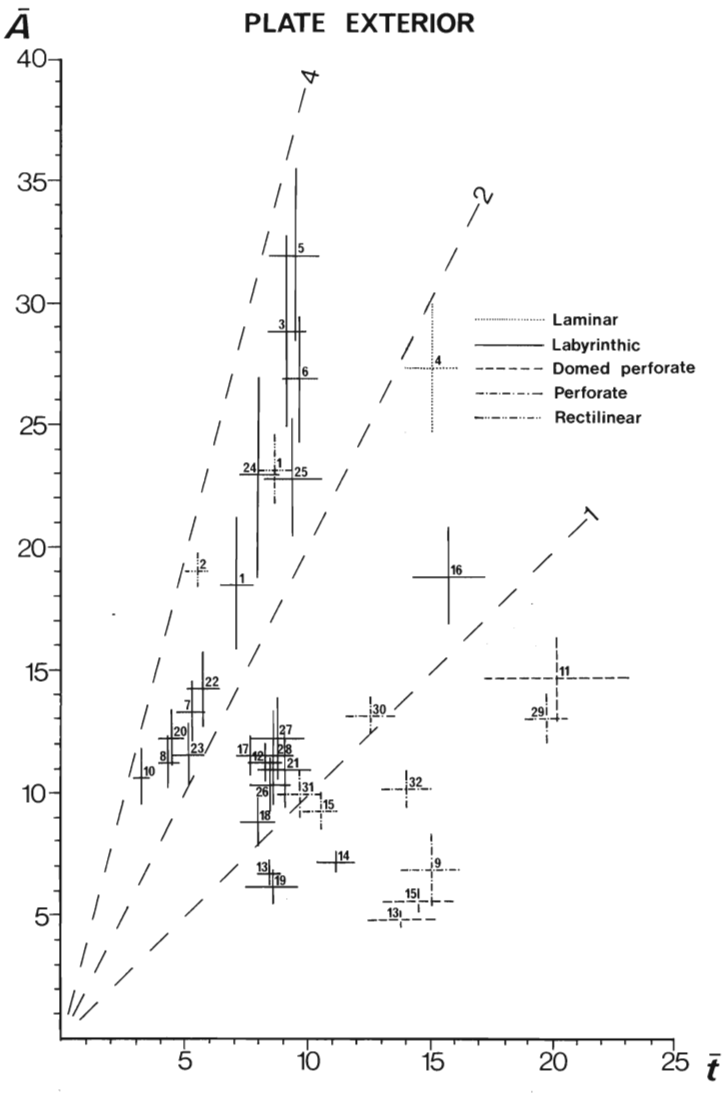

TEXT-FIG. 8. A plot of data on stereom of the outer plate surface which is overlain by integument. The mean ± 2 standard errors is given for each species. Species are listed in Table 3.

EXPLANATION OF PLATE 14

Figs. 1, 2, 4. *Brissopsis lyrifera*. 1, stereo view of an aboral interambulacral tubercle in cross-section, showing the thin labyrinthic stereom of the boss. 2, same, showing laminar stereom of the inner plate layer to the left and galleried stereom of the outer plate layer to the right. Outer surface to the top. 4, trabecular thorns on the outer surface, aboral interambulacral plate.

Fig. 3. Aboral interambulacral plate of *Paramaretia peloria* in cross-section.

Fig. 5. Plate section showing the aboral interambulacral/ambulacral suture in *Mellita quinquiesperforata*. Long, interpenetrating thorns can be seen.

Fig. 6. Large trabecular thorns on the surface of the perforate stereom layer which forms the outer surface of an aboral interambulacral plate of *Eupatagus hastingiae*.

Fig. 7. Labyrinthic stereom with many irregularly arranged and free-ended trabeculae typical of areas of muscle attachment. Stereom of the areole of a primary interambulacral tubercle of *Temnopleurus hardwickii*.

Scale bar in Fig. 6 = 10 μm; Figs. 4, 7 = 20 μm; Figs. 1, 5 = 40 μm; Fig. 2 = 200 μm; Figs. 3 = 400 μm.

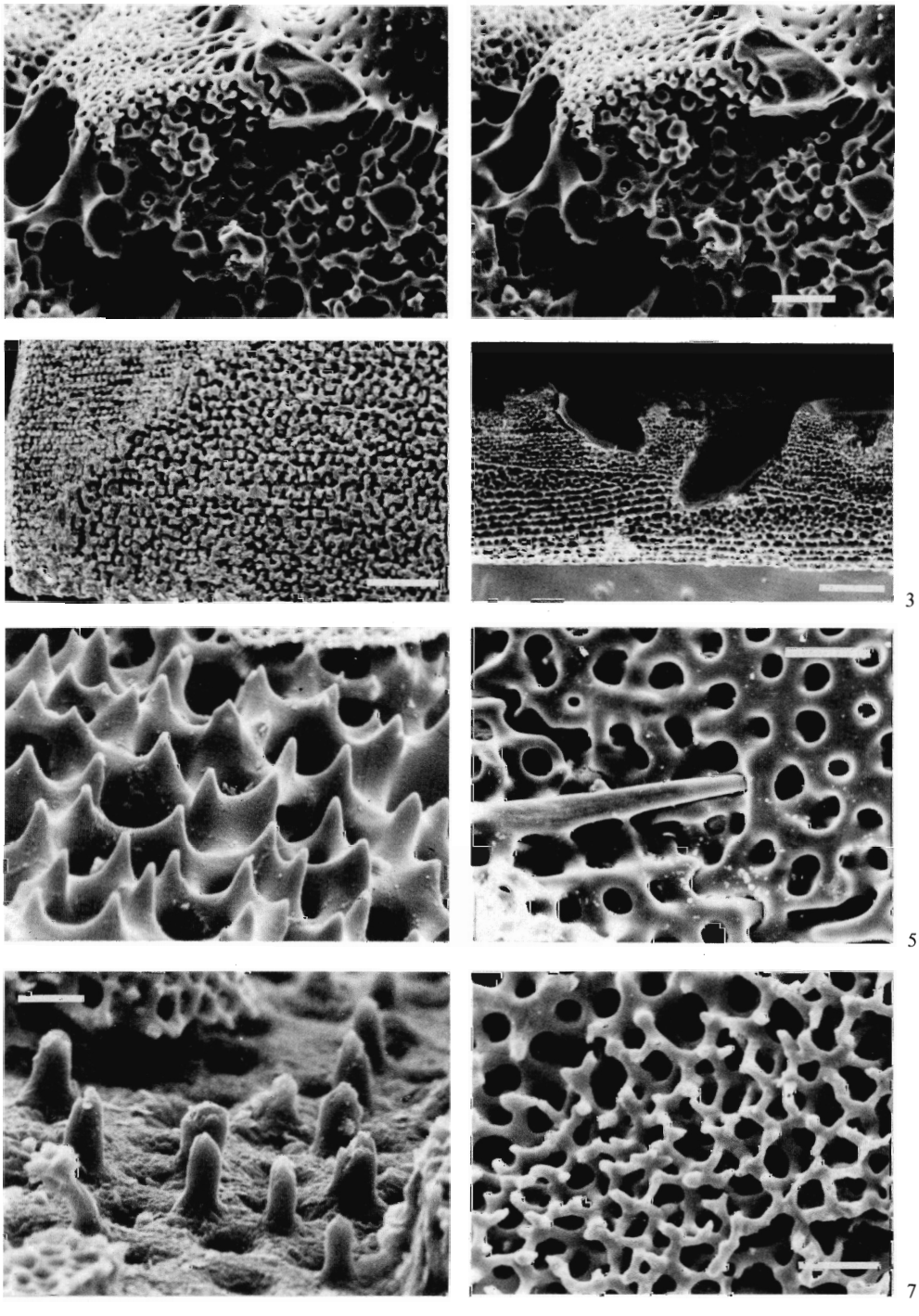

1 2 3 4 5 6 7

SMITH, plate surface stereom

5. Domed. In *Sphaerechinus* the plate surface is compact and large domes are developed in both interambulacral and ambulacral plates (Pl. 8, fig. 3). These domes may be aligned but are usually randomly arranged. Pores are small, roundish, and variable in size across the plate. A similar stereom organization occurs between isopores on the aboral and ambital surfaces of ambulacral plates of *Eucidaris* and *Psammechinus* and is reported by Oldfield (1976) from a number of other echinoids.

6. Laminar. Laminar stereom with oval pores underlies the integument of *Phormosoma* (Pl. 15, fig. 6). Trabeculae are variable in size and all intersections are smooth. Surface pore space is about 35%.

Boss

The boss of tubercles forms the area of attachment for the collagenous catch apparatus of the spine. These collagenous fibres enter into the pore space of the stereom (Pl. 16, fig. 1) and may penetrate to depths of more than 100 μm. In some cases the fibres loop around the surface layers of the stereom and do not penetrate further than the second or, at the most, third trabecular level (Pl. 23, fig. 2). In most cases the collagenous fibres are organized into discrete bundles, 4 μm to 12 μm in diameter, which penetrate deep into the stereom through many trabecular levels (Pl. 23, fig. 1). Groups of fibres branch from these bundles at intervals and loop under adjacent trabeculae to join with neighbouring bundles (Pl. 23, figs. 3, 4). Each fibre bundle runs along a gallery in the stereom. Galleried stereom is present where fibres penetrate the stereom in bundles whereas labyrinthic stereom is found where the catch apparatus fibres are less organized and loop around the surface layer of trabeculae. Results of stereom analysis are given in text-fig. 9.

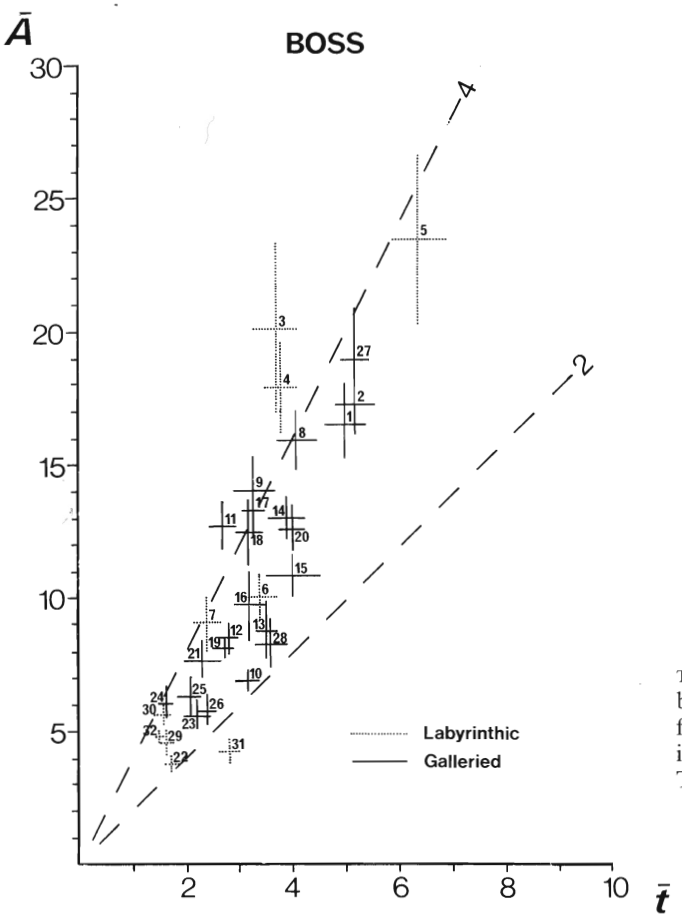

TEXT-FIG. 9. A plot of data on stereom of the boss where collagenous catch apparatus fibres insert. The mean ± 2 standard errors is given for each species. Species are listed in Table 3.

1. Galleried stereom. The galleries of the stereom always run perpendicular to the plate surface and show moderately good pore alignment (Pl. 2, fig. 4). The pores are randomly arranged and often vary markedly in size (unlike rectilinear stereom). Trabeculae are uniformly sized and in most cases have slightly swollen trabecular intersections. Small thorns may be present in some cases (Pl. 17, fig. 1). This stereom falls into a narrowly defined area when analysed quantitatively (text-fig. 9).

2. Labyrinthic stereom. A coarse labyrinthic stereom forms the outer surface of the bosses of *Calveriosoma*, *Phormosoma*, and *Centrostephanus*. It has very irregularly shaped and sized pores in a completely random arrangement (Pl. 16, figs. 2–4). Trabeculae are thin and fairly uniform in size. Trabecular intersections are often somewhat swollen but always lack thorns. In *Micropyga* the stereom of the boss is very similar. A fine labyrinthic stereom forms the bosses of *Salenocidaris*, *Spatangus*, *Echinocardium*, *Eupatagus*, *Clypeaster*, and small tubercles of *Brissopsis*. This has irregularly shaped and sized pores, haphazardly arranged, which is superficially identical to the stereom of the areole (Pl. 16, fig. 5). Trabeculae are fairly uniform in size and possess smooth or slightly swollen intersections. The average pore diameter for this stereom is less than 6 μm. In *Brissopsis*, the labyrinthic stereom of the boss can be seen, in cross-section, to form a moderately thick outer layer to the tubercle (Pl. 14, fig. 1). In some cases labyrinthic stereom forms the outer, superficial layer to tubercles which are normally composed of galleried stereom. This occurs because of growth banding in the stereom and it is often possible to see underlying pore alignment beneath the surface layer of trabeculae. Labyrinthic stereom is usually slightly coarser and more open than the associated galleried stereom.

Areole

The areole surrounds the tubercle boss and is defined here as the area on to which spine muscle fibres attach. Muscle fibres, which are arranged into bundles, attach on to the stereom by means of a connective tissue ligament. The muscle fibres do not themselves penetrate into the pore space of the stereom but the connective tissue ligament fibres are bound around the surface layer of trabeculae (Pl. 23, fig. 6). Ligament fibres never penetrate further than the first or second layers of trabeculae. A similar mode of attachment has been described for muscle of the starfish *Asterias* (Uhlmann, 1968). Although the areolar stereom is unmodified in some species, in the majority of echinoids a distinctive stereom is developed (text-fig. 10). The following types of stereom were found to support muscle fibres:

1. Unmodified plate stereom. Typical rectilinear stereom forms the areole in *Cidaris*, *Eucidaris*, *Poriocidaris*, and *Austrocidaris* (Pl. 1, fig. 1; Pl. 6, figs. 3, 6). In some cases pore alignment may be perpendicular to the plate surface but it may equally well be in any other orientation. The areole of *Centrostephanus longispinus* is composed of galleried stereom orientated parallel to the plate surface. In *Salenocidaris profundi* much of the areole may be composed of a similar galleried stereom although there may be a fine labyrinthic overlay developed near the tubercle (Pl. 22, fig. 4). In all these cases the stereom lacks the surface development of thorns found in the similar stereom underlying the integument. In *Calveriosoma* and *Phormosoma* spine muscle attaches on to an open laminar stereom with roundish to oval pores which are highly variable in size. Trabeculae are also rather variable in size and all intersections are smooth (Plate 17, fig. 2). The areolar stereom of *Calveriosoma* differs from the stereom underlying integument which forms a superficial overlay of labyrinthine stereom. In *Phormosoma* areolar stereom is identical to stereom underlying the integument in all respects. Similar laminar stereom forms the areole of *Micropyga* except that here trabecular intersections have thorns (Pl. 16, fig. 4).

2. Labyrinthic stereom. A large number of echinoids have an areole composed of medium or fine, open, labyrinthic stereom which forms a thin overlay (Pl. 18, figs. 4, 5) or superficial layer (Pl. 18, fig. 1) to the plate stereom. Thin trabecular struts may grow between existing plate stereom trabeculae to produce a finer, more irregular, stereom (Pl. 18, fig. 4). The pores are generally small and irregular in shape, with an average pore diameter of less than 15 μm. Many of the pores are angular and the stereom often has a ragged appearance imparted by the large proportion of trabeculae with free ends (Pl. 18, figs. 1–5). Trabeculae are often fairly variable in thickness, commonly swollen at intersections and pinched centrally. Trabecular intersections are largely without pegs or thorns, except in the case of *Echinostrephus* where small pegs are found at the larger trabecular intersections (Pl. 17, fig. 1). This type of labyrinthic stereom forms the areoles of many echinoids including *Centrostephanus nitidus*, *Stomopneustes*, *Arbacia*, *Temnopleurus*, *Tripneustes*, *Sphaerechinus*, *Colobocentrotus*, *Echinus*, *Psammechinus*, *Paracentrotus*, *Echinometra*, *Echinostrephus*, *Echinoneus*, *Echinolampas*, *Cassidulus*, *Apatopygus*, *Fellaster*, and *Clypeaster*. It is rather poorly developed in *Stomopneustes*, *Centrostephanus*, and *Colobocentrotus*.

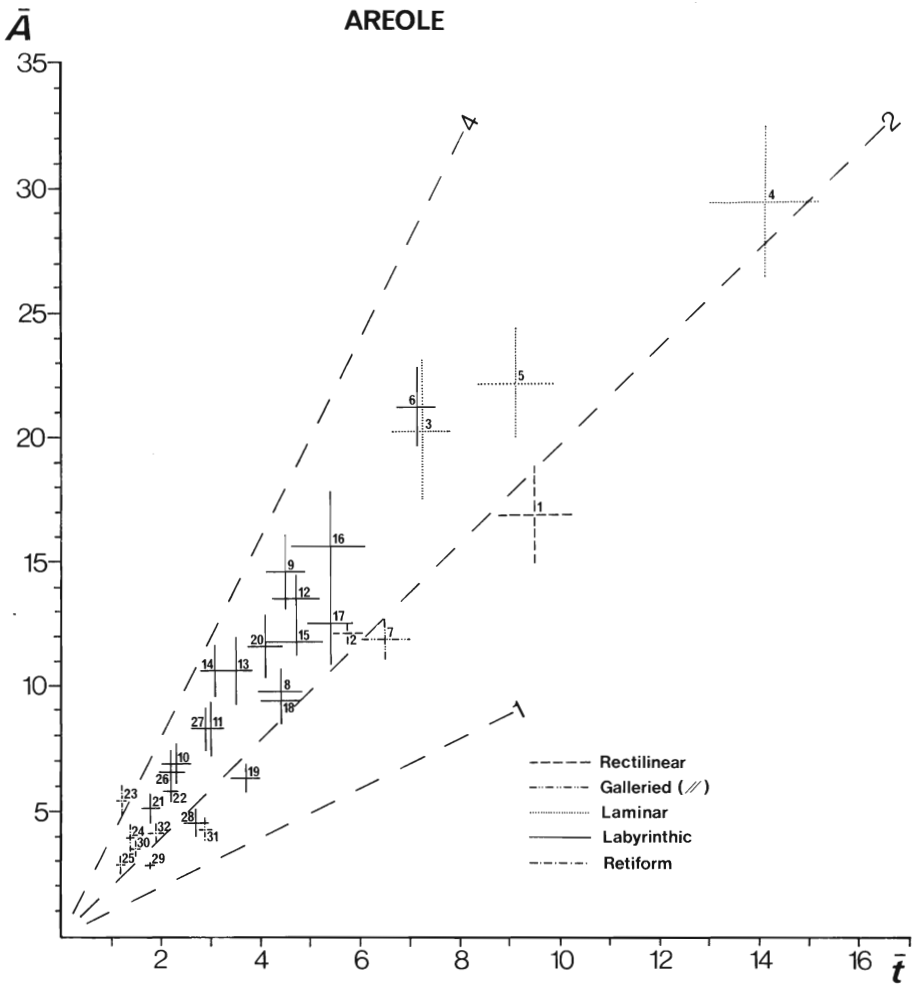

TEXT-FIG. 10. A plot of data on stereom of the areole where spine muscle fibres insert. The mean ± 2 standard errors is given for each species. Species are listed in Table 3.

EXPLANATION OF PLATE 15

Fig. 1. Open labyrinthic stereom forming the outer surface of an oral interambulacral plate of *Clypeaster rarispina*.

Fig. 2. Labyrinthic stereom of the surface of an ambital interambulacral plate of *Paracentrotus lividus*.

Fig. 3. Dense labyrinthic stereom forming the outer surface of an aboral interambulacral plate of *Echinolampas crassa*.

Fig. 4. Stereom of the surface of an ambital interambulacral plate of *Colobocentrotus atratus* showing some development of pore alignment.

Fig. 5. Perforate stereom forming the outer surface of an ambital interambulacral plate of *Brissopsis lyrifera*.

Fig. 6. Laminar stereom forming the outer surface of an aboral interambulacral plate of *Phormosoma placenta*.

Fig. 7. A pegged perforate stereom forming the outer surface of an oral ambulacral plate of *Brissopsis lyrifera* (from Amb. III).

Fig. 8. Irregular, pegged, perforate stereom forming the outer surface of an ambital interambulacral plate of *Echinometra mathaei*.

Scale bar in Fig. 3 = 20 μM; Figs. 1, 2, 4–6, 8 = 40 μm; Fig. 7 = 100 μm.

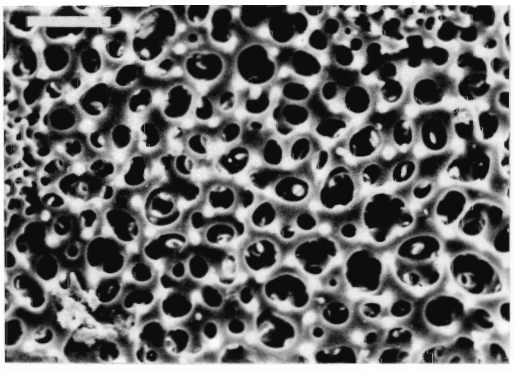

1

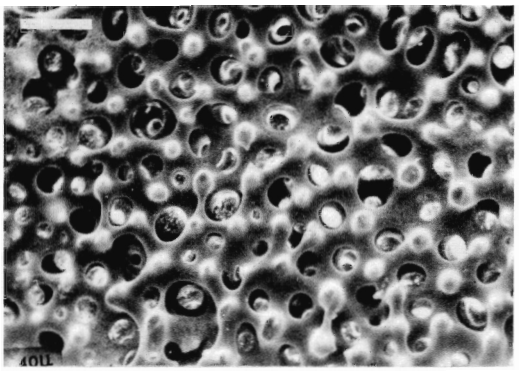

2

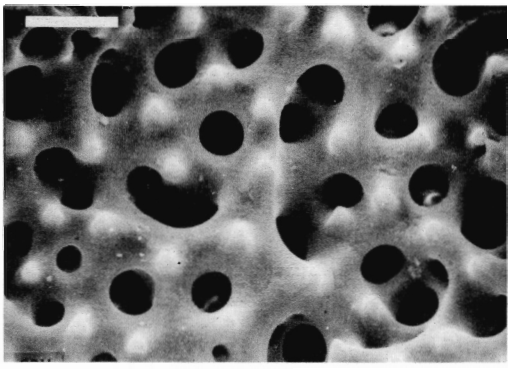

3

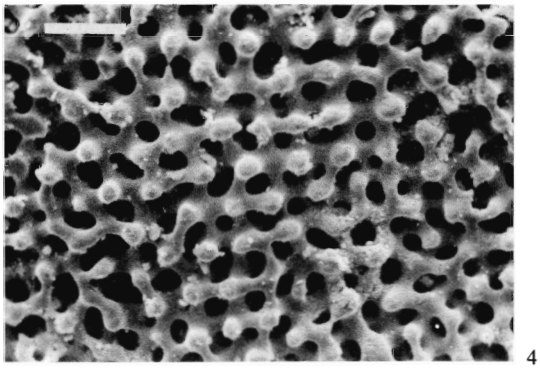

4

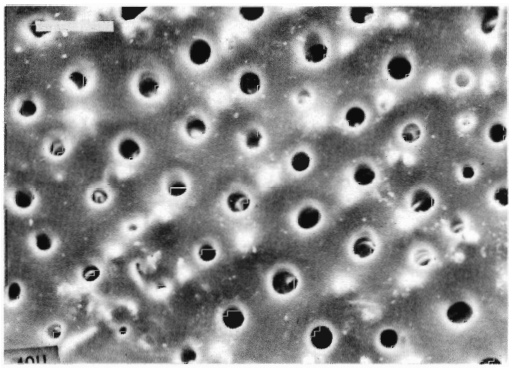

5

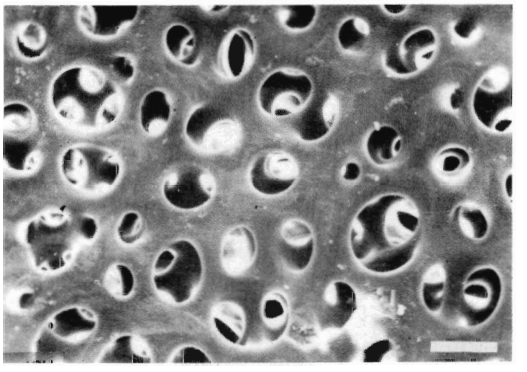

6

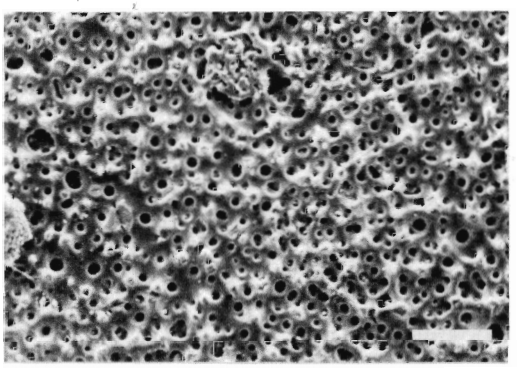

7

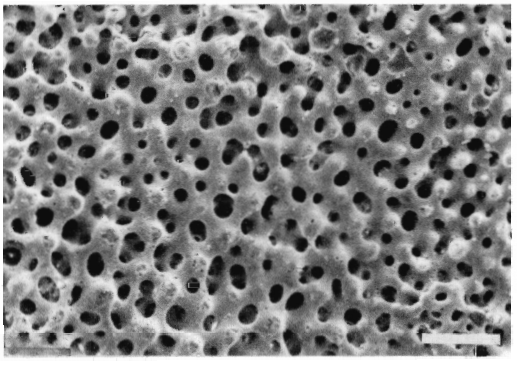

8

SMITH, plate surface stereom

Stereom pores are rounded and rather variable in size. Trabecular intersections are always smooth (Pl. 19, fig. 2). Such stereom is found in *Echinometra*, *Paracentrotus*, *Apatopygus*, *Fellaster*, *Mellita*, *Encope*, *Brissopsis*, *Spatangus*, and *Echinocardium*. It may also be found in some tubercles of *Echinolampas* and *Cassidulus* in the vicinity of the boss. In some echinoids the stereom of the area lying between the boss and areole resembles the stereom which lies outside the areole except that thorns may be absent or only poorly developed. This is true for *Centrostephanus nitidus*, *Temnopleurus*, *Tripneustes*, *Echinus*, and *Echinoneus* (Pl. 17, fig. 4). In the sunken tubercles of *Clypeaster*, *Cassidulus*, and *Echinolampas* the stereom of the area between the boss and the areole is commonly galleried and orientated parallel to the plate surface (Pl. 19, fig. 1). In *Calveriosoma* and *Phormosoma* the lower part of the boss is composed of a coarser labyrinthic stereom than the rest of the boss (Pl. 17, fig. 3). Collagenous catch apparatus fibres still insert into this stereom, however, although not very deeply.

Tube foot attachment area

Each tube foot attachs on to the stereom by its collagen layer and collagen fibres from the tube foot are looped around the surface layer of trabeculae (Pl. 23, fig. 5). Occasionally fibres may penetrate down to the next layer of trabeculae. The collagen layer of the tube foot inserts at the outer margin of the attachment area and, where there are many muscle fibres, extends inwards forming a thin ligamentous layer for the attachment of the muscle fibres. This ligamentous collagen is bound round the surface layer of trabeculae. The attachment of spine muscle and tube foot muscle is therefore very similar and, not surprisingly, the associated stereom is more or less identical (text-fig. 12).

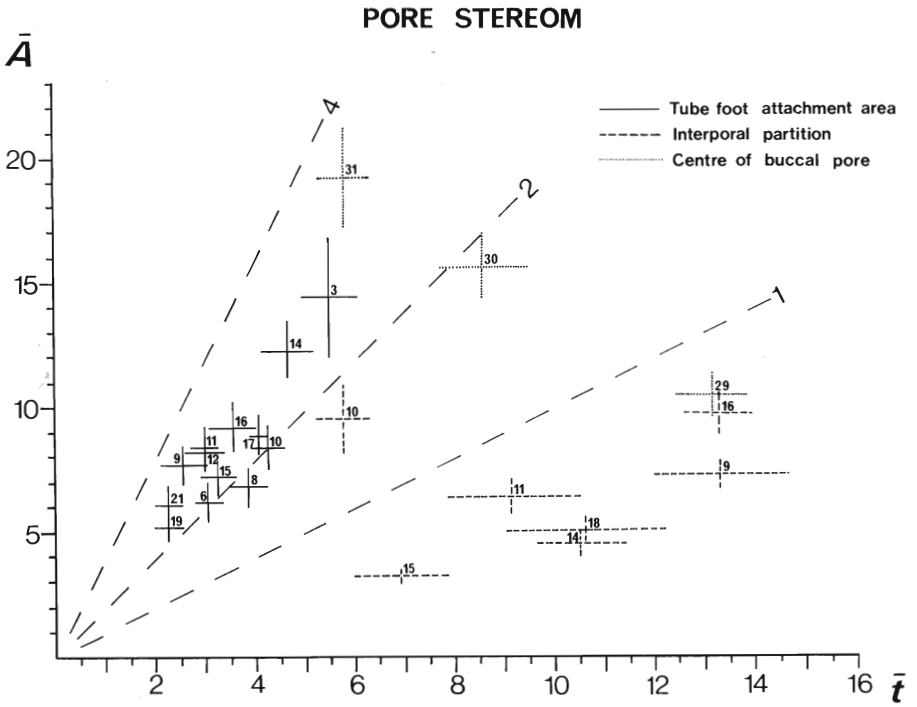

TEXT-FIG. 12. A plot of data on stereom of the tube foot attachment area and intrapodial area. The mean ± 2 standard errors is given for each species. Species are listed in Table 3.

3. Retiform stereom layer. In the spatangoids examined, muscle fibres attach on to a well-defined retiform layer (Pl. 5, figs. 1–4; Pl. 16, fig. 5). Average pore size for this stereom is less than 6 μm and the pores may be aligned. Trabecular intersections are always smooth. Spine muscle attaches to retiform stereom layers in *Mellita*, *Encope*, *Eupatagus*, *Brissopsis*, *Spatangus*, and *Echinocardium*.

Area separating the boss and areole

In most large tubercles of irregular echinoids there is a circular area, lying between the boss and the areole, on to which neither collagenous catch apparatus nor muscle inserts. Only a thin collagenous membrane extends across this stereom. Where this region is broad and well defined, as is found in most irregular echinoids, an open or sparse labyrinthic stereom is found (text-fig. 11).

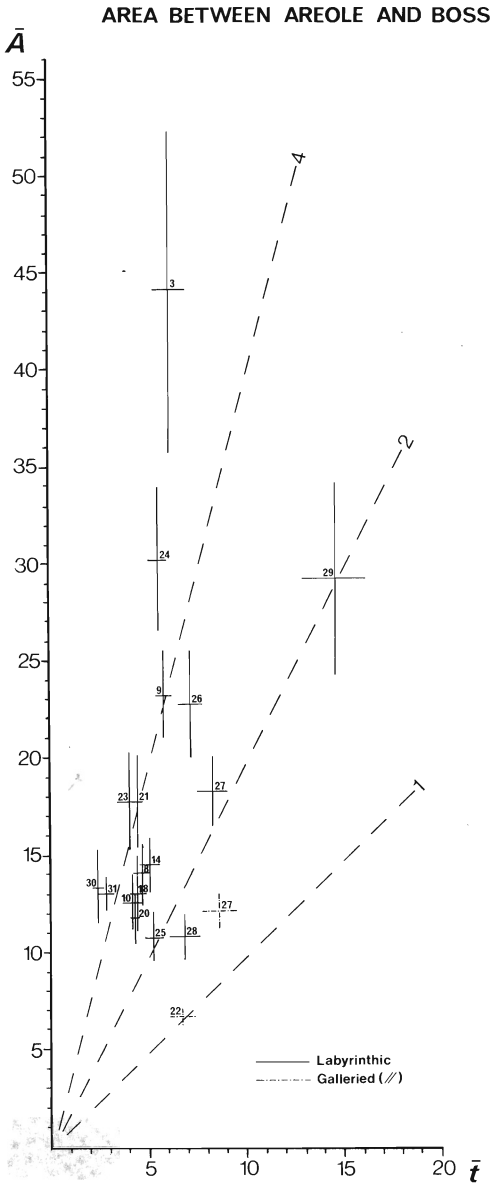

TEXT-FIG. 11. A plot of data on stereom of the region lying between the areole and boss associated with a thin collagenous membrane. The mean ± 2 standard errors is given for each species. Species are listed in Table 3.

In most cases the stereom of the tube foot attachment area is an open labyrinthic stereom overlay to the plate surface. The stereom pores are often angular and are variable in size. It has a rather ragged appearance because of the presence of numerous free-ended trabeculae which stick out in all directions (Pl. 20, figs. 1–3). Where the attachment area is narrow, the stereom often forms a prominent ridge. If the attachment area is broad then the trabeculae may form small pegs perpendicular to the plate surface. In *Tripneustes*, *Temnopleurus*, and aboral isopores of *Echinus* the attachment area is far less obvious but equally distinctive. Here the stereom pores become very much smaller and more numerous where the tube foot attaches (Pl. 19, fig. 6). Pore size and trabecular thickness are much the same as in other species.

Area lying within the tube foot attachment area

In isopores this includes only the interporal partition or conjugate furrow (Smith 1978*a*) but in unipores there is often a broad region of stereom to one side of the pore which is enclosed within the tube foot. These surfaces are covered by a single layer of squamous epithelial cells with occasional cilia. The underlying stereom is typically dense or compact (text-fig. 12). Where the interporal partition is narrow it is formed of an open labyrinthic stereom (the area available is too small to measure). In species with a broader interporal partition the stereom is denser and forms a perforate stereom layer. In *Echinoneus* the interporal partition is a smooth, imperforate stereom. The compact stereom of broad interporal partitions has surface domes or ridges which are commonly aligned (Pl. 20, fig. 4). The surface is perforated by small, circular to oval pores with a diameter of less than 10 μm. The periporal area of unipores was analysed only in the phyllode pores of *Brissopsis*, *Spatangus*, and *Echinocardium*. The associated stereom is varied (text-fig. 12). In *Spatangus* and *Echinocardium* the stereom is labyrinthic. Pores are rounded and trabeculae fairly uniform in size with smooth intersections. In *Brissopsis* the stereom varies from a dense, labyrinthic texture peripherally to a compact, perforate stereom with small, round, uniformly sized pores near the centre (Pl. 20, fig. 3). Trabecular intersections are smooth.

Pore wall

The ambulacral pores, which connect the external tube feet with their internal ampullae, are lined with a single layer of densely packed epithelial cells with horse-shoe shaped nuclei (Pl. 23, figs. 7, 8). These cells possess numerous cilia which extend well into the lumen of the pore. At the base of the epithelial layer fine branching muscle fibres may be present, running circumferentially. This is separated from the underlying connective tissue of the plate by a very thin basal membrane. The stereom of the pore wall shows great variation, even within the same pore, and galleried, perforate,

---

EXPLANATION OF PLATE 16

Fig. 1. Collagen fibres, arranged into bundles, penetrating into the boss of an ambital interambulacral plate of *Psammechinus miliaris* along galleries in the stereom.

Fig. 2. Labyrinthic stereom forming the boss of a primary ambital interambulacral tubercle of *Centrostephanus longispinus*.

Fig. 3. Labyrinthic stereom forming the boss of an aboral interambulacral tubercle of *Phormosoma placenta*.

Fig. 4. Labyrinthic stereom forming the lower part of the boss of an aboral interambulacral tubercle of *Micropyga tuberculata*.

Fig. 5. Stereo-view of an aboral interambulacral tubercle of *Spatangus raschi* showing the superficial similarity of labyrinthic stereom of the boss (to the left) and areole (to the right).

Scale bar in Figs. 1–3, 5 = 20 μm; Fig. 4 = 100 μm.

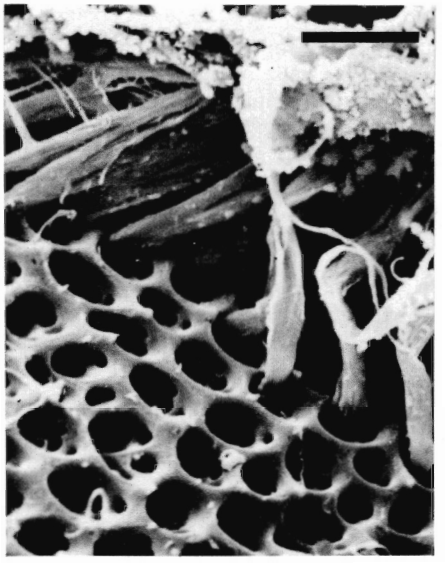

1

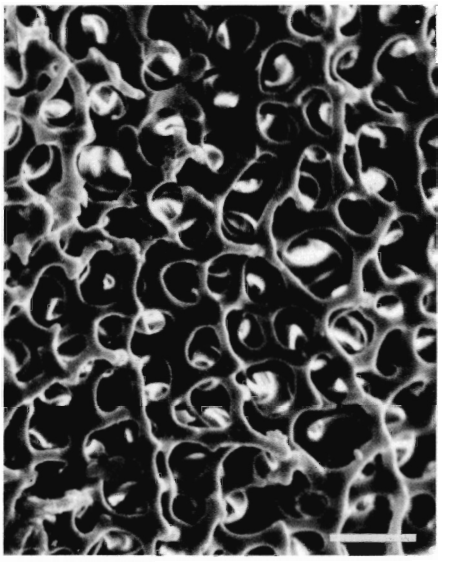

2

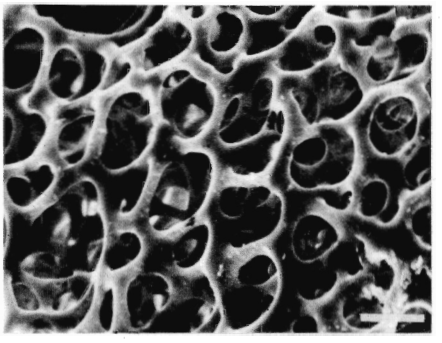

3

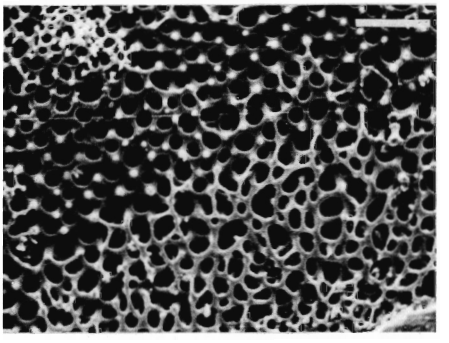

4

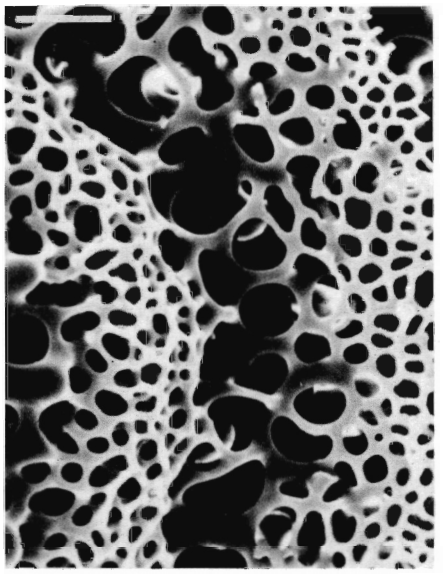

5

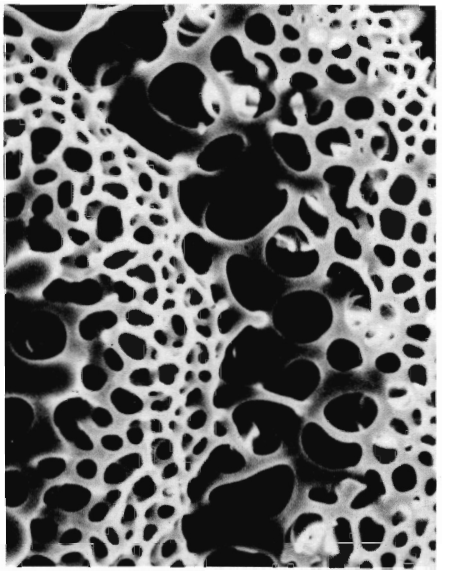

SMITH, boss stereom

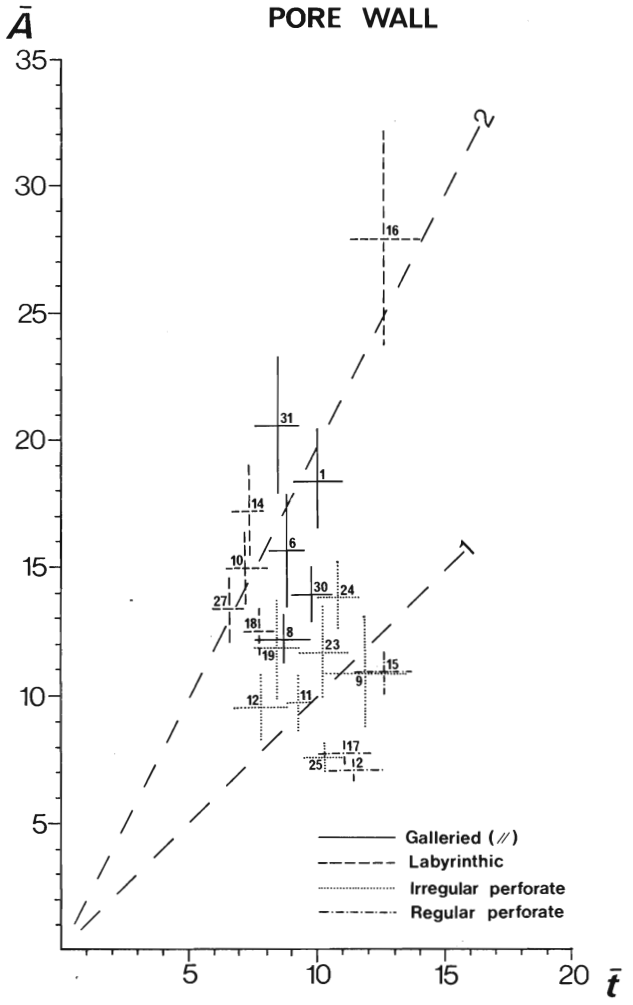

TEXT-FIG. 13. A plot of data on stereom forming the walls of ambulacral pores where ciliated endothelium is found. The mean ± 2 standard errors is given for each species. Species are listed in Table 3.

or labyrinthic stereom may be present (text-fig. 13; Pl. 20, figs. 5–7). In every case the trabeculae were seen to have smooth intersections. Perforate stereom of the pore wall usually displays some pore alignment. Because stereom fabric varies even within one pore little weight can be placed on the stereom analysis.

EXPLANATION OF PLATE 17

Fig. 1. Stereo view of a primary interambulacral tubercle of *Echinostrephus molaris*. The superficial labyrinthic stereom overlay of the areole can be seen in the upper part and galleried stereom of the boss in the bottom right of the electron micrograph.

Fig. 2. Side view of an oral interambulacral primary tubercle of *Calveriosoma hystrix* showing the laminar stereom of the areole surrounding the boss.

Fig. 3. Aboral interambulacral primary tubercle of *Phormosoma placenta* with laminar stereom of the areole to the bottom and labyrinthic stereom of the boss to the top.

Fig. 4. Stereo view of a primary interambulacral tubercle of *Echinus esculentus* showing galleried stereom of the boss at the top and a labyrinthic intergrowth of stereom forming the areole at the bottom.

Scale bar in Figs. 1 and 4 = 40 μm; Fig. 3 = 100 μm; Fig. 2 = 200 μm.

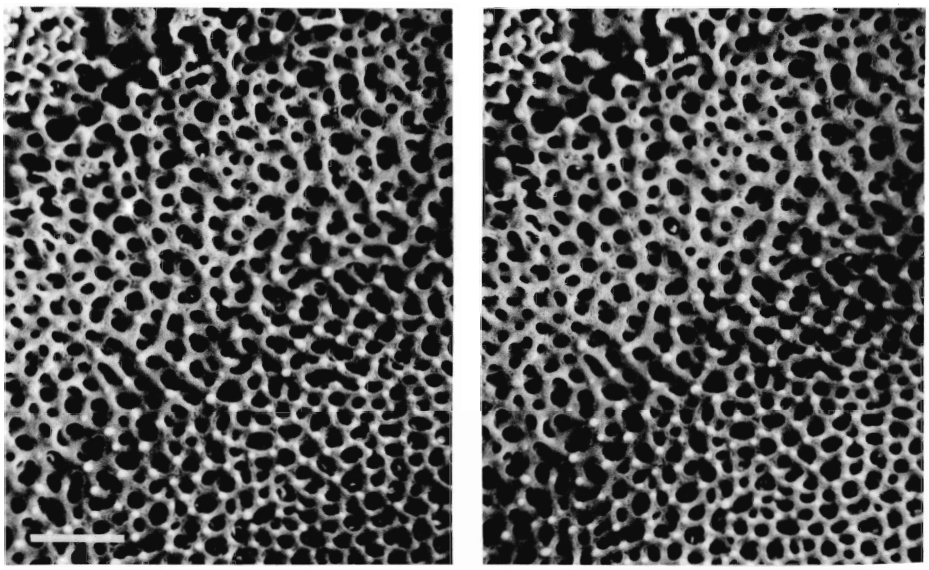

1

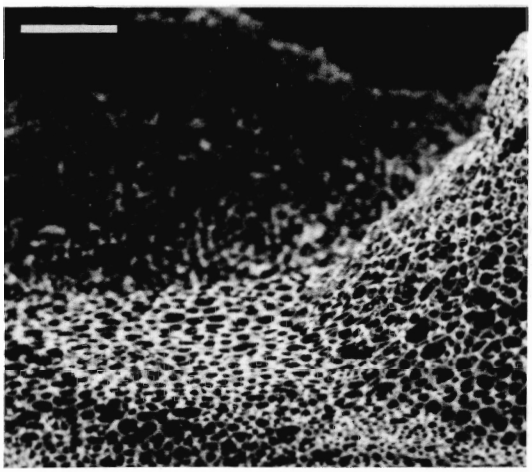

2

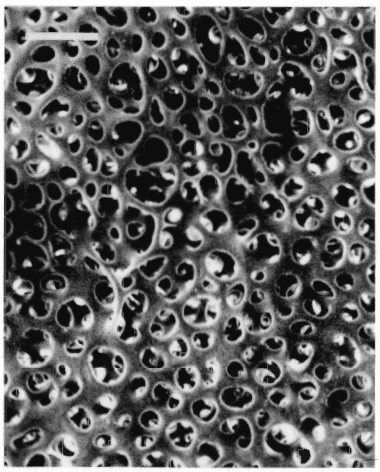

3

4

SMITH, areole stereom

Suture face

In echinoids with rigid tests, adjoining plates are bound together by collagen fibres. These fibres are arranged into bundles which may penetrate quite deeply into each plate following galleries in the stereom. As in the collagenous catch apparatus, groups of fibres periodically branch from the main bundles and pass under trabecular struts to merge with neighbouring bundles, thus looping the fibres around the trabeculae (Pl. 23, fig. 10). Deeper fibres terminate by looping themselves around a trabecula. Penetration occurs to an equal depth on either side of the suture. As would be expected, the stereom at suture faces has galleries running perpendicular to the surface.

The rods, which form the galleried stereom of the plate, are enlarged at the suture face to produce prominent pegs which interlock into depressions in the adjacent plates (Pl. 19, fig. 3). In some cases long thorns may be developed which penetrate deep into the neighbouring plate (Pl. 14, fig. 5). In the aboral ambulacra of *Fellaster*, the trabeculae of one plate may even grow around the trabeculae of the neighbouring plate (Pl. 19, fig. 4). In this case plate growth has presumably ceased in an apical/oral direction. The development of dowel-like interlocking pits and pegs on the suture face of plates of the Temnopleuridae is another device to strengthen the bond between plates. In the echinothuriids, which possess flexible tests, individual plates are embedded in a mass of connective tissue fibres (see Moss and Meehan, 1967). These fibres do not penetrate into the stereom of the plate and only small fibres are seen occasionally to enter the surface stereom layer. No suture face is present in these plates.

The stereom at the plate suture face is similar in all species examined (text-fig. 14). It has rather uniformly sized, circular, or oval pores separated by trabeculae which show little variation in thickness. Trabecular intersections extend outwards as pegs or thorns (Pl. 19, fig. 5). Pores are usually randomly arranged over the surface, though in some there is a tendency towards a linear arrangement, with pores paralleling the plate surface. Internal pore alignment varies from poor (Pl. 21, fig. 2) to excellent (Pl. 21, fig. 1). This variation stems from the stereom microstructural banding of the plate during growth. Stereom which shows only poor internal alignment commonly has a maze-like surface arrangement of trabeculae (Pl. 21, fig. 3). Plate suture faces of *Centrostephanus nitidus* have a central region of laminar stereom bounded both internally and externally by more normal galleried stereom (Pl. 6, fig. 7). This laminar layer is developed only towards the lateral sutures.

Internal plate surface

The inner surface of the test of echinoids is lined with a single layer of squamous epithelial cells with well-spaced nuclei. This layer is sparsely ciliated. As a result of the plate construction, the peripheral area of each plate often has a different stereom from the rest of the plate although both are

EXPLANATION OF PLATE 18

Fig. 1. Stereo view of labyrinthic stereom forming the areole in an ambital interambulacral tubercle of *Temnopleurus hardwickii.*

Fig. 2. Stereom of an ambital interambulacral tubercle of *Psammechinus miliaris.* Labyrinthic stereom of the areole is clearly distinguished from galleried stereom of the boss (bottom right) and perforate stereom of the plate surface (top left).

Fig. 3. Labyrinthic stereom of the areole of an oral interambulacral tubercle of *Mellita quinquiesperforata.*

Fig. 4. Stereo view of the thin labyrinthic stereom overgrowth forming the areole of an aboral interambulacral tubercle of *Echinoneus cyclostomus.*

Fig. 5. Stereo view of the labyrinthic stereom veneer forming the areole of an aboral interambulacral tubercle of *Encope michelini.* Galleried stereom of the boss can be seen in the bottom left of the micrograph.

Scale bar in Figs. 1, 2 = 40 μm; Figs. 3–5 = 20 μm.

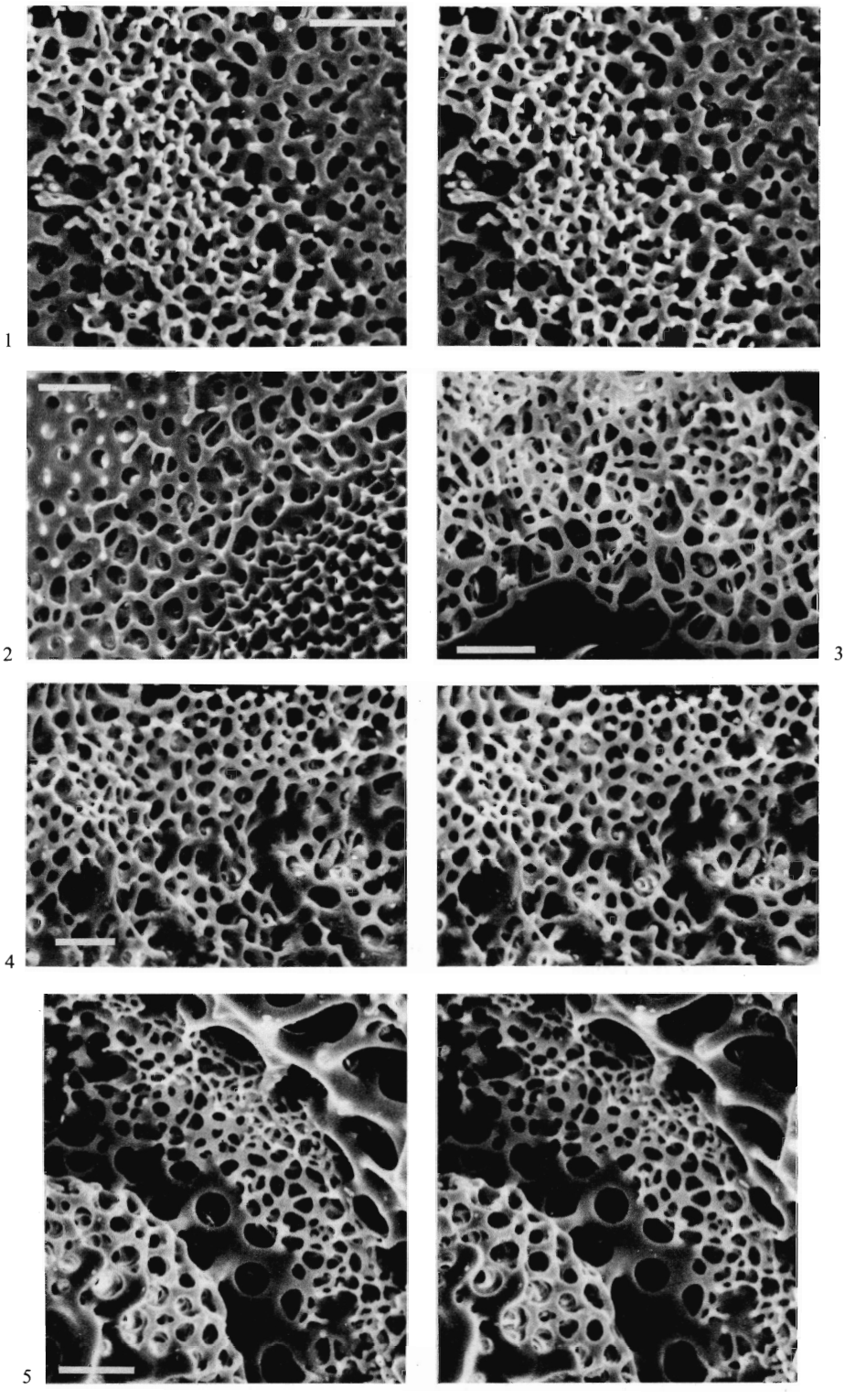

SMITH, areole stereom

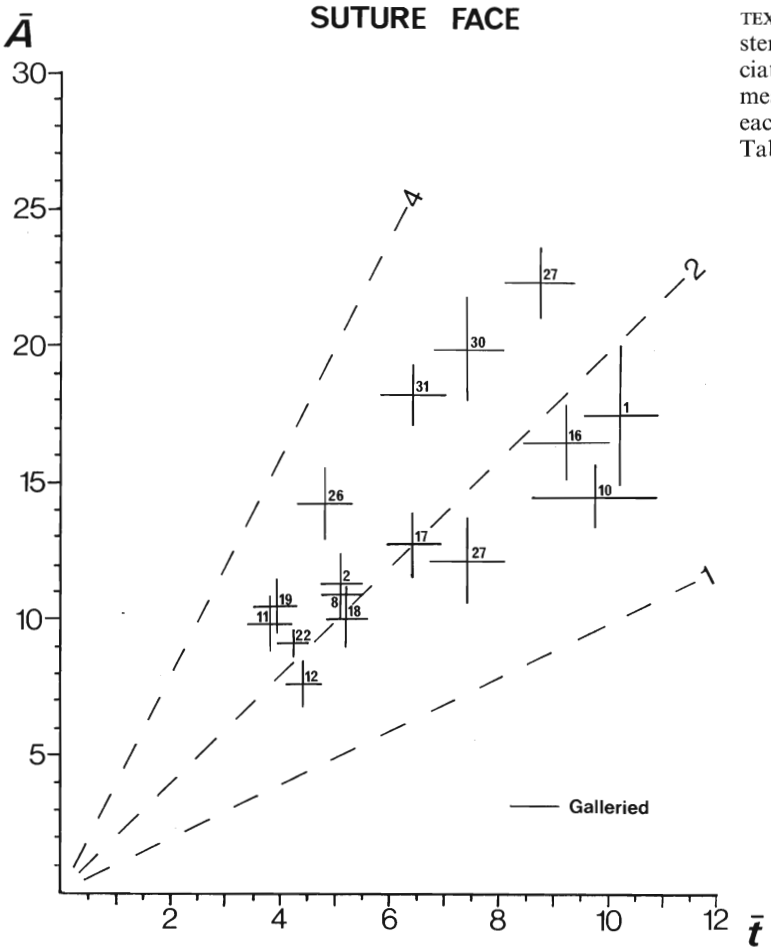

TEXT-FIG. 14. A plot of data on stereom of the lateral plate face associated with sutural collagen fibres. The mean ± 2 standard errors is given for each species. Species are listed in Table 3.

covered in the same endothelial layer. The stereom is no different where the radial nerve, or any of its branches, passed across the plate interior. Variation in internal stereom is quite marked between species (text-fig. 15) and the following surface arrangements can be identified:

1. Labyrinthic. A very coarse, sparse labyrinthic stereom is found on the inner surface of plates of *Cidaris*, *Calveriosoma*, and *Echinus esculentus* (Pl. 3, figs. 3, 4; Pl. 4, fig. 3). Pores are variable, both in size and shape, and trabeculae are relatively thin and uniform in size. All trabecular intersections are smooth. The extreme openness of the stereom fabric permits one to see deep into the plate interior. A similar, but somewhat less coarse, open labyrinthic stereom forms the inner plate surface of *Eucidaris*, *Echinometra*, *Paracentrotus*, *Clypeaster*, *Fellaster*, and some plates of *Tripneustes*. Dense labyrinthic stereom, presenting an almost planar surface, is found over much of the inner plate surface of *Arbacia*, *Echinostrephus*, and *Colobocentrotus* (Pl. 21, fig. 7). The pores of this stereom are irregularly shaped and randomly arranged. Trabecular intersections are smooth.

2. Planar. Without examining the cross-sectional construction of the plate, it is difficult to differentiate between laminar, perforate and microperforate stereoms simply from the superficial appearance. These have therefore been grouped together under the term planar stereom. Such stereom has circular pores irregularly arranged over a planar surface. Trabecular intersections are smooth in all specimens examined. The stereom is coarse and open where there is a perforate stereom layer as in plates of *Psammechinus*, *Tripneustes*, and *Stomopneustes* (Pl. 22, fig. 1; Pl. 8, fig. 4). The laminar stereom of *Brissopsis*, *Spatangus*, *Echinocordatum*, and *Eupatagus* is a little more dense (text-fig. 15; Pl. 4, fig. 6). In *Encope* and *Mellita* the internal surface is a thin consolidated

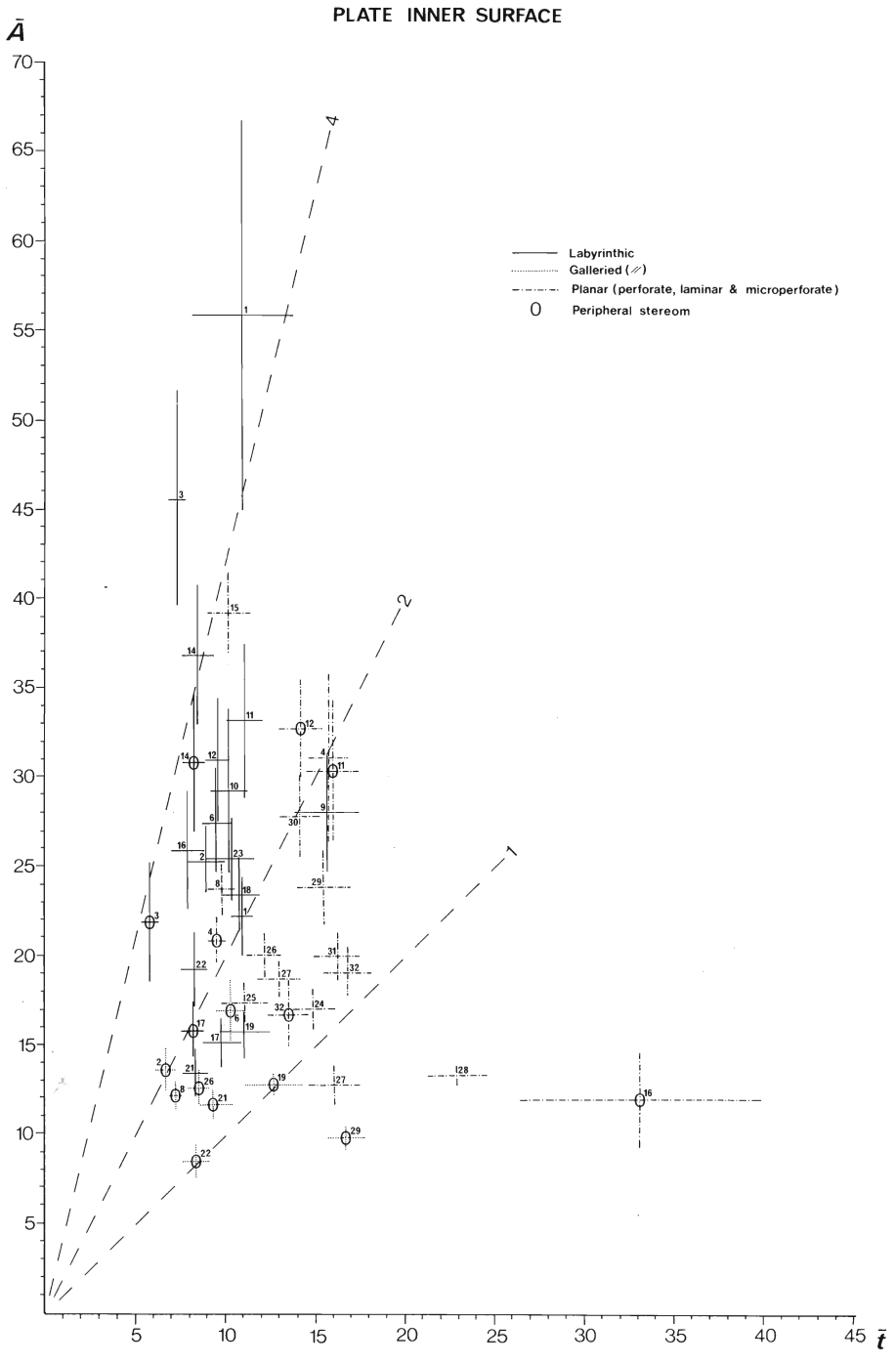

TEXT-FIG. 15. A plot of data on stereom of the inner plate surface where endothelium is found. The mean ± 2 standard errors is given for each species. Species are listed in Table 3.

layer which is indistinguishable from other planar stereoms (Pl. 21, fig. 6). The microperforate stereom of *Apatopygus* and *Echinolampas* is more compact than other planar stereoms and has smaller pores (Pl. 3, fig. 2). Variation in the pore size and porosity of the stereom found in the inner surface of plates of *Echinolampas* is likely to be the product of changes during growth of the stereom. In *Phormosoma* much of the interior of the plate is planar although the stereom is very irregular; much more so than the planar stereom of the outer plate surface. The retiform layer, seen in cross-sections of these plates, may appear at the inner plate surface towards the edge of the plate but this does not form a proper margin to the plate as it is very patchily distributed.

Towards the plate edge in other echinoids, pore size decreases while the number of pores increase (text-fig. 15; Pl. 21, fig. 4). There may also be a marked change in the stereom organization. The marginal zone of the inner plate surface in *Cidaris*, *Eucidaris*, *Stomopneustes*, *Echinostrephus*, *Echinoneus*, *Clypeaster*, *Cassidulus*, *Brissopsis*, *Echinocardium*, and *Eupatagus* is composed of galleried stereom orientated with the galleries paralleling the plate's inner surface (Pl. 21, fig. 8; Pl. 4, fig. 5). In this stereom, major rods run perpendicular to the plate margins and the pores are circular or oval and fairly uniform in size. Trabecular intersections are smooth. In *Echinus esculentus* and *Calveriosoma*, stereom at the plate periphery is much the same as at the centre of the plate and is composed of open labyrinthic stereom with smooth trabecular intersections. In *Psammechinus* and *Tripneustes* the marginal stereom, which is a smooth perforate stereom, is a little less coarse than stereom at the plate centre. There is also little variation over the inner plate surface in *Arbacia*, *Temnopleurus*, *Colobocentrotus*, *Echinometra*, *Echinolampas*, *Fellaster*, *Encope*, and *Mellita*. In all of these echinoids the stereom at the periphery of the plate is less coarse than, but similar in construction to, stereom towards the plate centre. In *Paracentrotus* the marginal area of the inner surface of the plates is a compact perforate stereom and, in places, comes close to being imperforate. This rather rough-surfaced stereom is perforated by small irregular-shaped pores in no particular arrangement (Pl. 7, fig. 8). The compact layer is overlain centrally by labyrinthic stereom. Only the very central part of the inner surface of plates of *Centrostephanus* is composed of open labyrinthic stereom. Surrounding this, and forming the major part of the inner plate surface, is a dense planar stereom (Pl. 21, fig. 5). This stereom has oval or irregular-shaped pores and all trabecular intersections are smooth.

Other areas

Small, raised regions of the plate surface, which are commonly termed granules, were found in *Arbacia*, *Echinus acutus*, and the cassiduloids that were examined. These granules are overlain by integument which does not appear to differ in detail from the surrounding integument of the plate surface. The superficial stereom of these structures is very compact, with only occasional small circular pores (Pl. 22, fig. 2). In some cases the stereom is imperforate (Pl. 22, fig. 3). The surface of these granules is covered in pronounced thorns.

EXPLANATION OF PLATE 19

Fig. 1. Stereo view of an oral interambulacral tubercle of *Clypeaster rarispina* showing the galleried stereom which separates the labyrinthic stereom of the areole (top left) from labyrinthic stereom of the boss (bottom right).

Fig. 2. Stereo view of an aboral interambulacral tubercle of *Encope michelini* showing the sparse labyrinthic stereom which separates the labyrinthic stereom of the areole (right) from galleried stereom of the boss (left).

Fig. 3. Aboral ambulacral/interambulacral plate suture of *Cidaris cidaris* (internal surface) showing interdigitation of stereom pegs.

Fig. 4. Aboral ambulacral/ambulacral plate suture of *Fellaster zealandiae* (external surface) showing intergrowth of trabeculae.

Fig. 5. Stereo view of galleried stereom of the lateral face of an aboral interambulacral plate of *Echinolampas crassa*.

Fig. 6. Stereo view of the attachment area in an aboral isopore of *Temnopleurus hardwickii* (seen as a horizontal band of smaller pores). Part of the interporal partition appears towards the base.

Scale bar in Fig. 4 = 10 μm; Fig. 3 = 20 μm; Figs. 1, 2, 5, 6 = 40 μm.

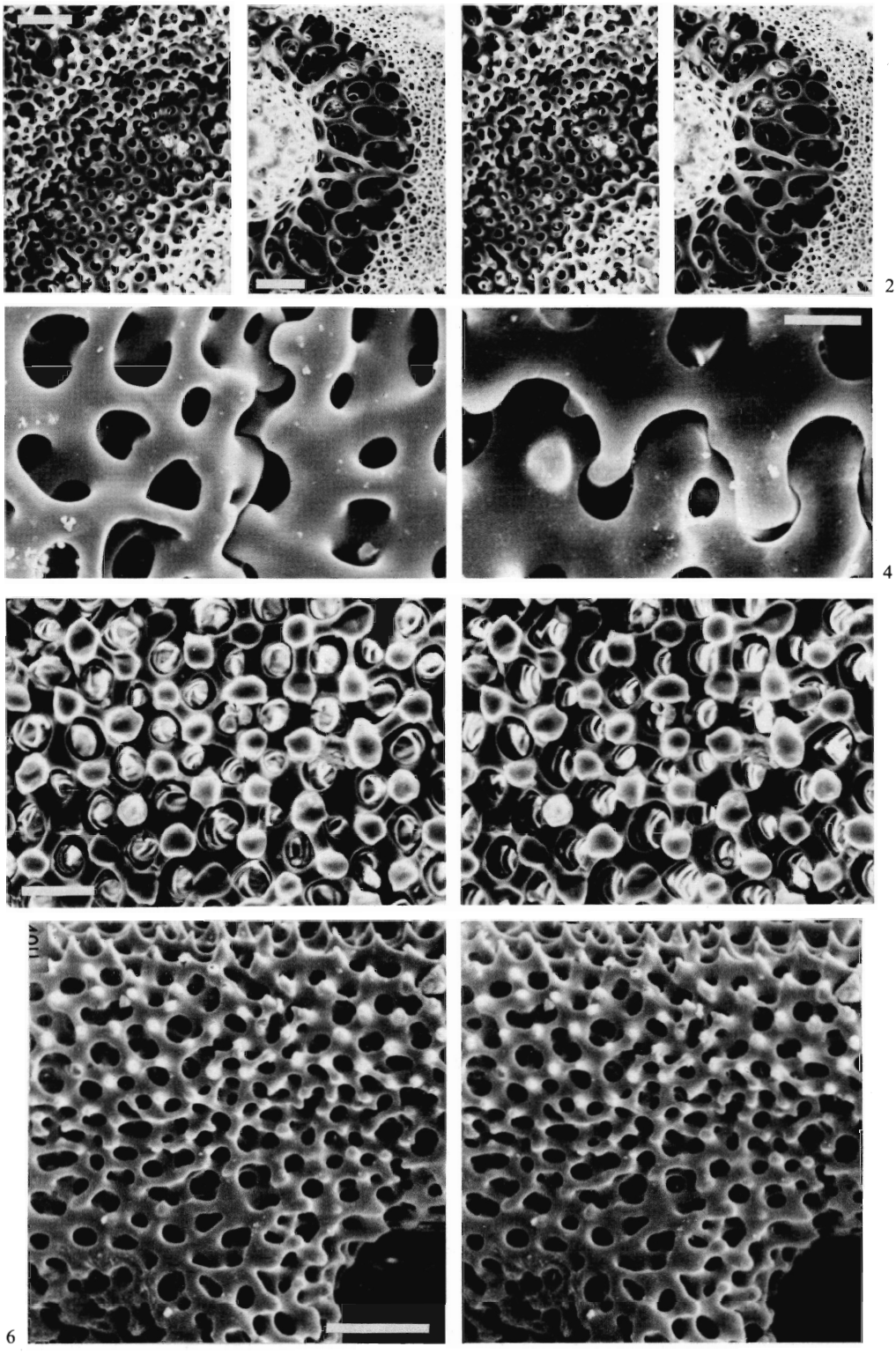

SMITH, echinoid stereom

RELATIONSHIP TO INVESTING SOFT TISSUE

It is clear that the stereom pattern at the surface of the plate is largely dependent upon the construction of the plate. Resorption, stereom growth rate and associated soft tissue all act to modify the stereom to a greater or lesser extent. This modification is less pronounced in the more primitive groups of echinoids. If the aim of microstructural analysis is the identification of associated soft tissues, plate construction and growth must be fully understood before surface variation of the stereom can be interpreted.

One of the major stumbling blocks to producing a generalized scheme for interpreting stereom microstructure arises from the variation in plate construction within the Echinoidea. In practical terms this means that, although stereoms supporting different tissues are quite distinct in most groups of closely related species (with a similar plate construction) (text-figs. 16, 17) the distinctions become blurred with the incorporation of data from other groups of echinoids which may have a very different plate construction and stereom texture. Another difficulty is posed by seasonal variation in stereom during growth. Changes in the growth rate of the plate not only affect the texture and density of the stereom but may also produce a change in the actual lattice structure. As the stereom analysis herein is drawn largely from single specimens of each species, it will not encompass all the stereom variation that may be encountered in those species. Other specimens, collected at different

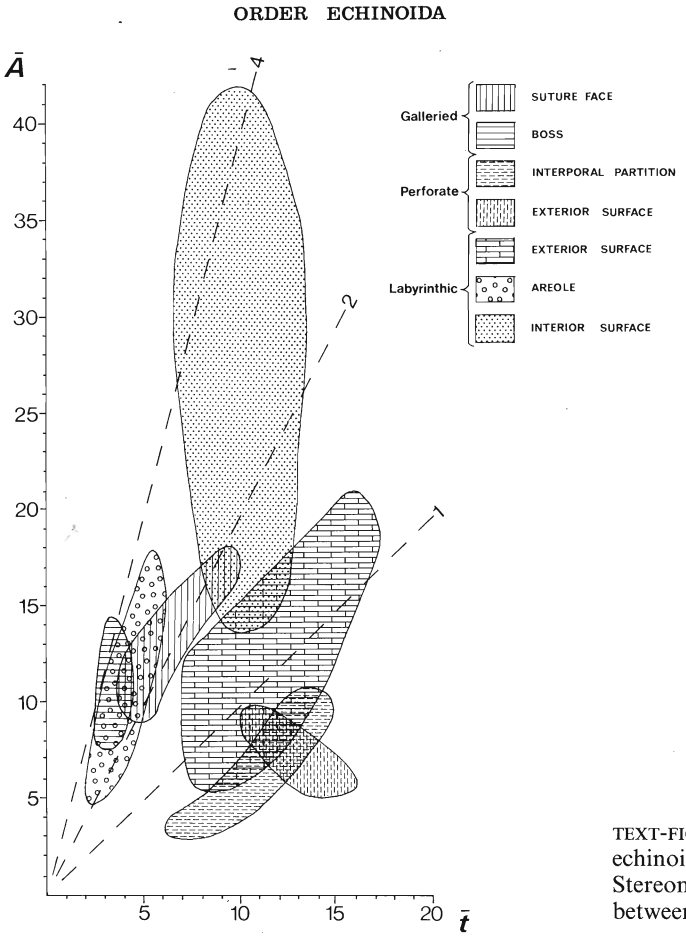

TEXT-FIG. 16. Stereom data on seven species of echinoids from the order Echinoida (see Table 1). Stereom of the inner plate surface can alternate between perforate and labyrinthic design.

times of the year, may have a different superficial stereom in regions of the plate where growth banding occurs. However, by combining the data from all echinoid species examined, it is possible to define graphically areas within which stereom is associated with one particular tissue. Because of the number and diversity of species covered, I believe that there is a good coverage of the variation that might be expected to occur. Measurements of pore size and trabecular thickness are of little use on their own without taking into consideration the three-dimensional stereom arrangement. For this reason galleried, labyrinthic, and planar stereoms have been treated separately. These three stereom arrangements should be readily distinguishable even in fossil material, especially if plate cross-sections are available. The stereom distributions are illustrated in text-figs. 18, 19, and 20. It can be seen from this that quantitative data, on their own, are not sufficient to allow the distinction of stereoms associated with different tissues. In some cases there is considerable overlap of stereom supporting different tissues, although any one species very rarely has more than one stereom in the zone of overlap. Surface microstructure often provides additional evidence for the differentiation of stereoms. Table 4 lists the different superficial stereom fabrics encountered in this study and gives the soft tissues with which each was associated. Scrutiny of this table will show that some stereom arrays may be found with a number of different tissues whereas others are associated with only one. In no case is one tissue found to be restricted to a single stereom array. The stereom patterns associated with each type if tissue will now be dealt with in turn.

Collagenous fibres

The stereom associated with collagenous fibres is often distinctive because of the presence of galleries running perpendicular to the plate surface. Collagenous fibres are arranged into bundles which penetrate into the plate along these galleries. It is thought that stereom growth is restricted by the presence

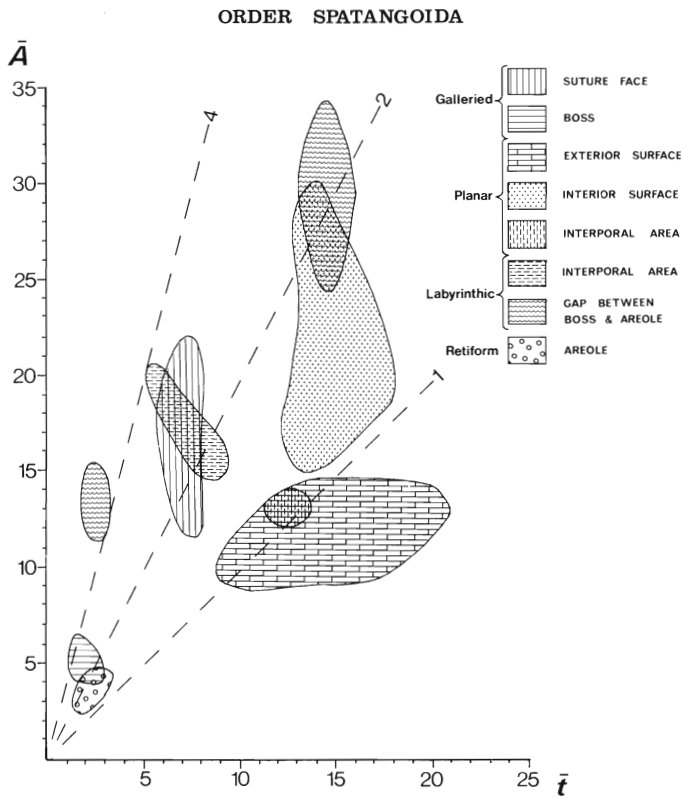

TEXT-FIG. 17. Stereom data on four species of echinoids from the order Spatangoida.

TABLE 4. Summary of stereom types and associated soft tissue.

Lattice	*Surface organization*	*Plate*	*Associated soft tissue*
Rectilinear	Linearly arranged galleries.	Plate 1, fig. 1	Ectoderm, muscle, catch apparatus
Galleried	Galleries perpendicular to plate surface: trabecular intersections smooth or with small thorns.	Plate 2, fig. 3	Catch apparatus
	Galleries perpendicular to plate surface: trabecular intersections developed into large pegs or thorns.	Plate 19, fig. 5	Sutural collagen
	Galleries parallel to plate surface: trabecular intersections smooth.	Plate 4, fig. 5 Plate 20, fig. 7	Coelomic epithelium, muscle
	Galleries parallel to plate surface: trabecular intersections with thorns or pegs.	Plate 22, fig. 4	Ectoderm
Perforate	Surface planar and smooth.	Plate 20, fig. 6	Coelomic epithelium
	Surface planar with prominent thorns.	Plate 15, fig. 5	Ectoderm
	Surface with pronounced domes.	Plate 8, fig. 3	Ectoderm, coelomic epithelium of the interporal partition
Laminar	Pores round and uniform in size.	Plate 4, fig. 6	Coelomic epithelium
	Pores oval and variable in size and shape.	Plate 15, fig. 6	Ectoderm, muscle
Microperforate	Surface planar and smooth.	Plate 3, fig. 2	Coelomic epithelium
Labyrinthic	Coarse, dense to sparse stereom: trabecular intersections smooth.	Plate 4, fig. 3	Coelomic epithelium
	Dense to open stereom with a medium to coarse texture: trabecular intersections with prominent thorns or pegs.	Plate 15, fig. 1	Ectoderm
	Fine to coarse, open or sparse stereom with very irregular pore size and shape: trabecular intersections largely smooth and with some free-ended trabeculae. Forms a surface layer of moderate thickness.	Plate 16, figs. 2, 3	Catch apparatus
	Medium to fine, open stereom forming an overlay to the plate surface of only one or two trabecular layers: trabeculae variable in size: intersections swollen, sometimes with pegs or thorns: pores irregular in shape and often angular, with many free-ended trabeculae.	Plate 18, fig. 1	Muscle
	Medium to fine, open stereom formed by the intergrowth of small trabeculae between existing plate trabeculae. Forms a thin veneer of only one or two trabecular layers. Texture as above.	Plate 19, fig. 6	Muscle
Retiform	Pores in regular arrangement, or unorganized	Plate 5, figs. 1, 4	Muscle

of these fibres and that trabecular struts can only grow around fibre bundles, so that pore alignment is maintained during growth. Galleried stereom, with galleries running perpendicular to the plate surface, is always found to support collagenous fibres. This is not true for galleries in rectilinear stereom. The length of the galleries does not, however, reflect the depth of penetration of collagenous fibres. These fibres die off internally as growth proceeds so that penetration never usually exceeds 100 μm to 150 μm. During periods of minimal plate growth collagenous fibres become associated

with a superficial labyrinthic stereom. It is suspected that periods during which little growth occurs give time for the fibres to become reorganized thus destroying pore alignment. Stereom growth banding is readily apparent in cross-section.

In some species collagen fibres do not penetrate the stereom in bundles but are looped around the outermost trabecular layers (Pl. 23, fig. 2). The associated stereom superficially resembles the stereom of muscle attachment. In irregular echinoids such stereom is developed because of the small size of the collagenous fibre bundles. These bundles show only limited penetration and are bound irregularly around trabeculae. The resultant stereom has an average pore size of less than 7 μm. It can be distinguished from similar-sized stereom for muscle attachment in its three-dimensional construction; fine stereom for muscle attachment always forms a single layer of labyrinthic or retiform construction whereas fine stereom with collagenous fibres forms rather a thicker veneer of at least three or four trabecular levels. Collagenous catch apparatus fibres are also found with a coarser-textured labyrinthic stereom. Here the fibres show little or no organization into bundles and penetration into the boss is limited, with most of the fibres looping around the outer trabeculae. Where

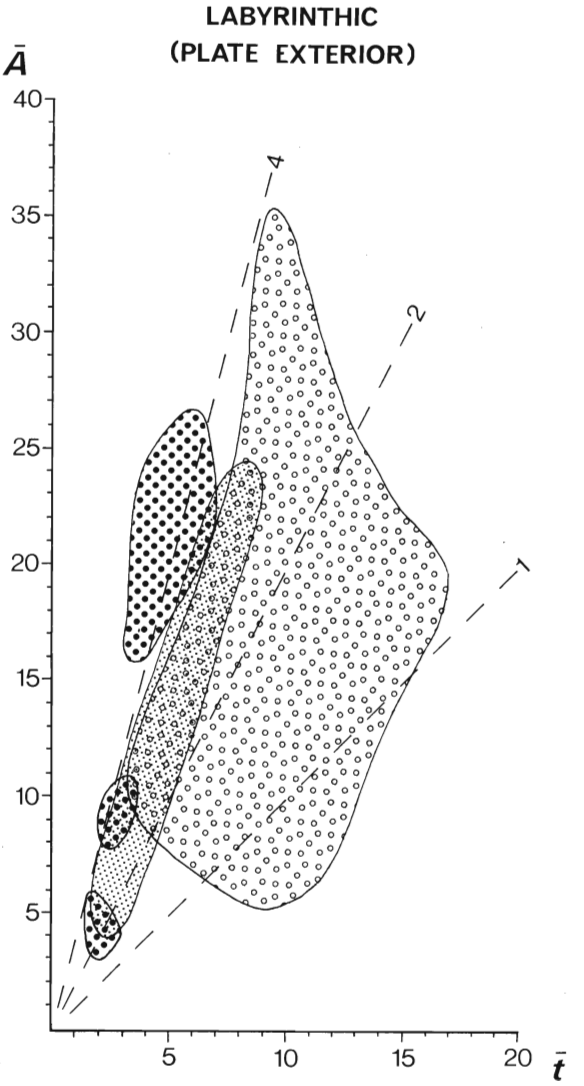

TEXT-FIG. 18. Summary of all data on labyrinthic stereom from the outer plate surface (circles), areole and tube foot attachment area (small dots), and boss (large dots).

such an arrangement is found, stereom for muscle attachment is poorly differentiated, if at all. The identification of such stereoms as areas of collagenous fibre attachment is therefore important since they could easily be mistaken for areas of muscle attachment. The coarser stereoms, with an average pores size greater than about 15 μm, are, in general, more open textured than similar-sized stereoms of muscle attachment, though a slight zone of overlap does occur (text-fig. 18). Stereoms with a smaller average pore size cannot be distinguished quantitatively from labyrinthic stereoms of muscle attachment. Plate cross-sections show that labyrinthic stereom supporting collagenous catch apparatus fibres forms a moderately thick veneer to the plate surface compared with stereoms to which muscle fibres attach.

The difference in the stereom fabric of the boss is a direct result of a difference in tubercle growth. Most large tubercles increase in size gradually over a number of seasons so that catch apparatus fibres insert into an actively outward-growing surface. These fibres can therefore exert some control on the trabecular organization and so produce a galleried arrangement. Small tubercles of scutellids and spatangoids, on the other hand, grow rapidly within a short period of time by forming a core of fascicular stereom. These tubercles do not increase in size periodically. It is only as the tubercle approaches its full size that a layer of fine labyrinthic stereom is deposited to form the surface of the boss. A very similar construction is found in the tubercles of diadematoids and echinothuriids and these are likely to have a similar method of growth. It therefore appears that collagenous fibres attach by looping around stereom of non-growing surfaces but penetrate into actively growing surfaces producing galleried stereom. This explains why fluctuation in the rate of plate growth results in the observed stereom banding of the middle plate layer.

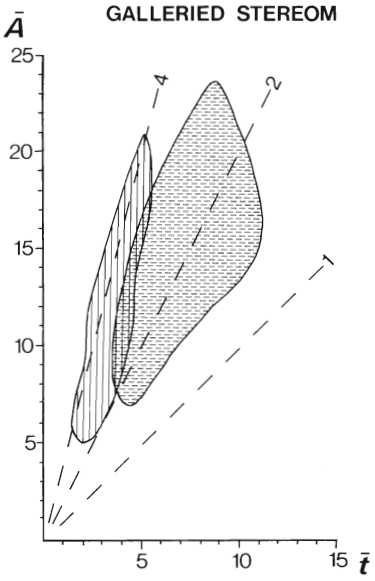

TEXT-FIG. 19. Summary of all data on galleried stereom. Vertical lines —boss: dashes—suture face.

Galleried stereom with collagenous catch apparatus fibres is more open in texture and has relatively thinner trabeculae than galleried stereom found with sutural collagen fibres (text-fig. 19). At suture faces the rods, which compose the galleried stereom, are extended outwards to form thick pegs or, occasionally, thorns and the interconnecting struts tend to be quite broad. This reflects a difference in the function of the stereom rather than a difference in the soft tissue. Whereas the stereom of the boss has only to provide attachment for the catch apparatus fibres, stereom at the suture face has also to interlock rigidly with neighbouring plates well enough to distribute external loading forces across the whole test (Moss and Meehan, 1967). Trabeculae are thickened to increase their strength

EXPLANATION OF PLATE 20

Figs. 1, 4. *Tripneustes gratilla*. 1, stereo view of the adoral attachment area and neural groove of an ambital isopore. 4, domed perforate stereom forming the interporal partition of an ambital isopore.

Fig. 2. Adapical attachment area of an ambital isopore of *Centrostephanus longispinus*.

Fig. 3. Perforate stereom of the intraporal area of a buccal unipore of *Brissopsis lyrifera*. The attachment area can be seen to the right.

Fig. 5. Labyrinthic stereom forming the pore wall of an ambital ambulacral plate of *Temnopleurus hardwicki*.

Fig. 6. Perforate stereom, showing some alignment, forming the pore wall of an aboral ambulacral plate of *Encope michelini*.

Fig. 7. Galleried stereom forming the pore wall of an ambital ambulacral plate of *Stomopneustes variolaris*.

Scale bar in Figs. 2 and 6 = 20 μm; Figs. 1, 4, 5, and 7 = 40 μm; Fig. 3 = 100 μm.

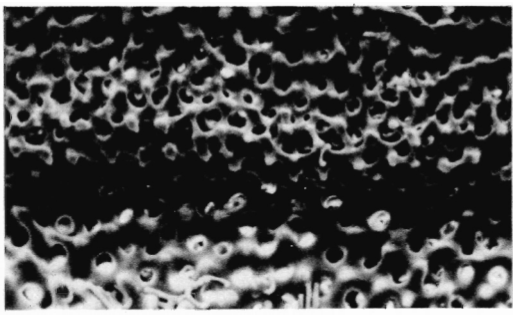

1

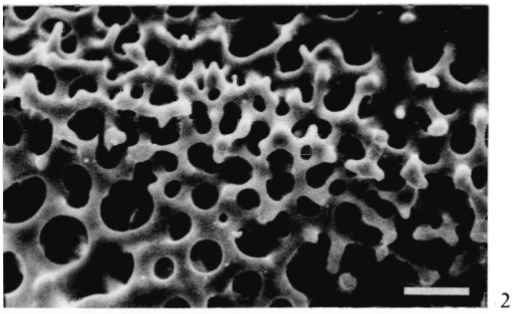

2

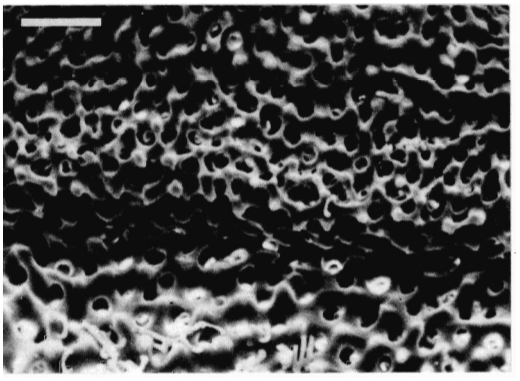

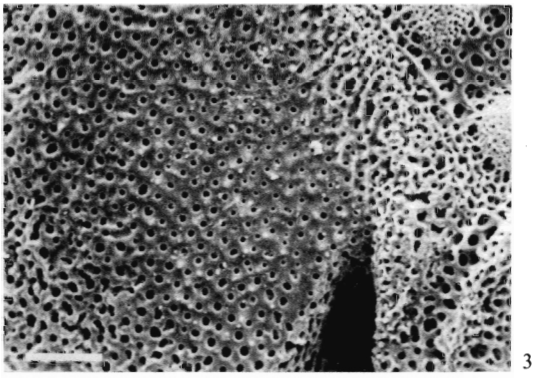

3

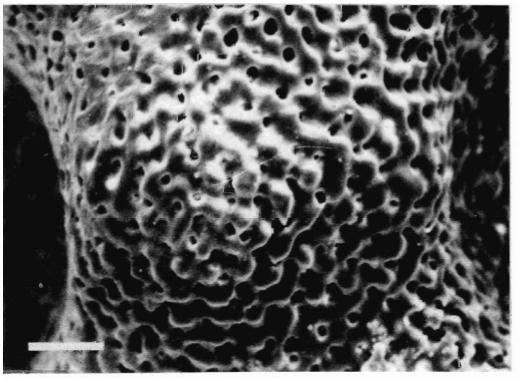

4

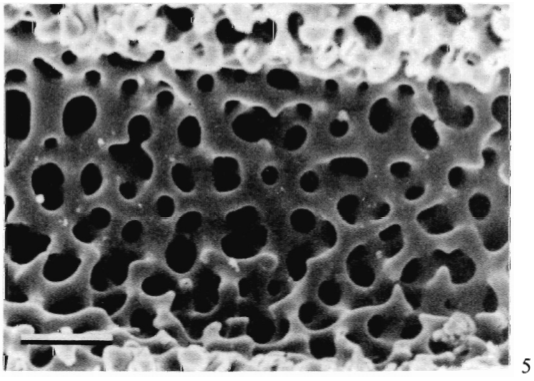

5

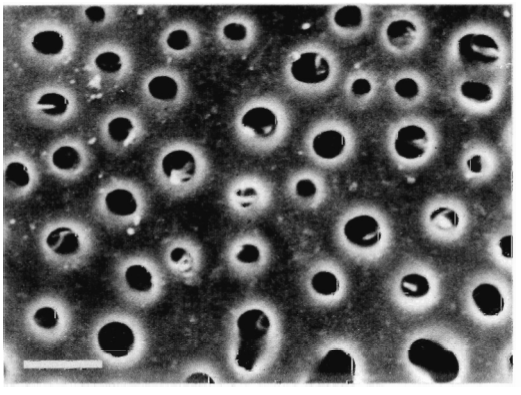

6

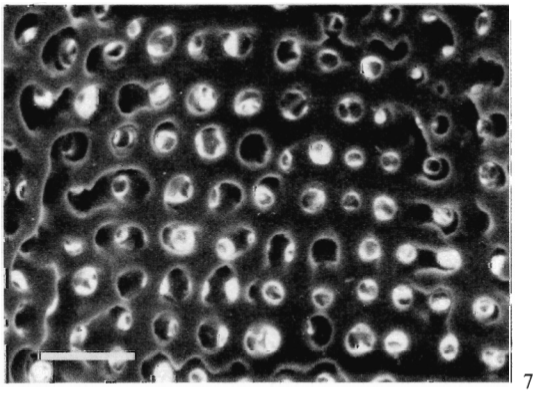

7

SMITH, ambulacral pore stereom

at the expense of pore size and pore space. Because of the interdigitation of pegs at suture faces the collagen fibres, binding the plates together, are not quite so well organized into discrete bundles as are the fibres of the catch apparatus.

Muscle fibres

In cidaroids, spine muscle fibres attach on to unmodified rectilinear stereom, which forms the upper layer of the plate, via a collagenous ligament. In *Centrostephanus longispinus* and *Salenocidaris profundi* a similar situation occurs except that the upper plate layer is composed of galleried stereom, orientated with galleries paralleling the plate surface. Areolar stereom may or may not differ structurally from the surrounding stereom which underlies the integument. The lack of thorns on the stereom of the areole may help to differentiate it from stereom underlying the integument, which is always thorned. Spine muscle fibres attach on to laminar stereom in *Calveriosoma*, *Phormosoma*, and *Micropyga*. This stereom forms the outer plate layer in *Phormosoma* and the presence of muscle fibres appears to have little or no modifying effect. The areole can be readily distinguished from the surrounding plate stereom in *Calveriosoma* and *Micropyga*, where the integument is underlain by thin development of labyrinthic stereom. In *Phormosoma*, however, there is no distinction between stereom supporting muscle fibres and stereom supporting integument.

In all other echinoids examined there is a specially developed stereom for muscle attachment. This is always markedly finer than the surrounding plate stereom in any one species and is readily distinguishable because of its fine, open, irregular construction. Quantitative analysis shows that this stereom falls into a narrowly defined area (text-fig. 18). It is a thin labyrinthic overlay with irregular-shaped pores and many free-ended trabeculae. Pegs may sometimes be present and the trabeculae are typically variable in thickness. In some cases the stereom is produced by the growth of fine trabeculae between existing trabeculae of the plate surface. It may also be formed by the modification of plate stereom with a reduction in pore size and increase in pore numbers. In most cases, however, the stereom for muscle attachment forms a thin overgrowth to the plate surface. Stereoms with an average pore size less than about 10 μm form an obvious thin veneer over the plate stereom. Where the average pore size is greater the superficiality of this stereom may be less immediately apparent. Although there is a considerable overlap of stereoms supporting muscle fibres and stereoms supporting integument (text-fig. 18) there is rarely any trouble in differentiating between these stereoms in individuals because of the markedly finer and commonly more open

---

EXPLANATION OF PLATE 21

Fig. 1. Galleried stereom forming the lateral plate surface of an ambital interambulacral plate of *Clypeaster rarispina*.

Fig. 2. Labyrinthic stereom of the lateral plate surface of an aboral interambulacral plate of *Echinocardium cordatum*.

Fig. 3. Maze-like appearance of poorly galleried stereom of the lateral plate surface of an ambital plate of *Temnopleurus hardwickii*.

Fig. 4. Ambital interambulacral/interambulacral plate suture of *Sphaerechinus granularis* (internal surface) showing the reduction in pore size by the suture.

Fig. 5. Ambital interambulacral plate of *Centrostephanus longispinus* showing a small central labyrinthic region surrounded by denser planar stereom.

Fig. 6. Planar stereom showing some pore alignment from near the margin of inner surface of an aboral interambulacral plate of *Mellita quinquiesperforata*.

Fig. 7. Central dense labyrinthic stereom of the inner surface of an ambital interambulacral plate of *Colobocentrotus atratus*.

Fig. 8. Galleried stereom forming the rim to the inner surface of an ambital interambulacral plate of *Eucidaris metularia*.

Scale bar in Fig. 1 = 20 μm; Figs. 2, 3, 6–8 = 40 μm; Fig. 4 = 100 μm; Fig. 5 = 400 μm.

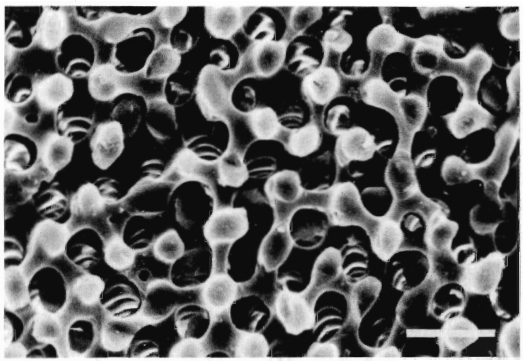
1

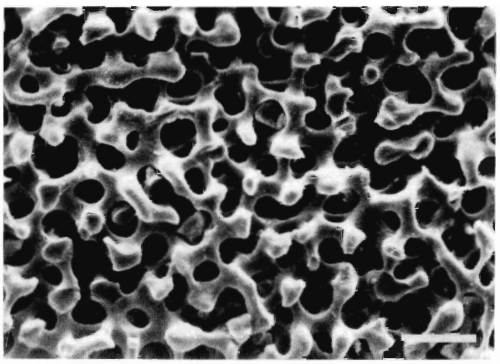
2

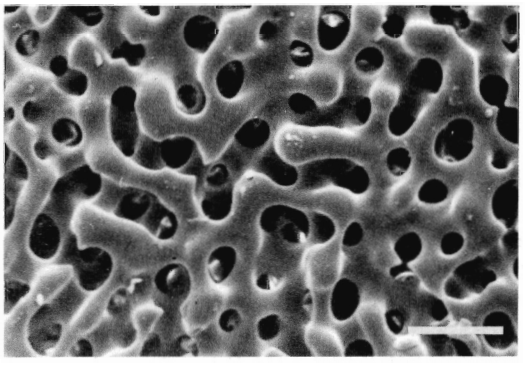
3

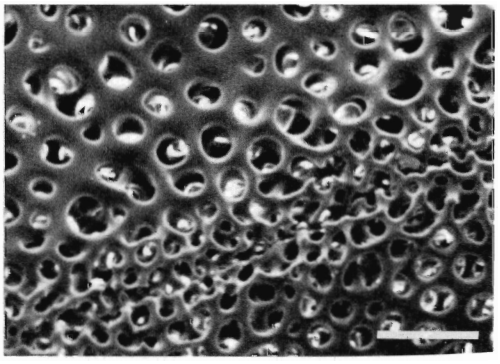
4

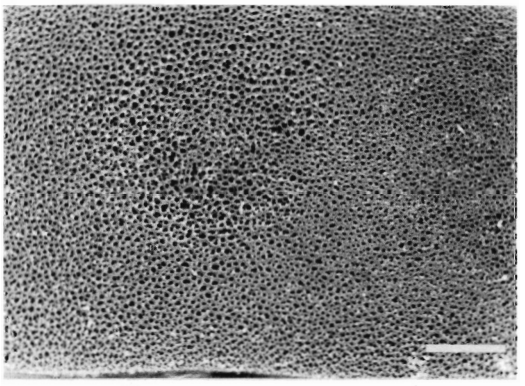
5

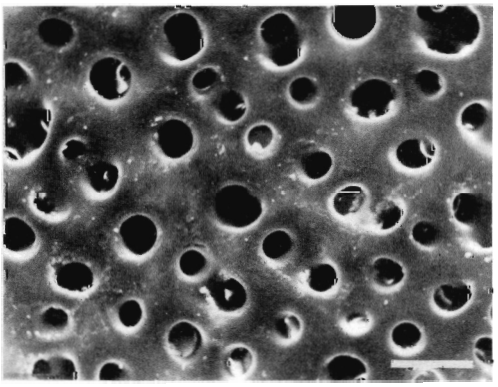
6

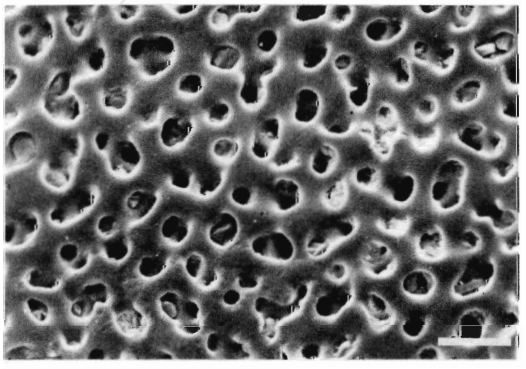
7

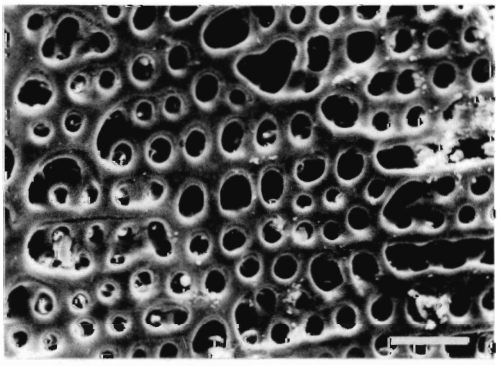
8

SMITH, lateral and inner plates surface

texture of stereoms for muscle attachment. The open irregular texture of these stereoms presumably provides much firmer anchorage to the muscle fibres than denser plate stereom. In almost all cases only one stereom is found in the area of overlap, the other being clearly placed in one or other of the areas. The superficial nature of this stereom helps to distinguish it from very similar stereom which supports collagenous fibres.

Integument

Stereom which underlies epidermal tissue is highly variable, largely because of differences in the cross-sectional design of the plates. The surface fabric ranges from coarse, open labyrinthic stereom to compact, perforate stereom. Stereom overlain by integument is always obviously coarser or denser than stereom supporting collagenous or muscle fibres in any one species although when all data are taken together there is a certain amount of overlap (text-fig. 18). Where galleried or rectilinear stereom forms the outer plate surface there is little apparent difference between stereom overlain by integument and stereom overlain by muscle fibres.

In the echinothuriids, where the integument has a basal layer of connective tissue fibres, the stereom of the plate surface is smooth and lacks thorns. In all other echinoids examined, stereom which is overlain by integument (which lacks a connective tissue layer) has thorns, or occasionally pegs or domes. From the findings of Heatfield (1971), it would be expected that thorns should be present on actively growing surfaces. The tetracycline labelling studies of Kobayashi and Taki (1969) and Markel (1975) have shown that growth on the outer plate surface is largely restricted to tubercle enlargement and that most plate growth occurs marginally and inwardly. Observations on the growth lines of *Psammechinus* plates confirms this but suggests that some upward growth of the outer plate layer must occur towards the periphery of an expanding plate. It is therefore somewhat surprising to find that, whereas the inner plate surface lacks thorns in all cases examined, the outer plate surface commonly possesses well-developed thorns, especially on planar dense surfaces where outward growth has obviously ceased (Pl. 14, fig. 6). Although pegged stereom and some thorned stereom may well be the result of active outward growth this cannot be true in the majority of cases. The thorns, unlike the larger domes and granules, do not increase the surface area of epithelium since they appear to penetrate into the integument without folding it. Thorns possibly mark the retention of calcite-secreting cells from which further growth could be initiated, but this is unlikely because thorns are absent from internal surfaces and because a resorption ring forms around expanding tubercles with the resultant loss of thorns. Roux (1974) found that striated muscle fibres in some crinoids attached on to a prominently thorned surface and suggested that the thorns' main function was to provide anchorage for these muscle fibres. Similar thorned facets have also been noted in crinoids by Macurda and Meyer (1975) where they are again associated with muscle fibre attachment.

EXPLANATION OF PLATE 22

Fig. 1. Stereo view of perforate stereom forming the inner plate surface of an ambulacral plate of *Psammechinus miliaris*. An ambulacral/ambulacral suture can be seen near the top.

Fig. 2. A granule, composed of perforate stereom, on the outer surface of an aboral interambulacral plate of *Echinolampas crassa*.

Fig. 3. Imperforate stereom forms the granules of the outer surface of an aboral interambulacral plate of *Arbacia lixula*.

Figs. 4, 6. *Salenocidaris profundi*. 4, stereo view of an ambital interambulacral plate showing radially arranged bands produced by outward movement of tubercles. Galleried stereom forms the areole. 6, stereo view of ambital ambulacral plates. Both isopores show clear trails of in-filled labyrinthic stereom deposited as they migrated marginally with plate growth.

Fig. 5. Stereo view of an aboral ambulacral primary tubercle of *Paracentrotus lividus* showing radial bands produced by lateral movement of the surrounding tubercles.

Scale bar in Figs. 1–3 = 100 μm; Fig. 6 = 200 μm; Figs. 4, 5 = 400 μm.

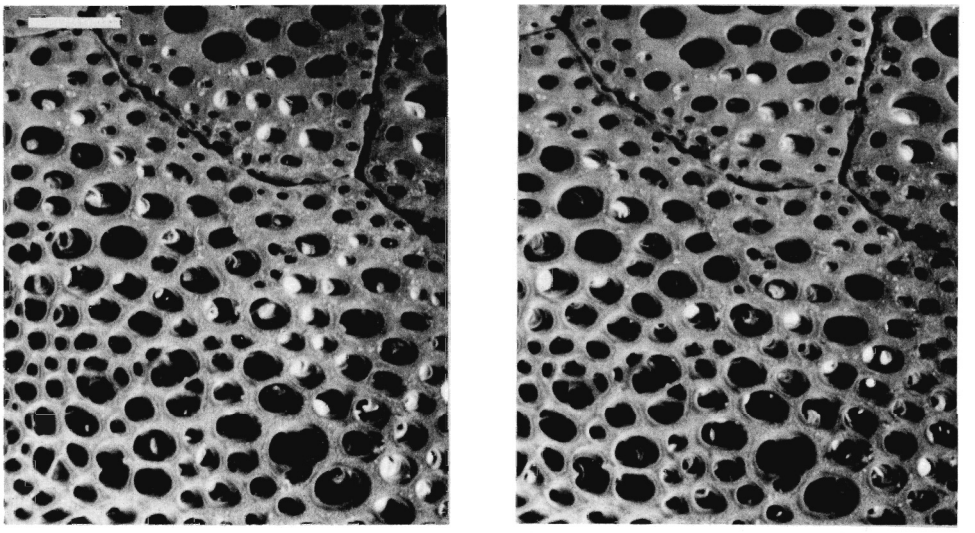

1

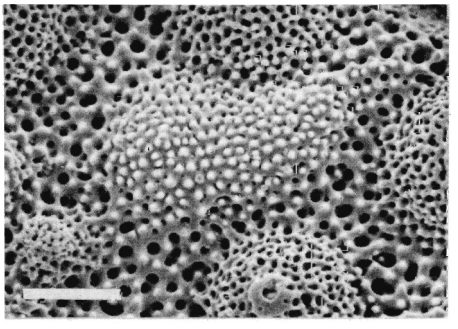

2

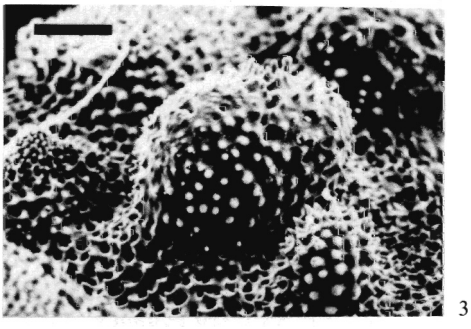

3

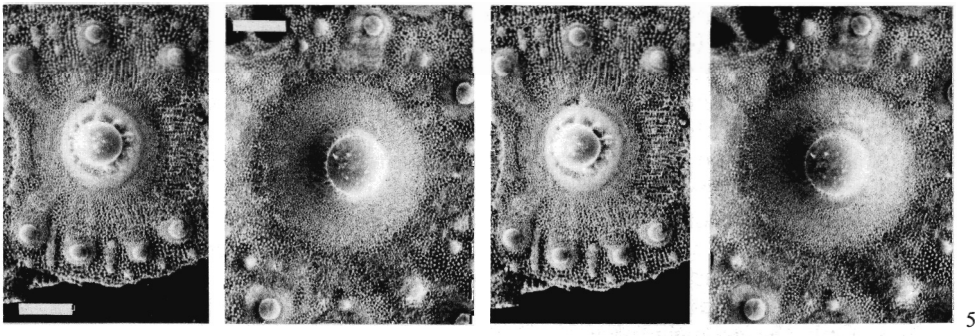

4 5

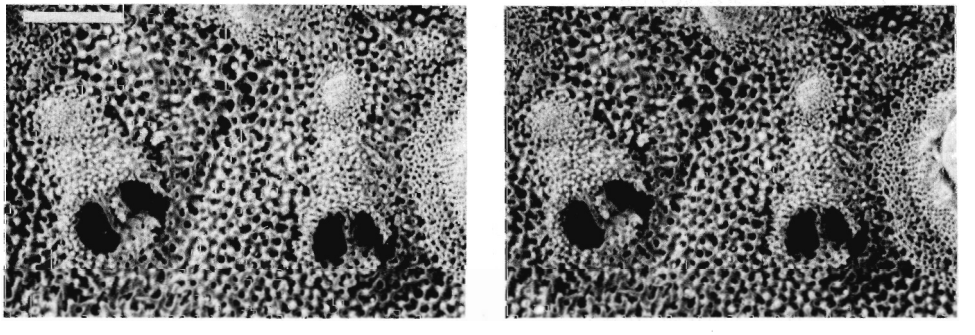

6

SMITH, surface details

This is not the function of the thorned surface of echinoid plates, and it is unlikely that thorns play part in the attachment of the integument. This leaves protection as the most likely function of these thorns. The sub-epidermal nerve plexus runs along the plate surface at the base of the thorns and must, to some extent, be protected by them. They cannot, however, act as a deterrent since they do not protrude through the integument. Abrasion of the ectoderm and surface skeleton by sediment particles must pose a major problem for many echinoids. In echinoid spines, where abrasion is most likely, the nuclei and a large part of the cytoplasm of ectodermal cells lies protected within grooves which run up the length of the spine. Thick trabecular wedges minimize the abrasion to this ectoderm. *Colobocentrotus atratus* can live openly in extremely turbulent environments because of its remarkably modified aboral spines which protect the integument and tube feet of the corona from scour. Living in burrows and crevices and the development of the covering reaction all help to protect echinoids from sediment abrasion. Thorns are best developed in urchins with only a thin outer layer of stereom. Large thorns are therefore thought to play a role in deflecting grazing damage and breaking impact of sediment particles. Instead of fracturing the outer stereom layer, impacting grains might be restricted to breaking only a few thorns. Not all thorns have a protective role however and many may be related to growth or muscle attachment.

Coelomic epithelium. This may overlie a broad range of stereom types (text-figs. 15 and 20) depending upon the construction of the plate. The coarse fabric of the stereom and its smooth trabecular intersections make it easily distinguishable from stereom of the outer plate surface. Quantitative data do, however, show some overlap between this stereom and stereom of the outer plate surface.

Imperforate Stereom. Although imperforate or compact perforate stereom forms both sides of the articulation surface between the mamelon and spine base, it may also be found in other situations not associated with articulation.

RESORPTION

The resorption of coronal plates at the peristomial margin has been described by Deutler (1926) and Gordon (1926); contrary evidence has recently been discussed by Markel (1975, 1976). The following account will be restricted to those minor resorptional features which can be found within plates and will not deal with evidence for or against complete resorption of early-formed plates. The resorption rim which surrounds expanding tubercles has been described and illustrated previously by Jensen (1972). Where resorption is taking place the stereom loses its thorns and forms a smooth, rather irregular surface. At the same time the stereom becomes denser by the occlusion of pore space, presumably brought about by the redeposition of resorbed calcite immediately beneath the zone of active resorption. As the major tubercles expand in size the surrounding smaller tubercles move outwards by active stereom growth at the leading margin and resorption at the trailing margin. This results in the formation of a superficial trail of dense, smooth stereom leading radially away from the major tubercle to each surrounding secondary tubercle (Pl. 22, figs. 4, 5). This marginal shift, produced by a combination of resorption and growth, is not confined to small secondary tubercles alone. Only the primary tubercle of each interambulacral plate of *Psammechinus* shows radially symmetrical growth. Other major tubercles all have an internal structure which shows that they have shifted laterally during growth (Pl. 12, fig. 2).

Sunken tubercles appear to be formed by resorption but without the production of compact stereom. This is best displayed by the large aboral interambulacral tubercles of *Paramaretia*. These tubercles are so deeply sunken that they penetrate through to the inner layer (Pl. 14, fig. 3). The stereom construction of the tubercles and the plate show complete continuity, suggesting that these tubercles were formed by resorption. The absence of the outer plate layer within the sunken tubercles of *Clypeaster* and *Echinolampas* is thought to be due partially to resorption and partially to differential growth. Resorption features are also apparent in the vicinity of ambulacral pores. The outward shift of pores, keeping them in contact with the expanding plate margin, is brought about by simultaneous resorption and deposition. Where the outer plate layer is thin or absent, as in *Salenocidaris*,

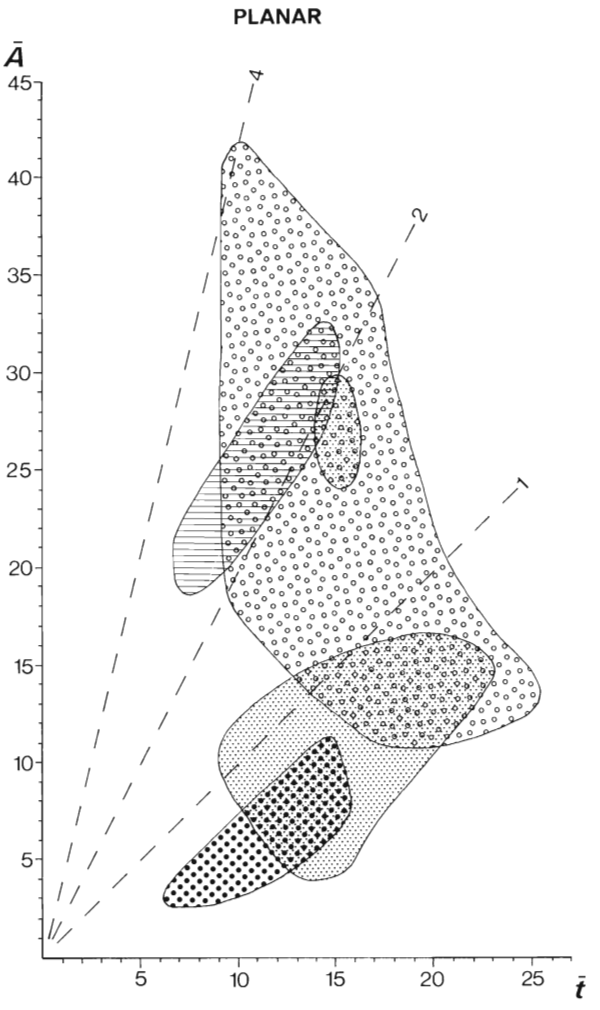

TEXT-FIG. 20. Summary of all data on planar stereom. Large circles—internal plate surface: small dots—external plate surface: horizontal lines —areole: large dots—intrapodial area.

the trail of back-filling stereom is clearly displayed (Pl. 22, fig. 6). The stereom which is deposited behind a pore as it shifts marginally is labyrinthic and is quite distinct from the galleried stereom which makes up much of the rest of the plate. Which stereom forms the pore wall therefore not only depends upon the plate construction, but also depends upon which side of the pore is examined. This explains why the stereom of the pore wall is so variable.

ECOLOGICAL SIGNIFICANCE OF SUPERFICIAL STEREOM MICROSTRUCTURE

Recent work by Oldfield (1976) has suggested that there is a correlation between the plate surface microstructure and the environment in Recent regular echinoids. In a survey of a large number of echinoid species she recognized a sequence of increasing stereom pore occlusion, from a simple unorientated mesh, through an organized mesh with enlarged trabecular intersections and well-developed thorns, to a very dense stereom with small pores and with either thorns or domes. She explains this variation by postulating that 'densely microstructured calcite with its associated high magnesium levels characterises areas of the coronal plate with higher growth rate' and asserts that

low growth rate echinoids, inhabiting 'low-energy' environments, tend to have a pronounced coronal plate ornamentation. Ebert (1975) has demonstrated that, in tropical waters, intertidal echinoids show significantly lower growth and mortality rates than subtidal echinoid species. In temporate species, no correlation between growth rate and bathymetric depth was found. Species from 'low-energy' environments therefore do not show low growth rates and may often show higher growth rates than species from high-energy environments. In this study it has been shown, by the use of stereom microstructural banding, that stereom deposited during the first bout of rapid growth tends to have thinner trabeculae and larger pores than stereom deposited towards the end of the growth period when the growth rate has decreased. During periods of minimal growth in the middle plate layer the stereom changes to a more open labyrinthic construction. However, in most cases, an increase in the stereom density is attributable to a decrease in growth rate rather than to an increase in growth rate.

Quantitative treatment of the stereom of the plate surface (text-fig. 8) shows that there is no obvious correlation between stereom density and environment (details of the habitats of these regular echinoids is given in an appendix to Smith, 1978). The surface stereom construction reflects the cross-sectional design of the plate which is itself affected by the growth strategy of the species. The growth strategy adopted by any particular species depends upon the environmental pressures it is subjected to. Such pressures as the predictability of recruitment success and the likelihood of skeletal damage and abrasion are likely to influence the growth strategy. There should therefore be an indirect relationship between the construction of the surface stereom and the habitat of the species, but this is often blurred by differences in the plate construction. In cidaroids, echinothuriids, diadematoids, and some clypeasteroids plates of the test possess no outer compact layer and epithelial tissue lies directly on top of open labyrinthic, rectilinear, or laminar stereom. In diadematoids and clypeasteroids this outer, coarse, labyrinthic stereom forms a thin overlay to the galleried stereom of the middle plate layer. In spatangoids, a thin perforate layer is developed on the outer surface and this is also present in interambulacral plates of *Tripneustes*. Large thorns are always developed between pores. In *Sphaerechinus*, this layer is thicker and domes are developed. Where the perforate layer is thin, the linear organization of the underlying galleried stereom imparts a similar linear pattern to the pores and to the thorns or domes of the overlying perforate layer.

Other species do not have such a well-defined, compact stereom layer. *Temnopleurus* and *Stomopneustes* have an open labyrinthic stereom deposited above the galleried stereom of the middle plate

---

EXPLANATION OF PLATE 23

Figs. 1, 3. *Temnopleurus hardwickii*. 1, primary interambulacral spine attachment showing the different mode of attachment for muscle and catch apparatus fibres, × 100. 3, insertion of catch apparatus fibres into the boss of a primary interambulacral tubercle, × 400.

Fig. 2. Primary interambulacral spine attachment in *Centrostephanus nitidus*. Notice the different method of attachment for catch apparatus fibres, × 400.

Figs. 4, 10. *Eucidaris metularia*. 4, insertion of catch apparatus fibres into the boss of a primary interambulacral tubercle, × 320. 10, collagenous fibres joining two aboral plates, × 320.

Fig. 5. Oral isopore attachment area of *Arbacia lixula* showing tube-foot retractor muscle fibre insertion, × 350.

Figs. 6, 9. *Echinostrephus molaris*. 6, attachment of spine muscle to the areole of an interambulacral tubercle, × 400. 9, integument covering an aboral interambulacral plate, × 450.

Fig. 7. Epithelial cells, with horseshoe-shaped nuclei, lining the pore wall of an ambulacral plate of *Cidaris cidaris*, × 620.

Fig. 8. Epithelial cells with underlying ?muscle fibres lining the pore wall of an ambulacral plate of *Tripneustes gratilla*, × 500.

m = muscle fibres; c = collagenous catch apparatus fibres; e = epithelium; n = nerve; s = stroma (connective tissue); > indicates plate surface.

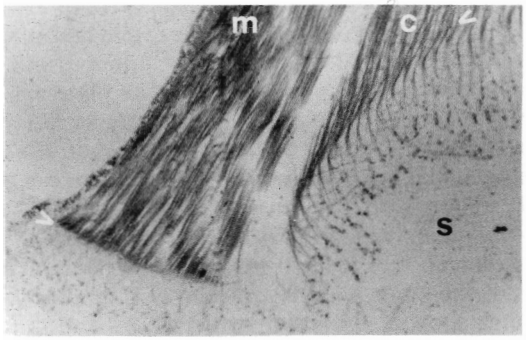

1

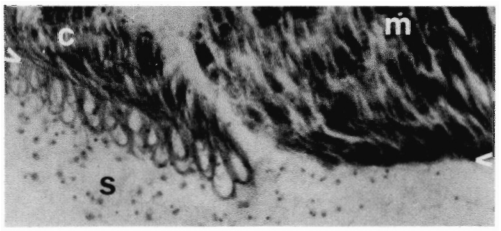

2

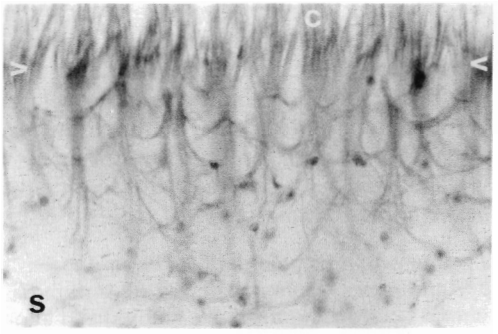

3

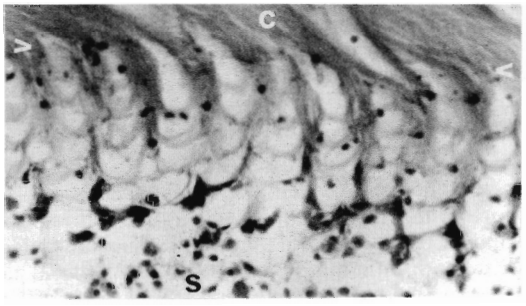

4

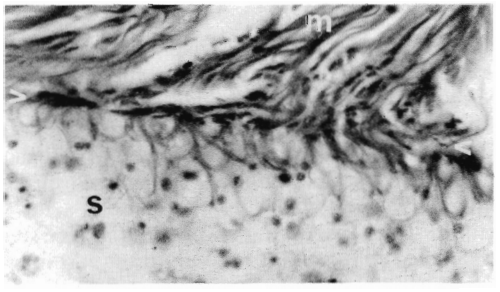

5

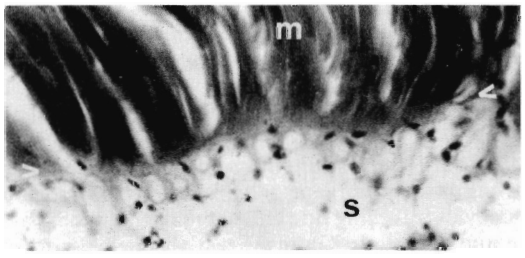

6

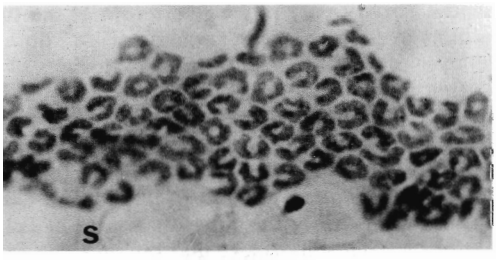

7

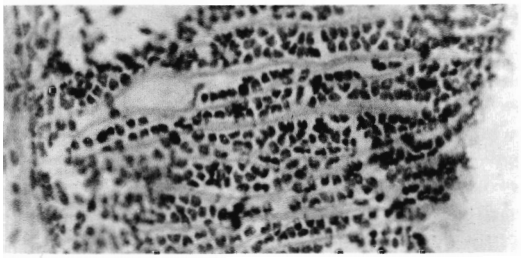

8

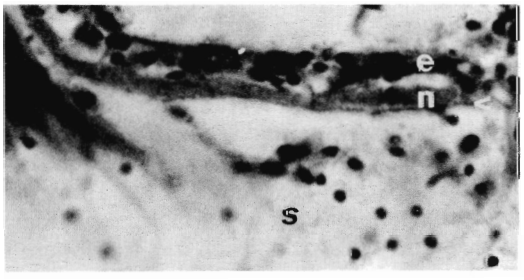

9

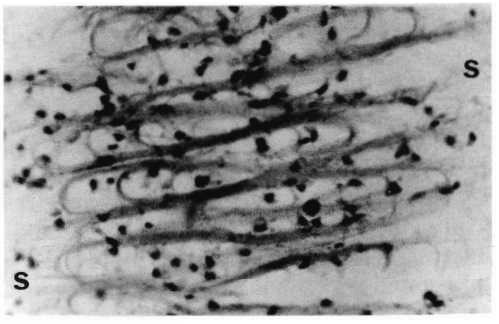

10

SMITH, histological sections

layer. The 'highly ordered stereom with sharp conical thorns' reported by Oldfield (1976) in *Temnopleurus reevsei* is developed only at the periphery of interambulacral plates and above ambulacral isopores of *Temnopleurus hardwickii*, where the thickness of the outer layer is minimal and the organization of the galleried layer of the plate dominates. Similar variation over the plate surface is marked in *Stomopneustes* and *Paracentrotus*. Some species have dense labyrinthic stereom on the outer plate surface. In some cases, as in *Arbacia*, this is exceedingly compact, whereas, in *Colobocentrotus*, outward growth of this thick layer maintains much of the organization of the underlying galleried stereom. However, in most cases, the dense labyrinthic stereom of the outer plate layer forms a moderately thick deposit and may show banded variation in density. The relationship between surface stereom design and the habitat of each species is far from straightforward. There is a generalized relationship between the thickness of the outer plate layer and the rate of growth. Species in 'lower-energy', more uniform environments show faster lateral growth rates and thinner outer plate layers than shallow water species from rocky habitats, which tend to build up the thickness of the outer plate layer. The thinner the outer plate layer is, the more likely it is to be a perforate stereom. However, exceptions are not uncommon and stereom microstructure of the plate surface cannot be used with certainty to identify the palaeoenvironment. Much clearer and more direct evidence comes from a study of the oral pore pair morphology of regular echinoids (Smith, 1978).

It is interesting to note that, in *Psammechinus* and *Eucidaris*, domed, perforate stereom is found only on ambulacral plates where it is described as pore-pair 'ornamentation' by Oldfield (1976). In both species, such stereom is developed only above ambital and aboral isopores where there are thin-walled tube feet important for gaseous exchange. This stereom is absent above oral isopores, from the rest of the ambulacral plate and from interambulacral plates (unlike *Sphaerechinus*). A perforate stereom with domes also forms the interporal partition in many species. Such surface granulation must act to increase the area of ciliated epithelium. The restriction of domed stereom to those tube feet with a respiratory function suggests that, in these species, domed stereom may be developed to enhance cilia-induced water circulation. It is unlikely that all domed stereom has this function. In many species doming is simply a consequence of growth of a perforate stereom layer. In crinoids, domed perforate stereom may be found at articulation surfaces (Macurda and Meyer, 1975, plate 19), where the rough surface presumably gives increased surface resistance and hence firmer clamping together of adjacent columnals.

From a superficial examination of the surface stereom fabric of *Paracentrotus lividus*, Regis (1977) concluded that galleried stereom plays an important part in transporting absorbed organic nutrients from the integument to the interior of the test. She envisages streams of coelomocytes travelling down the core of the spine, passing somehow across to the galleried stereom of the tubercle and penetrating into the test via the galleries. The objections to this theory are several: galleries do not run the thickness of the test but end at the dense outer plate layer of stereom; the articulation surfaces of both spine and tubercle are composed of extremely dense and often imperforate stereom; galleried stereom houses bundles of collagenous fibres which largely fill the pore space. Epithelial absorption undoubtedly occurs along the spine. The grooves of coarse, open stereom on spine shafts are areas of active absorption, not because of stereom porosity as implied by Regis (1977) but simply because, for protection against abrasion, this is where nearly all epithelial nuclei and the majority of their cytoplasm are sited. The intervening calcite wedges have only a thin skin of cytoplasm. Although epithelial absorption is probably an important source of nutrients for the tissues of appendages, there is little evidence that it has greater importance and the presence of galleried stereom is clearly irrelevant.

USES OF STEREOM MICROSTRUCTURE IN PALAEONTOLOGY

The coverage of fossil material in this survey has been limited because stereom microstructure can only be understood through detailed work on Recent species. Although stereom preservation is rarely as perfect as that in *Eupatagus hastingiae* from the Eocene of the Hampshire basin (Pl. 2, fig. 6) it is often good enough to permit quantitative analysis of pore and trabecula size over the plate surface. Stereom may be equally well preserved in other echinoderm groups as has been shown by Roux (1970, 1971), Macurda (1973), and Strimple (1972). The present work has shown that the microstructure of the echinoid plate is the product of three major interacting factors: phylogeny, the associated soft tissue, and the rate of growth. Environmental factors, such as the temperature (Davies *et al.*, 1972) or the availability of $CaCO_3$, may also influence the stereom construction.

Genetic factors control the basic pattern of stereom that is deposited and there are phylogenetic differences in the plate microstructure. Stereom is modified by the rate of plate growth and by the nature of the associated soft tissue. The interaction of all of these factors makes interpretation of the stereom microstructure rather more complex than had previously been assumed.

The method of plate growth and the ability to identify seasonal banding not only provides information on the age and growth rate of individuals but also on their growth strategy. Each major zone of stereom disruption, produced during periods of minimal plate growth, appears to coincide with a period of gonadal development. It is therefore possible to gauge the relative emphasis given to growth (lateral plate growth), strengthening (plate thickening), and gonadal development (stereom discontinuities). Such analysis can also be applied to other echinoderm groups. Stereom microstructure has been used to identify the mode of plate growth in cystoids (Paul, 1971) and in crinoids (Roux, 1971, 1975). It has also been used to identify probable composite elements formed by fusion of individual plates in a Carboniferous crinoid (Strimple, 1976).

Probably the most important use of stereom microstructure is in the identification of associated soft tissue. The stereom of echinoid plates varies considerably and, by using a combination of quantitative and qualitative data it is usually possible to deduce the nature of the overlying soft tissue. In this work, only coronal plate stereom has been systematically analysed but the stereom of other elements seems to show comparable variation. For example, the base of spines is formed of a lower band of galleried stereom accommodating the catch apparatus fibres, and an upper band of retiform stereom for muscle attachment. Muscle attachment in the lantern apparatus also appears to be associated with a retiform layer (Markel, 1978, fig. 1d).

Quantitative analysis of the surface stereom of the Jurassic *Plesiechinus ornatus* and the Eocene *Eupatagus hastingiae* shows that stereom microstructural variation in these fossils is quite comparable with that of Recent echinoids (see text-figs. 8–15). The similarity in the variation of surface stereom, going at least as far back as the Carboniferous, implies that the same interacting factors controlled stereom microstructure. This permits reconstruction of the soft tissue anatomy in fossil echinoids. This idea has been exploited in studies of ambulacral pores (Smith, 1978). The distinctive stereoms associated with tube foot attachment, integument, and endoderm are clearly recognizable even in Palaeozoic echinoids. It has therefore been possible to follow the evolution of tube feet from the microstructure of ambulacral plates.

Similarly the stereom microstructure of tubercles can provide a great deal of useful information as it gives direct evidence for the extent and development of muscle and catch apparatus fibres. Quantitative differences in stereom construction allow direct measurement of the breadth of muscle fibres, catch apparatus fibres, and the gap which separates the two. In many irregular echinoids the breadth of the areole is greater to one side and can be used to identify the direction of the power stroke of the spine.

The Carboniferous echinocystitoid *Lepidesthes* lacks primary tubercles and its small secondary tubercles are composed of a low platform of labyrinthic stereom without a distinct areole. In comparison with secondary tubercles of Recent regular echinoids, what few muscle fibres that were developed inserted around the edge of the labyrinthic platform. The fact that catch apparatus fibres in *Lepidesthes* are associated with labyrinthic rather than galleried stereom is presumably related to the growth rate. Where the boss has grown well above the plate surface the stereom is usually clearly galleried, as in the Carboniferous *Archaeocidaris* but where the boss is low and little outward growth has taken place, catch apparatus fibres are associated with a thin layer of labyrinthic stereom.

Even in Palaeozoic echinoids plate construction is variable. Plates of *Neobothryocidaris* from the Ordovician appear to be composed of rectilinear stereom, at least on their outer surface. In *Lepidesthes* there is a distinct outer plate layer composed of a dense perforate stereom. The middle plate layer is composed of labyrinthic stereom whilst the internal surface is planar and appears to be a laminar stereom. Plates of *Archaeocidaris* differ principally in lacking an outer dense layer and are rather similar in construction to plates of the Recent echinothurioid *Phormosoma*.

The plate construction in Jurassic holectypoids and cassiduloids differs from that of their Recent descendants. *Holectypus* has no dense outer plate layer and galleried stereom aligned perpendicular

to the sutures is clearly seen. *Galeropygus* has only a thin outer layer composed of a dense to open labyrinthic stereom which forms the low ridges between tubercles. The outer plate layer is better developed in *Clypeus* where it forms dense labyrinthic ridges with compact, low-profile granules. In Recent cassiduloids and in *Echinoneus* the outer plate layer is often exceedingly thick, possibly due to selection pressure by predatory gastropods.

Similar differences in surface stereom can be seen in regular Jurassic echinoids. The oldest species with granular stereom developed above ambital and aboral isopores that the author knows of is *Stomechinus intermedius* from the Bajocian. Unlike contemporary species it is found with, *Stomechinus* has phyllodes of P3-type isopores and is thus adapted for relatively high-energy environments. The other species have either little or no outer plate layer or possess a thin layer of dense labyrinthic stereom. They also lack phyllodes and have only P2-type isopores adorally. This is in direct contrast to the view of Oldfield (1976) that 'pore pair ornamentation' indicates a low-energy environment.

The conclusions drawn from this study not only appear to hold true for fossil echinoids but can also be applied to other groups of echinodermata. Muscle and collagen attachment areas in the arm ossicles of *Ophiura* (Macurda, 1973) and *Astrophyton* (Macurda, 1976) have a similar stereom microstructure to echinoids. Considerable information is available on the stereom microstructure of crinoids due to the efforts of Roux (1970, 1971, 1974*a*, *b*, 1975, 1977) and Macurda and Meyer (1975, 1976). The similarities between echinoid stereom and crinoid stereom are obvious and suggest that the results of this study can be applied to any group of echinodermata. Stereom microstructure is likely to prove an important line of evidence when assessing the palaeobiology of extinct and more problematic groups of echinodermata. The work on echinoid stereom has raised several important points which have not been considered in crinoid studies. First, it is important to distinguish between galleried stereom and rectilinear, for, although galleried stereom in echinoid plates is always found in association with collagen fibres, rectilinear stereom is found with a number of different tissues. Secondly, due to variation of the stereom during growth, collagen fibres may also be found associated with labyrinthic stereom and it is possible to differentiate areas of muscle and collagen attachment only by the three-dimensional construction. Thirdly, differences in stereom pore size cannot, by themselves, be used to identify the associated soft tissue, as was postulated by Lane and Macurda (1975). Although stereom for muscle attachment is commonly finer than other stereoms in the same element, this is not true in all cases and in plates of echinothurioids and *Centrostephanus* areas of collagen fibre attachment have very much finer stereom than the rest of the plate. Finally, the presence of thorns cannot be used to identify areas of striated muscle attachment, as was suggested by Roux (1971, 1974*a*) as they are rarely encountered in muscle attachment areas of echinoid plates (smooth muscle) or pedicellariae (striated muscle). In echinoids, large thorns are a distinctive feature of the outer surface of the plates where integument overlies.

Interpretation of surface stereom microstructure is not a simple task and a thorough understanding of the construction and mode of growth of an element must be gained before any attempt is made to analyse the surface stereom variation. A lot of useful biological information is encoded in the stereom construction of the echinoderm skeleton but great care must be taken in the interpretation of the microstructure.

Acknowledgements. I thank Professor David Nichols for help throughout this research and for criticisms of the draft manuscript. I also thank Miss A. M. Clark (British Museum (Natural History), London), Dr. D. L. Pawson (Smithsonian Institution, Washington), Dr. P. M. Kier (Smithsonian Institution, Washington), Dr. F. W. E. Rowe (Australian National Museum), Dr. A. N. Baker (New Zealand National Museum), Dr. C. Griffiths (University of Cape Town), Dr. F. J. Madsen (Universitetets Zoologiske Museum, Copenhagen) and Dr. C. D. Waterston (Royal Scottish Museum, Edinburgh) for making specimens available to me. This research was carried out under tenureship of an S.R.C. postgraduate research grant. The Universities of Liverpool and Exeter contributed towards publication costs.

REFERENCES

ALLAIN, J. Y. 1978. Age et croissance de *Paracentrotus lividus* (Lamarck) et de *Psammechinus miliaris* (Gmelin) des côtes nord de Bretagne (Echinoidea). *Cah. Biol. mar.* **19,** 11–21.

BECHER, E. 1924. Über den feineren Bau der Skelettsubstanz bei Echinoideen, insbesondere über statische Strukturen in derselben. *Zool. Jb. Abt. Zool. Physiol. Tiere*, **41,** 179–244.

BECHER, S. 1914. Über statische Strukturen und kristalloptische Eigentumlichkeiten des Echinodermenskeletts. *Verh. dt. zool. Ges.* **24,** 307–327.

BIRKLAND, C. and CHIA, F. S. 1971. Recruitment risk, growth, age and predation in two populations of sand dollars, *Dendraster excentricus* (Eschscholtz). *J. exp. mar. Biol. Ecol.* **6,** 265–278.

BOOLOOTIAN, R. A. 1966. Reproductive physiology. *In* BOOLOOTIAN, R. A. (ed.) *Physiology of Echinodermata.* John Wiley & Sons (Interscience Publishers), New York, Ch. 25.

CHADWICK, H. C. 1929. Regeneration of spines in *Echinus esculentus. Nature, Lond.* **124,** 760–761.

CHESHER, R. H. 1969. Contributions to the biology of *Meoma ventricosa* (Echinoidea: Spatangoida). *Bull. mar. Sci.* **19,** 72–110.

CRAPP, G. B. and WILLIS, M. E. 1975. Age determination in the sea urchin *Paracentrotus lividus* (Lamarck), with notes on the reproductive cycle. *J. exp. mar. Biol. Ecol.* **20,** 157–178.

DAVIES, T. T., CRENSHAW, M. A. and HEATFIELD, B. M. 1972. The effect of temperature on the chemistry and structure of echinoid spine regeneration. *J. Paleont.* **46,** 874–883.

DEUTLER, F. 1926. Über das Wachstum des Seeigelskeletts. *Zool. Jb. Abt. Anat. Ontog. Tierre*, **48,** 119–200.

DIX, T. G. 1972. Biology of *Evechinus chloroticus* (Echinoidea: Echinometridae) from different localities. 4. Age, growth and size. *N.Z. Jl mar. freshw. Res.* **6,** 48–68.

DURHAM, J. W. 1955. Classification of clypeasteroid echinoids. *Univ. Calif. Pubs geol. Sci.* **31,** 73–198.

EBERT, T. A. 1967. Negative growth and longevity in the purple sea urchin *Strongylocentrotus purpuratus* (Stimpson). *Science, N.Y.* **157,** 557–558.

—— 1968. Growth rates of the sea urchin *Strongylocentrotus purpuratus* related to food availability and spine abrasion. *Ecology*, **49,** 1075–1091.

—— 1975. Growth and mortality of post-larval echinoids. *Amer. Zool.* **15,** 755–775.

FELL, H. B. 1960. Archibenthal and littoral echinoderms of the Chatham Islands. *Bull. N.Z. Dep. scient. ind. Res.* **139** (2), 55–75.

FERBER, I. and LAWRENCE, J. M. 1976. Distribution, substratum preference and burrowing behaviour of *Lovenia elongata* (Gray) (Echinoidea; Spatangoida) in the Gulf of Elat (Aquaba), Red Sea. *J. exp. mar. Biol. Ecol.* **22,** 207–225.

FOUCAT, M. F. 1966. Localisation du collagène dans le test d'un oursin (Echinoderme). *Bull. Acad. r. Belg. Cl. Sci.* **52** (2), 316–319.

FUJI, A. 1967. Ecological studies on the growth and food consumption of the Japanese common littoral sea urchin *Strongylocentrotus intermedius. Mem. Fac. Fish Hokkaido Univ.* **15,** 83–160.

GIESE, A. C. 1967. Changes in body-component indexes and respiration with size in the purple sea-urchin *Strongylocentrotus purpuratus. Physiol. Zool.* **40,** 194–200.

—— KRISHNASWAMY, S., VASU, B. S., and LAWRENCE, J. 1964. Reproductive and biochemical studies on a sea urchin *Stomopneustes variolaris* from Madras Harbour. *Comp. Biochem. Physiol.* **13,** 367–380.

GLADFELTER, W. B. 1978. General ecology of the cassiduloid urchin *Cassidulus caribbearum. Mar. Biol.* **47,** 149–160.

GORDON, I. 1926. The development of the calcareous test of *Echinus miliaris. Phil. Trans. R. Soc. Lond.* B, **214,** 259–312.

HEATFIELD, B. M. 1971. Growth of the calcareous skeleton during regeneration of spines of the sea urchin *Strongylocentrotus purpuratus* (Stimpson); a light and scanning electron microscope study. *J. Morph.* **134,** 57–90.

HIGGINS, R. C. 1974. Observations on the biology of *Apatopygus recens* (Echinoidea: Cassiduloida) around New Zealand. *J. Zool.* **173,** 505–516.

HINES, J. and KENNY, R. 1967. The growth of *Arachnoides placenta* (L.) (Echinoidea). *Pacific Sci.* **21,** 230–235.

HOBSON, A. D. 1930. Regeneration of the spines in sea urchins. *Nature, Lond.* **125,** 168 only.

HSIA, W. P. 1948. On the relations between the number of coronal plates and the diameter of the test in three species of sea-urchins. *Contr. Inst. Zool. natn. Acad. Peiping*, **4,** 25–31.

HUMASON, G. L. 1972. *Animal tissue techniques* (3rd edn.). W. H. Freedman and Co., San Francisco, 641 pp.

JACKSON, R. T. 1912. Phylogeny of the Echini, with a revision of Palaeozoic species. *Mem. Boston Soc. nat. Hist.* **7,** 491 pp.

JENSEN, M. 1969*a*. Age determination of echinoids. *Sarsia*, **37,** 41–44.
—— 1969*b*. Breeding and growth of *Psammechinus miliaris* (Gmelin). *Ophelia*, **7,** 65–78.
—— 1972. The ultrastructure of the echinoid skeleton. *Sarsia*, **48,** 39–48.
KAWAGUTI, S. and KAMISHIMA, Y. 1964. Electron microscopic study on the integument of the echinoid *Diadema setosum*. *Annotnes zool. jap.* **37,** 147–152.
KAWAMURA, K. 1966. On the age determining character and growth of a sea urchin, *Strongylocentrotus nudus* [in Japanese, with English summary]. *Sci. Rep. Hokkaido Fish. exp. Stat.* **6,** 56–61.
——1973. Fishery biological studies on a sea urchin *Strongylocentrotus intermedius* (A. Agassiz) [in Japanese with English summary]. Ibid. **16,** 1–54.
KIER, P. M. 1974. Evolutionary trends and their functional significance in the post-Paleozoic echinoids. *Paleont. Soc. Mem.* **5,** 95 pp.
KOBAYASHI, S. and TAKI, J. 1969. Calcification in sea urchins: I. A tetracycline investigation of growth of the mature test in *Strongylocentrotus intermedius*. *Calcif. tiss. Res.* **4,** 210–223.
KUME, M. 1929. On the growth of the test in sea urchins [in Japanese]. *Rigakukai*, **27,** 209–213.
LANE, N. G. and MACURDA, D. B. 1975. New evidence for muscular articulations in Paleozoic crinoids. *Paleobiology*, **1,** 59–62.
LEWIS, J. B. 1958. The biology of the tropical sea urchin, *Tripneustes esculentus* Leske in Barbados, British West Indies. *Can. J. Zool.* **36,** 607–621.
MCCLELLAND, J. 1841. On *Cyrtoma*, a new genus of fossil Echinida. *Calcutta J. nat. Hist.* **1,** 155–187.
MCPHERSON, B. F. 1965. Contributions to the biology of the sea urchin *Tripneustes ventricosus*. *Bull. mar. Sci. Gulf Caribbean*, **15,** 228–244.
MACURDA, D. B. 1973. The stereomic microstructure of the blastoid endoskeleton. *Contrib. Mus. Paleont. Univ. Michigan*, **24** (8), 69–83.
—— 1976. Skeletal modifications related to food capture and feeding behaviour of the basketstar *Astrophyton*. *Paleobiology*, **2,** 1–7.
—— and MEYER, D. L. 1975. The microstructure of the crinoid endoskeleton. *Univ. Kansas Paleont. Contrib.* **74,** 1–22.
—— —— 1976. The morphology and life habits of the abyssal crinoid *Bathycrinus aldrichianus* Wyville Thomson and its paleontological implications. *J. Paleontol.* **50** (4), 647–667.
MARKEL, K. 1975. Wachstum des Coronarskeletes von *Paracentrotus lividus* Lmk. *Zoomorphologie*, **82,** 259–280.
—— 1976. Struktur und Wachstum des Coronarskeletes von *Arbacia lixula* Linné (Echinodermata, Echinoidea). Ibid. **84,** 279–299.
—— 1978. On the teeth of the Recent Cassiduloid *Echinolampas depressa* Gray, and on some Liassic fossil teeth nearly identical in structure (Echinodermata, Echinoidea). Ibid. **89,** 125–144.
—— KUBANEK, F. and WILLGALLIS, A. 1971. Polykristallin Calcit bei Seeigeln. *Z. Zellforsch.* **119,** 355–377.
MOORE, H. B. 1935. A comparison of the biology of *Echinus esculentus* in different habitats. Part II. *J. mar. biol. Ass., U.K.* **20,** 109–128.
—— 1936*a*. The biology of *Echinocardium cordatum*. Ibid. **20,** 655–671.
—— 1936*b*. A comparison of the biology of *Echinus esculentus* in different habitats. Part III. Ibid. **21,** 711–719.
—— JUTARE, T., BAUER, J. C., and JONES, J. A. 1963*a*. The biology of *Lytechinus variegatus*. *Bull. mar. sci. Gulf Caribbean*, **13,** 23–53.
—— —— JONES, J. A., MCPHERSON, B. F., and ROPER, C. F. E. 1963*b*. A contribution to the biology of *Tripneustes esculentus*. Ibid. **13,** 267–281.
—— and MCPHERSON, B. F. 1965. A contribution to the study of the productivity of the urchins *Tripneustes esculentus* and *Lytechinus variegatus*. Ibid. **15,** 855–871.
MOSS, M. L. and MEEHAN, M. 1967. Sutural connective tissues in the test of an echinoid *Arbacia punctulata*. *Acta anat.* **66,** 279–304.
—— —— 1968. Growth of the echinoid test. Ibid. **69,** 409–444.
NISSEN, H. U. 1969. Crystal orientation and plate structure in echinoid skeletal units. *Science, N.Y.* **166,** 1150–1152.
OLDFIELD, S. C. 1976. Surface ornamentation of the echinoid test and its ecological significance. *Paleobiology*, **2,** 122–130.
PAUL. C. R. C. 1971. Revision of the *Holocystites* fauna (Diploporita) of N. America. *Fieldiana Geol.* **24,** 1–166.
PEARSE, J. S. 1968. Patterns of reproductive periodicities in four species of Indo-Pacific echinoderms. *Proc. Indian Acad. Sci.* **68,** 247–279.
—— 1969. Reproductive periodicities of Indo-Pacific invertebrates in the Gulf of Suez. II. The echinoid *Echinometra mathaei* (de Blainville). *Bull. mar. Sci. Gulf Caribbean*, **19,** 580–613.

——1972. A monthly reproductive rhythm in the diadematid sea urchin *Centrostephanus coronatus* Verrill. *J. exp. mar. Biol. Ecol.* **8,** 167–186.

——and PEARSE, V. B. 1975. Growth zones in the echinoid skeleton. *Amer. Zool.* **15,** 731–753.

——and PHILLIPS, B. F. 1968. Continuous reproduction in the Indo-Pacific sea urchin *Echinometra mathaei* at Rottnest Island, Western Australia. *Aust. J. mar. Freshwat. Res.* **19,** 161–172.

RAUP, D. M. 1966. The endoskeleton. In BOOLOOTIAN, R. A. (ed.), *Physiology of Echinodermata.* J. Wiley and Sons, (Interscience Publishers), New York. Ch. 16.

——1968. Theoretical morphology of echinoid growth. *J. Paleont.* **42,** 50–63.

REGIS, M. B. 1977. Organisation microstructurale du stéréome de l'Echinoide *Paracentrotus lividus* (Lamarck) et ses eventuelles incidences physiologiques. *C.R. Acad. Sc., Paris,* **285, D,** 189–192.

ROUX, M. 1970. Introduction à l'étude des microstructures des tiges de crinoides. *Geobios,* **3,** 79–98.

——1971. Recherches sur la microstructure des pédonculés de crinoides post-Paléozoique. *Trav. Lab. Paléontol., Orsay,* 86 pp.

——1974*a*. Les principaux modes d'articulation des ossicules du squelette des Crinoides pédonculés actuels. Observations microstructurales et conséquences pour l'interprétation des fossiles. *C.R. Acad. Sc. Paris,* **278,** 2015–2018.

——1974*b*. Observations au microscope électronique à balayage de quelques articulations entre les ossicules du squelette des crinoides pédonculés actuels (Bathycrinidae et Isocrinina). *Trav. Lab. Paléontol., Orsay,* 10 pp.

——1975. Microstructural analysis of the crinoid stem. *Univ. Kansas Paleontol. Contrib.* **75,** 7 pp.

——1977. The stalk-joints of Recent Isocrinidae (Crinoidea). *Bull. Br. Mus. nat. Hist. (Zool.),* **32,** 45–64.

SMITH, A. B. 1978. A functional classification of the coronal pores of regular echinoids. *Palaeontology,* **21,** 759–790.

STRIMPLE, H. L. 1972. Porosity of a fossil crinoid ossicle. *J. Paleontol.* **46,** 920–921.

SUMICH, J. L. and MCCAULEY, J. E. 1973. Growth of a sea urchin *Allocentrotus fragilis* off the Oregon coast. *Pacific Sci.* **27,** 156–167.

SWAN, E. F. 1952. Regeneration of spines by sea urchins of the genus *Strongylocentrotus. Growth,* **16,** 27–35.

——1966. Growth, autonomy and regeneration. In BOOLOOTIAN, R. A. (ed.), *Physiology of Echinodermata.* J. Wiley and Sons (Interscience Publishers), New York, Ch. 17.

TAKI, J. 1972*a*. A tetracycline labelling observation on growth zones in the test plate of *Strongylocentrotus intermedius* (in Japanese, with English abstract). *Bull. Jap. Soc. scient. Fish.* **38,** 117–121.

——1972*b*. A tetracycline labelling observation on growth zones in the jaw apparatus of *Strongylocentrotus intermedius* (in Japanese, with English abstract). Ibid. **38,** 181–188.

THUM, A. B. and ALLEN, J. C. 1976. Reproductive ecology of the lamp urchin *Echinolampas crassa* (Bell) 1880 from a subtidal biogenous ripple train. *Trans. roy. Soc. S. Afr.* **42,** 23–33.

TOWE, K. M. 1967. Echinoderm calcite: single crystal or polycrystalline aggregate. *Science, N.Y.* **157,** 1048–1050.

UHLMANN, K. 1968. Über die Verbindung der Muskulatur mit dem skelett bei dem Echinodermen, *Asterias rubens* L. *Z. Zellforsch.* **87,** 210–217.

VADAS, R. L. 1977. Preferential feeding: an optimization strategy in sea urchins. *Ecol. Monogr.* **47,** 337–372.

VALENTIN, G. 1841. Anatomie des Echinodermes. In AGASSIZ, L., *Monographies d'Echinodermes vivants et fossiles.* Petitpierre, Neuchatel, 1–126.

VEVERS, H. G. 1966. Pigmentation. In BOOLOOTIAN, R. A. (ed.), *Physiology of Echinodermata.* J. Wiley and Sons (Interscience Publishers), New York, Ch. 11.

WAINWRIGHT, S. A., BIGGS, W. D., CURREY, J. D., and GOSLINE, J. M. 1976. *Mechanical design in organisms.* Edward Arnold (Publishers) Ltd., London, 423 pp.

WEBER, J. N. 1969. The incorporation of magnesium into the skeletal calcites of echinoderms. *Amer. J. Sci.* **267,** 537–566.

—— GREER, R., VOIGHT, B., and WHITE, E. 1969. Unusual strength properties of echinoderm calcite. *J. ultrastruct. Res.* **26,** 355–366.

ANDREW B. SMITH

Jane Herdman Laboratory of Geology
University of Liverpool
Liverpool L69 3BX

Final typescript received 17 August 1979